NASA CR-72122

FINAL REPORT
VOLUME II

FLOW OSCILLATIONS IN FORCED CONVECTION BOILING

by

A. H. Stenning and T. N. Veziroglu

prepared for

NATIONAL AERONAUTICS AND SPACE ADMINISTRATION
NASA GRANT NsG-424

Mechanical Engineering Department
University of Miami
Coral Gables, Florida

Requests for copies of this report should be referred to

National Aeronautics and Space Administration
Office of Scientific and Technical Information
Attention: AFSS-A
Washington, D.C. 20546

NASA CR-72122

FINAL REPORT

VOLUME II

FLOW OSCILLATIONS IN FORCED CONVECTION BOILING

by

A. H. Stenning and T. N. Veziroglu

prepared for

NATIONAL AERONAUTICS AND SPACE ADMINISTRATION

February 1967

NASA GRANT NsG-424

Technical Management
NASA Lewis Research Center
Cleveland, Ohio

James J. Watt

MECHANICAL ENGINEERING DEPARTMENT
UNIVERSITY OF MIAMI
CORAL GABLES, FLORIDA

FLOW OSCILLATIONS IN FORCED CONVECTION BOILING

by

A. H. Stenning and T. N. Veziroglu

ABSTRACT

The stability of flow in forced-convection boiling in a horizontal, electrically heated tube has been investigated experimentally using Freon-11 and water as the test fluids. Two major modes of oscillation have been identified, and studied analytically, with major emphasis on the conditions governing the onset of instability. Variations in heat transfer during oscillations appear to have a strong effect on stability.

CONTENTS

FLOW OSCILLATIONS IN FORCED CONVECTION BOILING

by

A. H. Stenning and T. N. Veziroglu

University of Miami

1. SUMMARY

The stability of flow in forced-convection boiling has been studied analytically, and also experimentally using Freon-11 and water as the test fluids.

Two major modes of oscillation have been identified. The first occurs when the pressure drop across the test section decreases with increasing flow rate, and is associated with relatively low exit vapor fraction. The period of these oscillations is mainly governed by the volume and compressibility of the vapor in the system. In this report these oscillations will be called "Type I" oscillations. In other publications by the present authors they have been given the name "pressure-drop" oscillations.

The second mode of oscillation occurs with higher exit vapor qualities than are found with Type I oscillations, and also when the working fluid is completely evaporated and super-heated. These oscillations are caused by the dynamic interaction between pressure drop, flow rate and mass storage within the heater. Their period is of the same order of magnitude as the residence time of a particle in the heater, and in the system tested was usually substantially less than the period of Type II oscillations. In other publications they have been given the name "density-wave" oscillations.

In addition to these two major modes, a third mode of oscillation was observed for a short period of time when studying Type II oscillations with film boiling in Freon-11. The third mode of oscillation was characterised by very large changes in tube-wall temperature, and appeared to be associated with operation near the negative slope region of the heat flux versus temperature difference curve, between the critical heat flux and the film boiling region. This mode of oscillation is here termed "Type III" oscillation, and elsewhere has been called the "thermal oscillation" mode.

When using Freon-11 as the working fluid, it was always possible to eliminate all these oscillations by introducing a flow resistance at the heater inlet, unless the pressure level was so low that cavitation occurred before the heater. With water, it was impossible to stabilise the system with an inlet restriction for the system pressure levels used in the experiments.

The general characteristics of Type I oscillations are predicted by the theoretical analysis, and the flow rate at which the instability commences is also predicted with good accuracy, although the predicted periods of the oscillations are considerably larger than the measured periods.

The analysis of Type II oscillations suggests that transient heat transfer coefficients may differ considerably from those measured in steady flow.

In the case of Type III oscillations, the instability appears to be associated with a hysteresis loop in the heat transfer characteristics. Only a partial explanation of this phenomenon is available at present.

The present report forms Volume II of the final report on two-phase flow instabilities. Volume I* covers instabilities in two-component two-phase flows.

* Oscillations in Two-Component Two-Phase Flow, NASA GRANT NsG-424, Final Report, Volume I, NASA CR-72121, February 1967.

2. INTRODUCTION

Many different types of instability have been observed in forced convection boiling, ranging from simple flow excursions of the Ledinegg type [1]* to complex periodic phenomena [2]. As the geometric arrangement of the evaporator becomes more complicated, with multiply connected tubes, the number of instability modes also increases.

The objective of this investigation was to study the modes of oscillation in the simplest possible forced convection boiling system, a single-tube horizontal heater fed from a pressurized tank, with a constant pressure at the system exit. With Freon-11 as the test fluid, the whole range of conditions from nucleate boiling to film boiling could be covered without encountering excessive heater wall temperatures. A limited amount of testing could also be carried out using water as the test fluid.

---

* The numbers in square brackets refer to references at the end of the Report on page 91.

3. EXPERIMENTAL APPARATUS

The apparatus is shown schematically in Fig. 1. The test system consists of a surge tank, an inlet valve, a heater, an exit valve, and (in the case of superheat experiments) an exit plenum connected by tubing. All the tubing in the system, including the heater, is made of nichrome with 0.1475 inch inside diameter and 3/16 inch outside diameter. The heater tube, 37 1/2 inches long, is itself used as the electrical resistance for providing heat input. D.C. voltage is applied at the ends of the heater tube, and power input up to 5 k.w. can be obtained with a maximum current of 200 amperes. To reduce the heat losses to a minimum, a vacuum jacket containing a radiation guard was built around the heater. The vacuum jacket is connected to a vacuum pump to evacuate air and other gases. At the inlet side of the heater a sight glass tube was included in the system for observation of any bubbles present in the liquid entering the heater. The surge tank was installed after several pressure gages were damaged during the early experiments, with the objective of reducing the amplitude of the pressure oscillations in the system. The surge tank is made of stainless steel (4 inches diameter x 9 inches height) with a glass level indicator. The surge tank was provided with a bicycle type check valve for pumping in air as needed, since it was found that the trapped air would flow out through the system in between the experiments and be replaced by vapor which in turn would condense during the experiments as pressures were increased. To decrease the possiblity of air escape, a 1/8 inch thick and

3 7/8 inch diameter disc was used as a float on the free liquid surface in the surge tank. During the superheat experiments, an exit plenum, 7 inches long and 4 inches in diameter, was added to the downstream side of the test section, to simulate the thrust chamber geometry of nuclear rocket engines. The exit plenum was connected to a 3/4 inch diameter exit pipe - in which the pressure was atmospheric - through a 6 inch long and 0.1475 inch inside diameter nichrome tube and a needle valve. Two flow-through copper-constantan thermocouples were inserted into the system before and after the heater to measure the inlet and exit temperatures of the test fluid. Five copper-constantan thermocouples were fixed to the outer wall surface of the heater to measure heater wall temperatures. They were electrically insulated from the heater by means of 0.0015 inch thick mica flakes. Three bourdon type Heise pressure gages and two strain gage type pressure transducers were installed in the test section to measure the pressures at various stations across the system, and sense the pressure oscillations. A differential pressure transducer, Sanborn Model 270, was installed at the upstream side of the heater to record the line pressure drop and sense the flow oscillations. The outputs from the pressure and differential pressure transducers were recorded on a Sanborn chart recorder and an X-Y plotter. The outputs from the thermocouples were recorded on an Esterline-Angus chart recorder during the earlier experiments and on a Sanborn chart recorder for the later experiments.

The experimental set-up included a liquid container on the upstream side of the test section, and a liquid recovery system on the downstream side. The container has a volume of 4 cubic feet and is made of stainless steel to withstand pressures up to 150 p.s.i.g. The liquid inlet temperature was controlled by a 2 k.w. immersion heater with a thermostat installed in the container. During the experiments liquid in the container was pressurized by high pressure nitrogen, using a constant pressure regulating valve to maintain flow into the test section, via a filter, a micrometer control valve, and a rotameter. Superheated vapor or a mixture of saturated vapor and liquid leaving the test section was led into the recovery system. This system was essentially a heat exchanger where vapor was condensed in a helical aluminum tube cooled by refrigerated brine at 32°F.

4. CLASSIFICATION OF OSCILLATIONS

In each set of tests, the geometry of the test section, the inlet temperature of the liquid, and the power input were fixed. The flow rate through the heater was then varied over the range allowed by the flowmeter and the steady flow and dynamic characteristics of the system studied within this flow range. In general, the system would be stable within portions of the flow range and unstable in other portions.

The different modes of oscillation can best be introduced by relating the sequence of events in three sets of test runs with Freon-11, two at approximately 1200 BTU/hr. power input with nucleate boiling throughout the heater, and one at 2390 BTU/hr. power input with both nucleate boiling and film boiling occurring.

4.1. Experiments with Nucleate Boiling

These tests were carried out with the surge tank installed. In obtaining the series of test points, the supply tank pressure was first set at 75 psia. The liquid Freon temperature was 67° F (57° subcooling at heater inlet). The valve after the heater (No. 3) was set to the desired position, and not changed during the series of tests. The valve before the heater (No. 2) was opened wide so that there was very little pressure drop between the surge tank and the heater. The valve between the supply tank and the surge tank (No. 1) was used to control the flow, and was opened wide to obtain the first test point. Power was turned on in the heater, and set at 1170 BTU/hr. When the temperatures, pressures and flow reached equilibrium all data were recorded. The system was stable at this flow rate (2.6 lbs/min), and there was no vapor generated. The maximum tube wall temperatures were of the order of 130°F.

The flow was then reduced in small steps using valve No. 1, allowing the system to come to steady state each time before making a further change. The pressure drop from the surge tank to the exit from valve No. 3 (where the pressure was constant and equal to atmospheric pressure) is plotted in Figure 2 against flow rate, and the vapor mass fraction leaving the heater is also shown on this diagram.

As the flow was reduced, the pressure drop across the test section also fell, until a flow rate of 2.22 lbs/min was reached, at which point the liquid leaving the heater was almost saturated. Further reduction in flow was accompanied by an increase in pressure drop as bulk boiling commenced. For flows between 2.22 lbs/min and 0.60 lb/min, the slope of the pressure drop versus flow curve was negative.

At a flow of 1.68 lbs/min, sinusoidal pressure oscillations of small amplitude were observed with a period of 42 seconds. The pressure recordings upstream and downstream of the heater are reproduced in Figure 3(a) and the point at which the recordings were made is marked (a) in Figure 2. The oscillations continued as the flow was reduced, and the amplitude of the oscillations increased until at a mean flow of 1.42 lbs. per minute the total variation in pressure during one oscillation was 2.5 psi. (Fig. 3(b)). At this point the period was 48 seconds, and the liquid level in the surge tank moved up and down in phase with the pressure oscillations. With further reduction in flow the amplitude of the oscillations decreased (Fig. 3(c)) until at a flow of 1.16 lbs. per minute steady, stable conditions were obtained. Between 1.16 lbs. per minute and 0.43 lb. per minute (a condition where the pressure-drop versus flow curve once again displayed a positive slope), higher frequency non-sinusoidal oscillations were observed with a period of 3.3 seconds (Fig. 3(d)) and these oscillations persisted as the flow was reduced further. Liquid level changes in the surge tank were negligible during the higher frequency oscillations.

Observations of heater wall temperature behavior during both low frequency and higher frequency oscillations showed a maximum fluctuation of 2°F for the low frequency oscillations, and no noticeable temperature fluctuation during the higher frequency oscillations. The wall temperature fluctuations for the low frequency oscillations were in phase with the pressure, and approximately equal to the change in saturation temperature of the liquid.

The power input was next increased to 1330 BTU/hour, to see whether relatively small changes in power could have a significant effect on the stability. Again, the flow was started at the maximum attainable value and reduced in small steps. The pressure drop versus flow curve is shown in Fig. 4, with exit vapor mass fraction shown above the flow scale. The pressure oscillations are displayed in Fig. 5, and the corresponding points in Fig. 4 are indicated with arrows. Low frequency oscillations with a period of 43 seconds were encountered at a flow of 1.95 lbs. per minute (Fig. 5(a)). These oscillations increased in amplitude as the flow was reduced to 1.80 lbs. per minute (Fig. 5(b)). At a mean flow rate of 1.59 lbs. per minute (Fig. 5(c)) an interesting change was observed in the pressure traces, a sharp disturbance appearing on the rising pressure portion of each cycle. With further reduction in mean flow to 1.23 lbs. per minute, the single sharp disturbance became a burst of higher frequency oscillations on the rising pressure portion of the cycle, with a period of 3 seconds (Fig. 5(d)). At a flow of 1 lb. per minute, the low frequency oscillations had a period of 90 seconds, while the superimposed higher frequency oscillations had a period of 3 seconds (Fig. 5(e)). At 0.89 lb. per minute, the flow became stable, and remained stable until 0.64 lb. per minute, when sustained higher frequency oscillations commenced with a period of 4 seconds (Fig. 5(f)). These higher frequency oscillations persisted at lower flows.

To determine the conditions required to stabilize the low frequency oscillations, the heater inlet valve (valve No. 2) was closed until stable flow was obtained in the range 0.8 to 2.0 lbs. per minute. With this valve setting, it was also found that the higher frequency oscillations did not appear in the flow range 0.4 to 0.6 lb. per minute. The pressure drop across the test system with the inlet restriction added is shown as a chain-dotted line in Figure 4. There is still a region with negative slope, but the maximum negative slope is less than the value without the inlet restriction, and the flow range in which negative slope occurs is greatly reduced.

The behavior described in the test runs at 1170 BTU/hr. and 1330 BTU/hr. is representative of that encountered in many other tests with Freon-11 and water. The low frequency oscillations, now called Type I oscillations, were only found when the slope of the pressure drop curve was negative. The higher frequency oscillations, termed Type II oscillations were observed at higher exit vapor mass fractions, in regions where the pressure drop increased with increasing flow, and where the ratio of inlet liquid density to mixed mean density leaving the heater was of the order of 40 or greater. In some cases, bursts of Type II oscillations were observed in the Type I oscillations, but in other cases the two types of oscillations were completely independent. When using Freon-11, the system could always be stabilized against both types of oscillation, provided no cavitation occurred between the surge tank and the heater, by providing a pressure drop across valve No. 2. However, in some cases where the supply pressure was very low, cavitation occurred in valve

No. 2. The compressibility of this vapor cavity at the heater inlet was then apparently sufficient to provide the equivalent of a surge tank after the valve which allowed oscillations to occur even when the valve was almost closed. In this case, it was impossible to distinguish between the two types of oscillations on the basis of frequency. Due to the small volume of the vapor cavity, the Type I oscillations would have frequencies of the same order as the Type II oscillations, and no intervening stable zone was found. With water as the test fluid, the system could not be stabilized.

4.2. Experiments with Film Boiling

During the film boiling experiments, the surge tank and valve No. 1 were not installed. With valves No. 2 and No. 3 at a fixed setting, the flow was controlled by changing the nitrogen pressure in the supply tank. At the power levels required to obtain film boiling within the useful range of the flowmeter, the exit vapor mass fraction was greater than 25% over the whole flow range of the flowmeter and the pressure drop versus flow curve had positive slope. Consequently, Type I oscillations were never encountered, though there is no reason to believe that they would not have occurred if a higher flow had been attainable.

As in the tests at lower power, the procedure was to set the power level and the valves, then reduce the flow until oscillations were encountered. It was expected that stable flow would occur until Type II oscillations appeared, and that the oscillations would then persist at lower flows, just as had been observed in the earlier experiments. In many of the film boiling tests, these expectations were realized, and nothing untoward occurred. Type II oscillations were observed at density ratios (heater inlet to heater outlet) of 40 or more with nucleate boiling in the first 25 inches of the heater and film boiling in the remaining 12 inches. However, in some experiments a completely different type of oscillation was also observed, and one of these experiments will be described below.

In this series of tests, the power was set at 2390 BTU/hr., and the liquid Freon inlet temperature was 79° F. The flow rate was reduced by lowering the nitrogen pressure in the supply tank until, at a tank pressure of 50 psia and a flow rate of 0.59 lb. per minute, small Type II oscillations appeared, with a period of 2.7 seconds. The pressure oscillations at the heater inlet are shown in Figure 6(a). At this point, the mean pressure at the heater inlet was 47 psia and the pressure at the exit from the heater was 41 psia. A pressure drop of 26 psi occurred across the exit tubing and valve No. 3. Heater wall temperatures are plotted in Figure 7 against length from heater inlet. The saturation temperature was approximately 144° F. From comparison with a typical Freon-11 boiling curve (Fig. 8) by Blatt and Adt [3] it can be seen that nucleate boiling prevailed throughout the tube. The mean flow was then reduced about 5% with the expectation of generating fully developed Type II oscillations. Instead, a highly non-linear oscillation appeared with a period of 80 seconds, involving short bursts of Type II oscillations at regular intervals. The wall temperatures measured at the first three thermocouples on the heater remained constant and without appreciable fluctuation. However, the temperatures measured at the last two thermocouples near the exit showed large fluctuations. At the twenty-seven inch station, the wall temperature fluctuated periodically between 262° F and 396° F, while at the thirty-five inch station the wall temperature fluctuated between 360° F and 390° F. Apparently, the last twelve inches of the heater was now operating in the film boiling region, and the instability was caused by the behavior of the film boiling zone. The pressure oscillations at the heater inlet and the temperature fluctuation at a point twenty-seven inches from the heater inlet are displayed in Figure 6(b). The slow oscillations were called Type III oscillations because the wall temperature behavior was clearly different from the other types. The Type III oscillations continued as the flow was reduced further, until at a mean flow rate of about 0.45 lb. per minute they were replaced by fully developed Type II oscillations with a period of 2.1 seconds (Fig. 6(c)). The wall temperatures throughout the tube then became steady, with nucleate boiling at the first three measuring stations (wall temperature about 150° F) and film boiling at the last two stations (wall temperature about 380° F). The Type II oscillations persisted at lower flows.

The factors which caused the Type III oscillations to occur in some cases and not in others have not yet been determined. When they occurred, it was always just after the onset of Type II oscillations with nucleate boiling and they were always replaced by fully developed Type II oscillations with film boiling when the flow was reduced further. The Type III oscillations were not obtained after the heater tube became badly fouled and was replaced by a new tube, so surface conditions may have a strong influence on them.

5. EXPERIMENTAL RESULTS

After establishing the existence of the three modes of oscillation, careful experiments were carried out with the objective of studying the characteristics of each type separately. A considerable body of data was obtained for Type I and Type II oscillations using Freon-11. A smaller quantity of data was obtained with water, due to difficulties associated with excessive tube-wall temperatures. As has been mentioned earlier, Type III oscillations were not obtained after a new heater tube was installed, and in consequence the discussion in section 4.2 contains most of the information which was obtained about this phenomenon.

5.1. Type I Oscillations in Freon-11

In early experiments on Type I oscillations, considerable difficulty was encountered in attempting to repeat results on different occasions. Even with the exit valve in a fixed position, and apparent repeatability in liquid inlet temperature, substantial variations in the heater pressure drop characteristics occurred. After investigating the reasons for this behavior, it was observed that a change of one degree in the inlet temperature would have a noticeable effect on the steady and dynamic characteristics of the system. In consequence, for the experiments reported below, a stainless steel coil was installed in the liquid Freon line just before the surge tank. The Freon flowed through this coil, which was cooled by essentially constant temperature city water at 78.4 ± 0.5 F. In addition, the exit valve was removed and replaced by a 0.059 inch diameter sharp-edged orifice which produced overall pressure drop characteristics favorable for the occurrence of Type I oscillations. With this arrangement, excellent repeatability of data was obtained. From the observations discussed in section 4.1, it was apparent that the pressure drop characteristics of the system had a major effect on the occurrence and amplitude of Type I oscillations. It was therefore essential to obtain the steady-state pressure drop from the surge tank to the system exit with valve 2 fully open as a function of flow rate and heater power input. Since the system was unstable over part of the flow range with valve 2 fully open, it was necessary to stabilise the system by partially closing valve 2, then to measure the pressure drop downstream of valve 2 as a function of flow rate and heat input, and finally to add the pressure drop contributions of valve 2 when fully open, and the short section of tubing between the valve and the surge tank. Figure 9 shows the results of the steady state pressure drop measurements, plotted as pressure drop downstream of valve 2 versus flow rate for different heat inputs. It can be seen that the right-hand portion of each curve approaches an envelope which is, in fact, the pressure drop with liquid flowing throughout and zero heat input. There is an intermediate region on each curve with negative slope, and a left-hand portion with positive slope. The dotted line at the bottom of the figure represents the additional pressure drop which must be added to the values shown in the curves to obtain the total pressure drop from the surge tank to the system exit.

In addition, steady state heat transfer data was taken, yielding the curves for average heat transfer coefficient over the tube shown in Figure 10. These curves show a very rapid and unexpected increase of heat transfer coefficient with mass flow rate at flows above 2 pounds per minute. However, the possible errors in h^* at these flow rates are approximately $\pm$ 50% because the average ΔT was only about 2 degrees F, and the estimated maximum error in ΔT is of the order of $\pm$ 1 degree F. In consequence, it is quite possible that the measured heat transfer coefficients are incorrect at high flow rates.

After the steady state curves were obtained, valve 2 was opened fully and a set of tests were carried out at constant power input, reducing the flow using valve 1 until oscillations were encountered, and then taking recordings of the limit cycles which occurred as the flow was reduced further. Callahan has reported the complete results of these tests [4]. The discussion given here will be limited to the results of the test at 1170 BTU/hour.

Oscillations were first encountered at a mean flow rate of 2.35 pounds per minute, and the limit cycle at this flow is shown on the pressure drop-flow rate plane as curve A in Figure 11. As the mean flow was reduced further, the amplitude of the flow and pressure oscillations increased as shown by the curves B, C and D. All the limit cycles

* A nomenclature is included at the end of the Report on page 95.

travel in the clockwise direction. From the superimposed steady flow pressure drop curve at 1170 BTU/hr, it can be seen that for curve D the minimum flow rate during the oscillation is slightly larger than that corresponding to the peak of the pressure drop curve. A further reduction in mean flow produced limit cycle E, which moved to the left of the peak, and went through several Type II oscillations before recovering and completing the cycle. The pressure and flow oscillations are shown separately in Figure 12 for each limit cycle.

In Figure 13, the limit cycle of curve D is depicted, with the time taken to reach each point in the cycle from an arbitrary zero recorded on the curve. The period of the cycle was 63 seconds. Considering the cycle as a roughly four sided figure, it can be seen that the time taken to move along each side was approximately the same (about 15 seconds). The slowest portion of the cycle occurred between 50 and 60 seconds, when the flow rate changed so slowly that the heat input into the fluid was equal to the electrical power input. This was the only portion of the cycle for which the system followed the steady state pressure drop curve at 1170 BTU/hr.

To summarise, Type I oscillations in Freon-11 were characterised by limit cycles which commenced at a flow rate to the left of the minimum on the test section pressure drop curve. The amplitude of the oscillations at first increased as the mean flow rate was reduced, and if the transient flow fell below that corresponding to the peak of the pressure drop curve, Type II oscillations occurred during part of the cycle. In some cases, direct transition from Type I to fully developed Type II oscillations occurred with further reduction in mean flow. In other cases (as shown in Figure 2) a region of stable flow was observed between the Type I and Type II oscillations. In such cases, Type II oscillations were not observed on the Type I oscillations. The right-hand portion of the steady state pressure drop curve always formed one boundary of the limit cycles.

5.2. Type II Oscillations in Freon-11

The experiments for investigating the stability boundaries for Type II oscillations in Freon-11 were broadly separated into three classes: (1) Experiments with partial boiling, and approximately constant inlet temperature; (2) Experiments with superheated vapor leaving the system, and approximately constant inlet temperature; and (3) Subcooling experiments, in which the temperature of the Freon-11 at the inlet to the system was varied. Accordingly, the system geometry and the procedure used in each group of experiments will be outlined separately.

5.2.1. Experiments with partial boiling

The early experiments with partial boiling were run without the surge tank, and the later ones with the surge tank in place. Consequently, in the early experiments the Freon-11 container acted as the surge tank, and the friction and inertia of the fluid between the container and the heater contributed to the system dynamics. All the experiments with partial boiling were run without the exit plenum. With the exceptions noted here, the general set-up conformed to the description given under section 3.

In these experiments, liquid Freon-11 was first run through the system with the inlet valve partly closed and the exit valve fully open, after pressurizing the Freon-11 in the container up to 50 to 60 p.s.i.g. The regulator valve kept the tank pressure constant within $\pm$ 0.1 p.s.i. during the experiments. Then the heater was started at a relatively low power level of about 100 watts. Its power was increased to a pre-determined test level by 50 watt increments. After each change in power, about 10 minutes was allowed to elapse before the next change. This procedure prevented unwanted transient instabilities. During the heater power level increases, the Freon-11 flow rate was increased by adjusting the control valve, and the pressure drop upstream of the heater was increased if necessary by adjusting the inlet valve so that the system was already operating within the stable zone at steady state. After the test power level was reached, the exit valve was set to provide a pre-determined exit pressure drop. Then the Freon-11 mass flow rate was brought to a pre-determined value, by adjusting the Freon-11 container pressure in the case of the experiments without the surge tank, and by adjusting the control valve in the case of the experiments with the surge tank. After setting the flow rate, the inlet valve was slowly opened till the onset of Type II oscillations was noticed. These oscillations could be observed from the periodic motion of the pressure gage pointers and also from the pressure recordings. Since the experiments indicated that there was no noticeable hysteresis effect, the stability boundary was always reached from the stable zone as this procedure resulted in some time saving. At the stability boundary the room temperature, barometric pressure, Freon-11 mass flow rate, heater voltage and current, and pressure and temperature (thermocouple) readings at various stations along the test system were recorded. After taking the readings, the pressure drop upstream of the heater was slightly reduced by opening the inlet valve a little more. This caused the system to operate in the unstable zone. At this stage, pressure recordings were made for more accurate frequency calculations. Figs. 14a and b show the pressure recordings at the stability boundary and within the unstable region for one experiment. The procedure described above was repeated for various flow rates, exit valve settings and heater power levels. Heater power level and Freon-11 mass flow rate combinations were so arranged that at all times the Freon-11 leaving the heater was a saturated mixture of vapor and liquid. This could be ascertained by checking that the Freon-11 exit temperatures were never above the saturation temperatures corresponding to the exit pressures.

An earlier analysis [5] suggested that the major parameters affecting the onset of Type II oscillations with partial boiling are overall density ratio ρ_{hi}/ρ_{se} (the inlet density of liquid divided by the exit density of the liquid and vapor mixture); the heat input fraction c' expended in removing subcooling; the inlet pressure drop fraction y (pressure drop upstream of heater divided by the overall system pressure drop) and the rate of change of heat transfer with flow rate, represented by the parameter $b = [1 - \frac{\dot{m}}{q} \frac{\partial q}{\partial \dot{m}}]$. The symbol b represents the fraction of the heat transfer coefficient which may be attributed to pool boiling. In addition, the inertia of the fluid is represented by a parameter involving the ratio of inlet dynamic pressure to overall system pressure drop, and the ratios of inlet and exit tubing lengths to the heater length. However, in the experiments reported here the effective inertia of the fluid was so small that it should not have had any significant effect on stability. Pressure drops were evaluated from the point where the pressure was maintained essentially constant ahead of the heater, that is from the Freon-11 container for the early experiments, and from the surge tank for the later experiments with the surge tank installed.

Using the experimental readings and the recordings the above parameters were calculated. In addition, the time period of the oscillations at the onset of instability τ_o, the residence time of a Freon-11 particle in the heater plus exit tubing τ_{ie}, and the residence time between the point where bulk boiling commenced and the system exit τ_{be} were calculated. The pressure recordings of the oscillations were used to obtain τ_o, and in calculating τ_{ie} and τ_{be} it was assumed that the heat flux was constant along the heater and the mixture was homogeneous with no slip between the phases.

The pressure and temperature distributions along the test sections, mass flow rate $\dot{m}$, heater heat flux q and most of the parameters are tabulated in Tables I and II for the test system geometries starting from the Freon-11 container and surge tank respectively. The calculations made from some additional heat transfer experiments indicated that the value of the parameter b was about 0.55 to 0.60 for all the onset conditions. The liquid temperature at the heater inlet ranged from 70°F to 80°F.

Because of the interdependence of the parameters affecting the stability boundary, it was not possible to keep all but two constant and investigate their relationship. Under these circumstances, to give a useful representation of the data, the overall density ratios ρ_{hi}/ρ_{se} were plotted against the heat fraction used in removing subcooling c' at different heater power levels and the resulting curves are shown in Figure 15 for the tests without the surge tank and in Figure 16 for the tests with the surge tank. These are in fact steady state operating curves for the system. Then the points corresponding to a constant c' were selected, and the inlet fraction of pressure drop y and the overall density ratio ρ_{hi}/ρ_{se} were determined for each point at the onset of oscillations. To keep c' constant, some of the points have been found by interpolation between two nearest onset points. The results are plotted for various values of c' in Figure 17 for the tests without the surge tank, and in Figure 18 for the tests with the surge tank. In the region above each curve the system is stable and in the region below it is unstable.

The transition from stability to instability was quite sharp, and a reduction of only 0.1 psi in the inlet pressure drop was sufficient to cause large oscillations when the system was on the stability boundary. The oscillation frequency changed very little as the system moved from a just-stable to an unstable condition.

From a study of Figs. 17 and 18, it can be seen that (1) increase in overall density ratio decreases stability, (2) increase in inlet fraction of pressure drop increases stability, (3) increase in fraction of heat used in removing subcooling decreases stability and (4) addition of the surge tank increases stability.

In comparing the stability maps for the system with the surge tank installed (Fig. 18) and without it (Fig. 17) it can be seen that (other things being equal) somewhat higher values of inlet pressure drop are apparently required to stabilize the system when the surge tank is not used. This trend is suprising, since the effective inertia of the fluid upstream of the heater is greater when the surge tank is left out.

Since earlier analyses [6] indicated that the time period τ_o of the density-wave two-phase flow oscillations should be of the order of the residence time τ_{ie} of a fluid particle from heater inlet to system exit, τ_{ie} was plotted against τ_o (Fig. 19). The points seemed to fall roughly on one straight line. The equation of the best straight line is $\tau_o = 2.29\ \tau_{ie}$.

5.2.2. Experiments with superheat

All the experiments with superheated vapor leaving the heater were run with the surge tank and the exit plenum installed (See Fig. 1).

The same procedure as for partial boiling was followed up to the point of obtaining the test power level in the heater. Throughout these experiments the needle valve - replacing the exit valve - was kept fully open. After the test power level was reached, the Freon-11 flow rate was adjusted with the control valve to obtain a few degrees of superheat at the heater exit. During this process the inlet valve opening was reduced if necessary to obtain stable flow. Then the inlet valve was slowly opened till the onset of Type II oscillations was noticed as described above under the experiments with partial boiling. The onset of the oscillations could be observed from the pressure and flow rate recordings. At the stability boundary all the pertinent readings were taken. Fig. 20 shows the recordings of heater inlet pressure and Freon-11 mass flow rate within the unstable region for one experiment. There is a 180 degree phase shift between them. The above procedure was then repeated, reducing the Freon-11 mass flow rate in steps with the control valve to obtain greater degrees of superheat. The experiments were repeated for other power levels. Heater power level and

Freon-11 mass flow rate combinations were so arranged that at all times the Freon-11 leaving the heater was superheated.

The overall density ratio from the heater inlet to the exit plenum is plotted in Figure 21 for different power levels and exit valve settings. Values of all the variables at the onset of instability are tabulated in Table III, and a crossplot of inlet pressure fraction versus mass flow rate at the stability boundary is presented in Figure 22. From a comparison of Figure 18 and Figure 22, it is apparent that the presence of superheated vapor introduces no discontinuity in stability. The overall density ratios are somewhat higher than those encountered with partial evaporation, and slightly larger inlet pressure drop fractions are necessary for stability.

The periods of the oscillations are not tabulated, but were again found to correlate well with computed residence times.

5.2.3.Subcooling experiments.

In all the experiments to study the effect of subcooling on the onset of Type II oscillations, the surge tank was installed before the heater and the downstream plenum was not used. During some of the experiments the exit valve was removed from the system and replaced by a 6 inch long piece of tubing to give the lowest possible exit pressure drop. In other respects the experimental apparatus conformed with the arrangement shown in Figure 1.

The pressurized (50 to 60 p.s.i.g.) Freon-11 in the container was heated to a pre-determined temperature level between the room temperature and the saturation temperature, using the immersion heater in the Freon-11 container and its thermostat controls. Stability was determined at each inlet temperature for a range of power inputs. When the inlet temperature was within a few degrees of the saturation temperature, cavitation occurred at the heater inlet and was accompanied by a substantial reduction in stability. To keep the number of variables down to a minimum, cavitation of Freon-11 before entry into the heater was avoided by limiting the inlet temperature to the heater. As a result the minimum subcooling allowable ranged from $7^{O}F$ at a heat flux of 8500 BTU/hr.ft.^{2} to $20^{O}F$ at a heat flux of 22650 BTU/hr.ft.^{2}.

Using the experimental readings and recordings the degree of subcooling ΔT_s, and the parameters mentioned under the experiments with partial boiling were calculated. The pressure and temperature distributions along the test section, mass flow rate, heater heat flux and most of the parameters are tabulated in Tables IV and V for the test sections with and without the exit valve. Figs.23 and 24 show subcooling (defined as the difference between the saturation temperature at the start of bulk boiling and the inlet temperature) versus mass flow rate at the stability boundary with the inlet valve wide open for various heater power levels, with and without the exit valve. Each line represents the boundary between stable and unstable operation. At a given value of ΔT_s, the system is unstable to the left of the line. From a study of the figures it can generally be observed that (1) increase in heat input decreases stability, (2) removal of the exit restriction has a slight beneficial effect on stability. The shapes of the curves, more clearly shown in Fig. 24, are interesting. They have, for the regions investigated, S shapes with rather sharp bends, indicating a sudden increase in stability as the subcooling is increased above a certain value (which increases with heater input). The curves show that for a given mass flow rate there may exist three different subcooling values at the stability boundary. Probably there would be at least one more subcooling value at the boundary, a value greater than any of the three indicated in the diagrams, since the upper branches of the curves must turn back towards the subcooling axis as the subcooling is increased above the range investigated. Another interesting feature of the results is the common envelope of the upper branches of the curves. Gouse and Andrysiak [7] have reported similar experiments using Freon-113 as the test fluid. Their results, plotted as subcooling versus mass flow rate at the stability boundary, do not show S shaped curves, but inverted C shapes. However, they indicate that the nature of closure at the bend is not quite clear.

Evidently, the effects of subcooling on stability shown in Figures 17 and 18 are limited to the inlet temperatures employed in those experiments, and cannot be used as a basis for prediction of stability with different inlet temperatures.

5.3. Type I Oscillations in Water

The procedure used in the water experiments was essentially the same as that employed in the Freon-11 experiments, except that the constant temperature bath was not installed upstream of the surge tank. For the first experiments on Type I oscillations in water, the exit valve was again replaced by a .059 inch diameter sharp-edged orifice. The immersion heater in the supply tank was adjusted to give a liquid inlet temperature of approximately 180 degrees F.

Preliminary experiments using water showed that the system could not be stabilized by inlet pressure drop when bulk boiling occurred, and in consequence it was not possible to generate complete curves of the type shown in Figure 9. Type I oscillations with Type II oscillations superimposed were observed to occur whenever the flow was reduced sufficiently to produce boiling in the tube (and hence an increase in pressure drop with a decrease in flow). Moreover, there appeared to be a marked lack of thermal equilibrium within the flow, since the onset of instability was generally associated with the appearance of some vapor in the liquid leaving the heater, and this would usually occur when the liquid exit temperature was still a few degrees below the saturation temperature.

The periods of the Type I oscillations in water ranged from 20 to 200 seconds.

Since the system could not be stabilized with bulk boiling occurring, pressure drop data could be obtained only for the right hand portion of the curve with liquid flowing throughout the system. The liquid pressure drop from the surge tank to the system exit with the inlet valve wide open is shown in Figure 25 as a function of mass flow rate. Data was taken at various levels of heat input as shown on the figure, and the points fell on one smooth curve. At each level of power input, instability occurred when bubbles appeared in the liquid leaving the heater, and at this point the liquid leaving the heater was still slightly subcooled by an amount which varied from one to seven degrees F. Figure 26 shows the point at which instability occurred for each heat input with the inlet valve wide open.

Type I oscillations with small limit cycles were never observed. As soon as the oscillations commenced, they immediately built up to large amplitude. A typical set of records of the oscillations just after the onset of instability is shown in Figures 27 and 28 for a heat input of 4130 BTU/hr. This behavior suggests that the damping effects which permitted stable operation on part of the negative sloperegion with Freon, and limited the amplitude of the Freon oscillations, were not present in water.

A number of experiments were carried out with partial closure of the inlet valve to determine whether stability could be improved. Up to a 10% reduction in the flow rate at which instability occurred could be obtained with an inlet restriction, but it was never possible to stabilize the system completely, even when the pressure drop across the inlet valve was substantially greater than the pressure drop from the heater inlet to the system exit. This result was in marked contrast with the behavior of the system using Freon 11, which could be stabilized completely with an inlet pressure drop less than 25% of the total pressure drop from the surge tank to the system exit. The principal difference in physical properties between Freon-11 and water was the liquid-to-vapor density ratio. For Freon-11, this quantity was of the order of 300 for the system pressure levels used in the experiments, whereas for water it was approximately 1400. By reducing the size of the exit orifice, it was possible to raise the heater inlet pressure from 18 psia to 60 psia and thus to reduce the liquid-to-vapor density ratio from 1400 to 400. This had no appreciable effect on stability, however, and it was still not possible to stabilize the system with bulk boiling present.

Systematic changes in inlet temperature were made to investigate the effect of subcooling on the onset of instability and the amplitude of the oscillations. As before, it was found that instability commenced when vapor bubbles were observed in the liquid leaving the heater. In general, the liquid temperature leaving the heater was still a few degrees below the saturation temperature at the onset of instability, which suggests that the instability was triggered by the appearance of subcooled boiling. Reduction of the liquid inlet temperature caused a substantial increase in the amplitude of the wall temperature oscillations during the limit cycles, and with inlet temperatures less than 150 degrees F it was necessary to shut off the power as soon as the oscillations commenced, or burnout of the heater tube would occur after a few limit cycles.

A detailed description of the water experiments is given by Mayer [8].

5.4. Type II Oscillations in Water

Type II oscillations were mostly observed in conjunction with Type I oscillations and (on the few occasions when it was possible to operate at very low flow rates without destroying the heater tube) occasionally on their own. The periods of Type II oscillations were of the same order as those measured for Freon-11, ranging from one to four seconds. No systematic study of Type II oscillations in water could be carried out because the system could not be stabilized with bulk boiling occurring, and in the low flow region where pure Type II oscillations occur the tube wall temperatures were too high for safe continuous operation. The general characteristics of Type II oscillations in water appeared to be the same as those observed for Type II oscillations in Freon-11.

6. THEORETICAL STUDIES

6.1. Type I Oscillations

Since the period of Type I oscillations is very much longer than the residence time of a fluid particle in the heater, it seems reasonable to assume that quasi-steady flow conditions prevail in the heater, and that each point in the oscillation corresponds to a steady state operating point on the set of pressure drop curves shown in Fig. 9.

Furthermore, one is tempted to assume that changes in heat transfer coefficient and temperature can be neglected, so that the power input into the fluid remains constant. Analyses using both these assumptions have been carried out and show that the system should become unstable as soon as the slope of the pressure drop versus flow curve attains a very small negative value [9] [10]. For mean flows only slightly smaller than that at which instability starts, large limit cycles ABCD should occur as shown in Fig. 29, with rapid jumps from B to C and D to A.

With water, the system behaves essentially in this manner, but with Freon-11 the system has been found to be much more stable than this analysis would predict. A finite negative slope can be sustained without instability, the amplitude of the cycles builds up very gradually as the mean flow is reduced, and no rapid transitions from one branch of the pressure drop curve to another are observed. Evidently, something is lacking in the first analysis, and a clue to the nature of the omission is derived from the plots of the

Freon limit cycles on the pressure-flow diagram (Fig.11). Since rounded loops are observed, it seems likely that the heat input into the fluid is varying, partly due to the effect of flow rate on heat transfer coefficient, and partly due to changes in wall temperature and fluid temperature.

An analysis which includes these effects has been developed, and is presented below.

6.1.1. System equations.

Let us consider the one-dimensional unsteady flow equations for the system shown schematically in Fig. 30. It is assumed that, during the pressure drop oscillations, the flow changes so slowly that quasi-steady flow conditions prevail in the evaporator i.e., the mass flow rate into the heater is always equal to the mass flow rate out. The dynamic equations governing the system are:

$$^{*}\quad P_1 - P_2 = K_1 Q_1^2 + \rho_\ell \frac{L_1}{A_1} \frac{dQ_1}{dt} \quad \ldots\ldots\ldots\ldots\ldots\ldots (1)$$

where Q_1 is the volume flow rate into the surge tank.

$$P_2 - P_3 = (P_2 - P_3)_s + \rho_\ell \frac{L_2}{A_2} \frac{dQ_2}{dt} \quad \ldots\ldots\ldots\ldots\ldots\ldots (2)$$

$$P_1 - P_3 = \text{constant} \ldots\ldots\ldots\ldots\ldots\ldots\ldots\ldots\ldots (3)$$

---

* Equation numbers start at (1) in each section, since there are many equations and no equation is referred to outside its own section.

where Q_2 is the volume flow rate out of the surge tank, and $(P_2 - P_3)_s$ is the steady flow pressure-drop across the system and is a function of Q_2 and the heat input into the fluid as shown in Fig. 9. The terms in dQ_1/dt and dQ_2/dt represent the pressure-drop required to accelerate the flow. ρ_ℓ is the liquid density, L is the tube length, and A is the cross sectional area.

For the surge tank, the continuity equation may be written as,

$$Q_1 - Q_2 - Q_{ev} = \frac{dV_\ell}{dt} \quad \text{..........................} \quad (4)$$

where Q_{ev} is the rate of loss of liquid volume due to evaporation, and V_ℓ is the volume of liquid in the surge tank.

$$\frac{dV_\ell}{dt} = -\frac{dV_g}{dt} \quad \text{..................................} \quad (5)$$

where V_g is the volume of gas in the surge tank, and

$$Q_{ev} = \frac{\rho_v}{\rho_\ell} \frac{dV_g}{dt} \quad \text{...............................} \quad (6)$$

where ρ_v is the density of saturated vapor. Hence,

$$Q_1 - Q_2 = -\left(1 - \frac{\rho_v}{\rho_\ell}\right)\frac{dV_g}{dt} \quad \text{......................} \quad (7)$$

Also, since the gas in the surge tank is a mixture of air and saturated vapor,

$$P_2 = P_{2a} + P_{2v} \quad \text{.................................} \quad (8)$$

where P_{2a} is the partial pressure of the air and P_{2v} is the partial pressure of the vapor. P_{2v} is constant if the liquid temperature in the tank is constant and thermal equilibrium prevails. Also,

$$P_{2a} V_g = P_{2ao} \ V_{go} = \text{constant} \ldots\ldots\ldots\ldots\ldots\ldots (9)$$

where the subscript "o" refers to steady-state.

Solving for V_g

$$V_g = \frac{P_{2ao} \ V_{go}}{P_{2a}} \ldots\ldots\ldots\ldots\ldots\ldots\ldots\ldots (9a)$$

Differentiating with respect to time

$$\frac{dV_g}{dt} = - \frac{P_{2ao} \ V_{go}}{P_{2a}^2} \frac{dP_{2a}}{dt} \ldots\ldots\ldots\ldots\ldots\ldots (10)$$

To this point the analysis is the same as that given in [10] except that $(P_2 - P_3)_s$ is now a function of power into the fluid as well as Q_2 and the assumption that power into the fluid is constant is not used.

With the inclusion of changing heat input into fluid, we have

$$M \ c_m \frac{dT_w}{dt} = H_o - \ H \ldots\ldots\ldots\ldots\ldots\ldots\ldots\ldots (11)$$

where, M is the mass of the heater element, c_m is the specific heat of the heater metal, T_w is the heater wall temperature, H_o is the power input to the heater, and H is the power input to the fluid. H is given by

$$H = h \ A \ (T_w - T_f) \ldots\ldots\ldots\ldots\ldots\ldots\ldots\ldots (12)$$

where A is the heater surface area, T_f is the saturation temperature of the Freon-11 in the heater and h is the heat transfer coefficient. The assumption is made that h is linearly dependent on Q_2

$$h = h_o \left(b + (1 - b) \frac{Q_2}{Q_{2o}}\right) \qquad (12a)$$

where h_o is the steady state heat transfer coefficient, Q_{2o} is the steady state flow, and b is the fraction of heat transfer independent of the flow rate (pool boiling heat transfer).

6.1.2. Linearized analysis

Using small perturbation analysis it is possible to linearize the differential equations describing the dynamics of the system. Upon finding the characteristic equation of the system from the linearized equations, the onset and frequency of the pressure-drop oscillations can be predicted. The order of the characteristic equation can be reduced by neglecting the inertia terms $\frac{dQ}{dt}$ in equations (1) and (2). This assumption can be made because when these terms are included their effect is found to be negligible for the system tested. Physically, since the period of Type I oscillations is large for this system, the inertia effects of flow rate changes can be neglected. Equation (1) then becomes

$$P_1 - P_2 = K_1 Q_1^2 \qquad (13)$$

Introducing the perturbed values

$$P_1 = P_{1o}$$

$$P_2 = P_{2o} + \delta P_2 \qquad (14)$$

$$Q_1 = Q_{1o} + \delta Q_1$$

where the subscript "o" indicates a steady-state value and the delta term is a small perturbation away from the steady-state. Substituting the perturbed values into equation (13)

$$P_{1o} - \delta P_2 - P_{2o} = K_1 \ (Q_{1o}^2 + 2Q_{1o}\delta Q_1 + \delta Q_1^2).$$

Since,

$$P_{1o} - P_{2o} = K_1 Q_{1o}^2$$

and neglecting second order terms

$$-\delta P_2 = 2K_1 Q_{1o} \delta Q_1 \qquad (15)$$

The terms of δP_2 and δQ_1 can be non-dimensionalized by multiplying both sides of equation (15) by $\dfrac{Q_{1o}}{P_{2o}}$.

Hence,

$$-\delta P_2' = 2 \ e \ \delta Q_1' \qquad (16)$$

where,

$$\delta P_2' = \frac{\delta P_2}{P_{2o}}$$

$$\delta Q_1' = \frac{\delta Q_1}{Q_{1o}}$$

$$e = \frac{P_1 - P_{2o}}{P_{2o}}.$$

For simplicity the primes (′) will not be carried in the remaining parts of the analysis, but all perturbation terms will have been non-dimensionalized.

Performing similar operations to that described above on equations (2), (7), (10), (11), and (12) yields the following equations:

$$\delta Q_1 - \delta Q_2 = \tau_1 \frac{d\ \delta P_2}{dt} \quad \ldots\ldots (17)$$

$$\delta P_2 = m_1\ \delta Q_2 + m_2\ \delta H \quad \ldots\ldots (18)$$

$$\delta H = \delta T_w - n_1\ \delta P_2 + n_2\ \delta Q_2 \quad \ldots\ldots (19)$$

$$\tau_2 \frac{d\ \delta T_w}{dt} = -\ \delta H \quad \ldots\ldots (20)$$

where,

$$\tau_1 = \left(1 - \frac{\rho_v}{\rho}\right) \frac{V_{go}}{Q_o} \frac{P_{2o}}{P_{2ao}}$$

$$\tau_2 = \frac{M\ c_m}{H_o} \left(T_{wo} - T_{fo}\right)$$

$$m_1 = \frac{Q_{2o}}{P_{2o}} \left(\frac{\partial\ (P_2 - P_3)}{\partial Q_2} \right)_o$$

$$m_2 = \frac{H_o}{P_{2o}} \left(\frac{\partial\ (P_2 - P_3)}{\partial H} \right)_o$$

$$n_1 = \frac{P_{2o}}{T_{wo} - T_{fo}} \left(\frac{d\ T_f}{d\ P_2} \right)_o$$

$$n_2 = \frac{Q_o}{h_o} \left(\frac{dh}{d\ Q_2} \right)_o$$

Combining equations (16) and (17)

$$\delta P_2 \left(\frac{1}{2e} + \tau_1 D \right) + \delta Q_2 = 0 \ldots\ldots\ldots\ldots\ldots\ldots\ldots (21)$$

where D is the differential operator with respect to time, $\frac{d}{dt}$.

From equations (18) and (19)

$$\delta P_2 (1 + m_2 n_1) + \delta Q_2 (-m_1 - m_2 n_2) + \delta T_w (-m_2) = 0 \ldots\ldots (22)$$

From equation (20)

$$\delta P_2 (-n_1) + \delta Q_2 (n_2) + \delta T_w (1 + \tau_2 D) = 0 \ldots\ldots\ldots\ldots (23)$$

The characteristic equation of the system is the determinant of the coefficients of equation (21), (22) and (23) and can be shown to be

$$A D^2 + B D + C = 0 \ldots\ldots\ldots\ldots\ldots\ldots\ldots\ldots\ldots\ldots (24)$$

where,

$$A = \tau_1 \tau_2 (m_1 + m_2 n_2)$$

$$B = \tau_1 m_1 + \tau_2 \left(1 + m_2 n_1 + \frac{m_1}{2e} + \frac{m_2 n_2}{2e}\right)$$

and

$$c = \frac{m_1}{2e} + 1$$

The stability criterion of a second order system is that all coefficients of the characteristic equation be positive. It can be shown by rearrangement of the coefficients that the conditions for stability of this system are:

From A,

$$m_1 > - m_2 n_2 \quad \ldots\ldots (25)$$

From B,

$$m_1 > - \frac{\tau_2}{(\tau_1 + \frac{\tau_2}{2e})} \left(1 + m_2 n_1 + \frac{m_2 n_2}{2e}\right) \quad \ldots\ldots (26)$$

From C,

$$m_1 > - 2e \quad \ldots\ldots (27)$$

Physically interpreted, m_1 is the normalized slope of the pressure drop versus mass flow rate curve. When the coefficient B (the damping coefficient term) goes to zero the frequency of the oscillations can be calculated as

$$\omega^2 = \frac{C}{A} = \frac{\frac{m_1}{2e} + 1}{\tau_1 \tau_2 (m_1 + m_2 n_2)} \quad \ldots\ldots (28)$$

An examination of the usefulness and accuracy of equations (25) to (28) for predicting the onset and frequency of pressure-drop oscillations was made for a power level of 1170 BTU/hr. This was done by taking several points on the steady-state curve shown in Fig. 11 and investigating the stability of the system at these points. Several system parameters defined for equations (16) to (20) were needed for this to be done and were obtained from the experimental data and thermodynamic property charts. A value for V_{go} of 53 cubic inches was estimated based on visual observation of the liquid level during the experiments. The product $M \cdot c_m$ was obtained from a transient heating experiment and found to be approximately 0.09 BTU/^{o}F. The parameters obtained for several flow rates along the above mentioned power curve and the results after substituting them in equations (25) to (28) are tabulated in the Appendix A. A point corresponding to a flow rate of 2.53 lbs./min. was first investigated and found to be stable. This was to be expected since the point is on the upper positive slope portion of the heater power input curve.[1] Stability of the system was investigated for a second and a third point, both on the negative slope portion of the steady-state curve. The first of these points (2.4 lbs./min. flow rate) was found to be stable and the second unstable (2.3 lbs/min.). The stability of a fourth point (2.35 lbs./min.) was investigated and found to be near the onset of pressure-drop oscillations. This was determined when both sides of equation (26) became nearly equal. In the four cases described, conditions (25) and (27) were always satisfied, meaning that the coefficients A and C of equation (24) were positive. The unstable conditions were indicated when condition (26) was not satisfied, making the coefficient B of the characteristic equation negative. If either A or C had gone negative the system

---

1 Remember to include the pressure drop from the surge tank to the inlet pressure transducer shown in fig. 9.

would have been described as statically unstable and would not have given rise to an oscillatory type of instability. With just the damping coefficient term (B) going negative, one can expect the system to oscillate about a steady-state value as was experimentally observed.

The frequency of the oscillations at onset was calculated using equation (28) and found to be approximately one third of the experimentally observed frequency. There is no apparent reason for this especially since the onset of oscillation is closely predicted by the analysis. However, the pressure drop slope m_1 is changing very rapidly in the vicinity of the point where instability occurs, so that large errors in estimating the other parameters could be made without much change in the predicted flow rate at the stability boundary. These errors would, however, have a substantial effect on the predicted period.

6.1.3. Non-linear analysis.

To obtain limit cycles, it is necessary to solve equations (1) to (12a) with time as the independent variable, and without introducing linearising assumptions for the behavior of the pressure drop as a function of flow rate and heat input to the fluid. This has been done, using an EAI TR-10 and a TR-20 analogue computer connected together to give the desired number of amplifiers. The Freon-11 pressure drop characteristics were represented using non-linear analog components, and over the flow range 1.0 to 3.5 lbs. per minute, and the power range 1050 to 1300 BTU per hour the Freon experimental values were reproduced within ±5%. The analog pressure drop characteristics are shown in Figure 31a. It was not possible to reproduce the positive slope region of the pressure drop curve which occurs at low flow rates, but since many of the limit cycles are confined to the flow range 1.0 to 3.0 lbs. per minute, this was not considered to be a serious disadvantage. The saturation temperature T_f was represented by the expression $T_f = 115 + 1.69\ P_2$.

The procedure followed was the same as that used in the experiments, that is to say the system was operated at a constant power input, and first stabilized at a flow rate to the right of the "valley" in the pressure drop curve. The value of K_1 was then increased slowly, to reduce the mean flow rate, and the dynamic behavior of the system was observed. When limit cycles occurred they were plotted on the pressure drop versus flow rate plane using an X-Y plotter.

It was found that the system dynamics were extremely sensitive to the values of b and h_o used, and good reproduction of the experimental limit cycles was only obtained within a narrow range of values. Figure 31b shows three Freon limit cycles at a power level of 1170 BTU/hr. These may be compared with the experimental limit cycles plotted in Figure 11, and it can be seen that the behavior is very similar. The values used for the system parameters are listed below.

$b = 0.1$

$Mc_m = 0.07$ BTU/°F

$h_o = 32.8$ BTU/hr/in^2/°F

$V_{go} = 53$ in^3

The value of h_o agrees well with the value observed experimentally for onset of oscillations at $\dot{m} = 2.5$ lbs/min and $H_o = 1170$ BTU/hr as does the low value of b if h_o and b are calculated from Figure 10. This suggests that the effect of flow rate on heat transfer shown in Figure 10 is real, and not produced by thermocouple errors.

The periods of the oscillations were longer than those experimentally observed, ranging from 100% greater at onset, to 40% longer at lower flow rates. Apart from the shape of the pressure drop curve, three variables have an effect on the period. These are V_{go}, Mc_m, and h_o. It can be seen from the linearized analysis that the period is proportional to the square root of their product, so that the experimental periods could be reproduced by reducing all of these variables by about 25% from the values listed above. Since considerable uncertainties existed in the determination of these quantities experimentally, such a variation is within the bounds of possibility. In addition, the analog pressure drop curves were much flatter near the minimum than the corresponding experimental curves, and it was observed that the computed variables changed very slowly in this portion of the cycle. In consequence, the shape errors may also bear some responsibility for the longer computed period.

The system was found to be stable for flows corresponding to the right hand region of positive slope on the pressure drop curves, in agreement with the experiments.

With water as the test fluid, it was not possible to stabilize the system with bulk boiling occurring, and therefore the data needed for comparison with theory could not be obtained. The behavior of the system using water is consistent with that predicted by analysis when a volume of non-condensible gas is present in the heater [9]. This suggests that the lack of thermal equilibrium between the steam and liquid water leaving the heater may have been responsible for the poor stability of the system with water as the test fluid.

6.2. Type II Oscillations

Type II oscillations have been observed by many investigators, using a variety of fluids [13] [14] [15], and the physical nature of these oscillations is now fairly well understood. They are caused by the dynamic interaction between pressure gradient, flow rate and mass storage within the heater, and can occur whenever a sufficiently large volume of vapor is generated in a flowing liquid. Pioneering work in analyzing these oscillations was carried out by Wallis and Heasley [16], who studied oscillations in a fluid with constant heat input and unity slip ratio, by Quandt [17], who presented an approximate integral method for studying stability, and by Meyer and Rose [18] and Jones [19] who developed methods suitable for use with digital computers.

The major difficulty encountered in predicting the occurrence of these oscillations is their dependence on all the parameters which are themselves so difficult to predict in two phase flows, such as void fraction, heat transfer coefficients, and pressure drop. Not only is it necessary to know the values of these quantities, but for a stability analysis their derivatives with respect to the other variables are also needed. These are extremely difficult to predict or measure. For this reason, the analyses of Type II oscillations carried out during the present investigation have been of the parametric type, concerned with discovering the influence of the basic variables on heater stability rather than with attempting to predict the stability of a given system directly.

Two analog computer studies of Type II oscillations were carried out at the beginning of the research program, one on systems with partial boiling, and the other on systems with superheat. The equations for each case are quite similar, but the system geometries were somewhat different, so that the analyses will be discussed separately.

6.2.1. Analog computer study with partial evaporation

The system under consideration is shown in Fig. 32. Liquid (subcooled or saturated) flows through an entrance duct and a valve to an evaporator in which partial evaporation occurs. The mixture of liquid and vapor then flows out through a second orifice. The pressure drop across the system is constant with time. Gravitational effects are neglected.

For analysis, the evaporator is broken up into seven pieces of equal volume and a continuity equation is written for each lump. The flow is assumed to be homogeneous and without slip. According to Meyer and Rose, this assumption leads to somewhat pessimistic estimates of system stability and is therefore on the conservative side.

For the n^{th} lump, as shown in Fig. 33, the continuity equation may be written as

$$\rho_n (UA)_n - \rho_{n+1} (UA)_{n+1} = \frac{V_n}{2} \frac{d}{dt} (\rho_n + \rho_{n+1}) \ldots\ldots\ldots \tag{1}$$

where ρ is density, U is flow velocity, and A is flow area. V_n is the volume of the lump. The average density is assumed to be the arithmetic mean of the inlet and outlet densities.

Dividing both sides of equation (1) by $\rho_{8s}(UA)_{8s}$, where ρ_{8s} is the density leaving the heater at steady state and $(UA)_{8s}$ is the volume flow rate leaving the heater at steady state, we obtain

$$r_n u_n - r_{n+1} u_{n+1} = \frac{V_n}{2(UA)_{8s}} \frac{d}{dt} (r_n + r_{n+1}) \ldots\ldots (2)$$

where

$$r = \frac{\rho}{\rho_{8s}}$$

Let $$u = \frac{(UA)}{(UA)_{8s}}$$

$$\frac{V_n}{2(UA)_{8s}} = \frac{V_t}{14(UA)_{8s}} = \tau$$

where V_t is the total heater volume. Then

$$r_n u_n - r_{n+1} u_{n+1} = \tau \frac{d}{dt} (r_n + r_{n+1}) = \frac{d}{dT} (r_n + r_{n+1}) \ldots\ldots\ldots\ldots (3)$$

where $T = t/\tau$

At steady state

$$r_n u_n = r_{n+1} u_{n+1} = r_8 u_8 = 1$$

since $r_8 = 1$ and $u_8 = 1$ at steady state.

The heat transfer into the fluid is assumed to be dependent only on the mass flow rate, and to be of the form shown in Fig. 34:

$$H_n = b H_{ns} + H_{ns}(1-b)\frac{[r_n u_n + r_{n+1} u_{n+1}]}{2} \ldots\ldots\ldots (4)$$

where H_n is the heat input into the fluid in the n^{th} lump per unit time, H_{ns} is the heat input at steady state, and b is the fraction of the heat input which is independent of mass flow rate. When b = 1, the heat input is time independent, corresponding to the cases of constant power input with small metal mass, or constant wall temperature with the heat-transfer coefficient independent of mass flow rate. When b = o, the heat transfer is directly proportional to mass flow rate. Therefore, b may range from zero to unity and can be evaluated experimentally for a given system or predicted approximately from available correlations of boiling heat transfer.

Experimental studies of the effects of forced convection and vapor quality on boiling heat transfer [20, 21] have shown that for conditions with up to 90 percent vapor by mass, the heat-transfer coefficient is often almost independent of quality. Equation (4) is therefore a reasonable representation of the boiling heat transfer with constant wall temperature for many systems.

The volume rate of vapor generation in the lump is given by the following equation:

$$Q_n = \frac{v_{fg}}{h_{fg}} \left[H_n - \rho_n (UA)_n c_\ell \Delta T_{sub} \right] \quad \ldots\ldots\ldots\ldots (5)$$

where v_{fg} and h_{fg} are the changes in specific volume and enthalpy respectively in going from saturated liquid to saturated vapor, c_ℓ is the liquid specific heat, and ΔT_{sub} is the degree of inlet subcooling. Changes in vapor density with pressure are neglected.

Substituting (4) in (5)

$$Q_n = \frac{v_{fg}}{h_{fg}} \left\{ bH_{ns} + \frac{(1 - b)}{2} H_{ns} \left[r_n u_n + r_{n+1} u_{n+1} \right] \right. \quad \ldots\ldots\ldots\ldots\ldots\ldots (6)$$

$$\left. - \rho_n (UA)_n c_\ell \Delta T_{sub} \right\}$$

Dividing both sides by $(UA)_{8s}$ and rearranging

$$q_n = q_{no} \left\{ b + \frac{(1 - b)}{2} \left[r_n u_n + r_{n+1} u_{n+1} \right] - cr_n u_n \right\} \quad \ldots\ldots\ldots\ldots\ldots\ldots (7)$$

where

$$q_n = \frac{Q_n}{(UA)_{8s}}$$

$$q_{no} = \frac{v_{fg} H_{ns}}{h_{fg} (UA)_{8s}}$$

$$c = \frac{c_\ell \Delta T_{sub} \rho_{8s} (UA)_{8s}}{H_{ns}}$$

and is the fraction of the heat input into the lump that is used to remove subcooling at steady state.

At steady state

$$q_{ns} = q_{no} (1 - c) \quad \ldots\ldots\ldots\ldots\ldots\ldots\ldots\ldots\ldots (8)$$

Since, in general, the heat required to remove the subcooling is very much less than the heat required to evaporate the same amount of liquid, it is assumed that the subcooling is removed in the first lump of the evaporator. The subcooling term therefore is used only in the first lump. For the lumps with no subcooling (i.e. for all the lumps after the first lump) equation (7) reduces to

$$q_n = q_{no} \left\{ b + \frac{(1 - b)}{2} \left[r_n u_n + r_{n+1} u_{n+1} \right] \right\} \qquad (9)$$

Since the volume of the lump is constant and compressibility effects are neglected, the volume flow rate out of the lump is greater than the volume flow rate into the lump by the amount of vapor generated, i.e.

$$(UA)_{n+1} - (UA)_n = Q_n \qquad (10)$$

Dividing both sides by $(UA)_{8s}$

$$u_{n+1} - u_n = q_n \qquad (11)$$

At steady state, if the heat input to each lump is the same, then

$$u_{1s} = u_{8s} - 7q_o + c\, q_o$$

where

$$q_o = \frac{Q_o}{(UA)_{8s}}$$

i.e.

$$u_{1s} = 1 - q_o\, (7 - c) \qquad (12)$$

and

$$r_1 = r_{1s} = \frac{1}{u_{1s}} = \frac{1}{1-q_o\, (7-c)} \qquad (13)$$

where r_1 is the ratio of liquid density to exit density at steady state, and is a constant even when the flow oscillates since the inlet density is constant.

The overall pressure drop ΔP_{0-9} is the sum of the orifice and heater pressure drops, and the inertial pressure drop. For the first orifice

$$\Delta P_{0-1} = K_1 \rho_1 U_1^2 \qquad (14)$$

For the second orifice

$$\Delta P_{8-9} = K_2 \rho_8 U_8^2 \qquad (15)$$

assuming that a relationship of this type is still useful for two-phase flow.

For a constant-area heater with an effective friction factor f and a linear velocity distribution from inlet to outlet

$$\Delta P_{1-8} = \frac{4fL}{D}\left[\frac{\rho_1 U_1^2}{4} + \frac{\rho_8 U_8^2}{4}\right] + \left[\rho_8 U_8^2 - \rho_1 U_1^2\right] \qquad (16)$$

where the first term is the friction pressure drop and the second is the momentum pressure drop.

Rearranging terms:

$$\Delta P_{1-8} = \rho_1 U_1^2 \left[\frac{fL}{D} - 1\right] + \rho_8 U_8^2 \left[\frac{fL}{D} + 1\right] \qquad (17)$$

Since $\rho_1 U_1 = \rho_8 U_8$ in steady flow for a constant-area heater, it follows that for overall density ratios of 20 or more, the first term of equation (17) is small in comparison with the second term and can be neglected.

Assuming for simplicity that all the inertia is lumped on the inlet side of the system, the dynamic pressure drop associated with the unsteady flow is obtained from the following equation:

$$\Delta P_d = \rho_1 \ (\Sigma\ L/A) \ \frac{d(UA)_1}{dt} \ \ldots\ldots\ldots\ldots\ldots\ldots\ldots\ldots (18)$$

where $\sum$ L/A is summed for all the ducting in the system. Then the pressure-drop equation is

$$\Delta P_{0-9} = \Delta P_{0-1} + \Delta P_{1-8} + \Delta P_{8-9} + \Delta P_d \ \ldots\ldots\ldots\ldots\ldots (19)$$

$$\Delta P_{0-9} = \left[K_1 + \frac{fL}{D} - 1\right]\rho_1 U_1^2 + \left[K_2 + \frac{fL}{D} + 1\right]\rho_8 \ U_8^2$$

$$+ \rho_1 \ (\Sigma\ L/A) \ \frac{d(UA)_1}{dt} \ \ldots\ldots\ldots\ldots\ldots\ldots\ldots\ldots (20)$$

Normalizing the right-hand side

$$\Delta P_{0-9} = K_3 r_1 u_1^2 + K_4 r_8 u_8^2 + \rho_1 (UA)_{8s} \ (\Sigma\ L/A) \ \frac{du_1}{dt} \ \ldots. (21)$$

where K_3, K_4 are new constants. The same expression is obtained for a heater of varying area if its resistance is approximated in terms of entrance and exit conditions.

At steady state

$$r_1 \ u_1 = 1, \ r_8 = 1, \ u_8 = 1, \frac{du_1}{dt} = 0$$

$$\Delta P_{0-9} = \frac{K_3}{r_1} + K_4 \quad \ldots\ldots (22)$$

Dividing (21) by ΔP_{0-9}, which is constant

$$1 = \left[\frac{K_3}{\frac{K_3}{r_1} + K_4}\right] r_1 u_1^2 + \left[\frac{K_4}{\frac{K_3}{r_1} + K_4}\right] r_8 u_8^2$$

$$+ \frac{\rho_1 (UA)_{8s} (\Sigma\, L/A)}{\Delta P_{0-9}} \frac{du_1}{dt} \quad \ldots\ldots (23)$$

Hence

$$1 = \left[\frac{K_3}{K_3 + K_4 r_1}\right] (r_1 u_1)^2 + \left[\frac{K_4}{\frac{K_3}{r_1} + K_4}\right] r_8 u_8^2$$

$$+ \tau_d \frac{du_1}{dt} \quad \ldots\ldots (24)$$

where

$$\tau_d = \frac{\rho_1 (UA)_{8s} (\Sigma\, L/A)}{\Delta P_{0-9}}$$

or

$$1 = y(r_1 u_1)^2 + (1-y) r_8 u_8^2 + \tau_d \frac{du_1}{dt} \quad \ldots\ldots (25)$$

where y is the fraction of the total pressure drop attributable to the upstream ducting at steady state. For high density ratios, y is equal to $\Delta P_{0-1}/\Delta P_{0-9}$ at steady state.

Making use of the relation $T = t/\tau$

$$\frac{du_1}{dT} = \frac{\tau}{\tau_d}\left[1 - y\ (r_1 u_1)^2 - (1-y)\ r_8 u_8^2\right] \qquad \text{..........(26)}$$

where

$$\frac{\tau}{\tau_d} = \frac{V_t\ \Delta P_{0-9}}{14(\Sigma\ L/A)\rho_1 (UA)^2_{8s}}$$

The analog-computer block diagram for equations (3), (7), (9), (11), and (26) is shown in Fig. 35. The conventional symbols are used for components with A denoting a summer, I an integrator, M a multiplier, and S a constant-voltage source.

The block diagram shown in Fig. 35, representing equations (3), (7), (9), (11), and (26), has been programmed on a Philbrick analog computer. The equations were not linearized. In operation, the system parameters were adjusted until small oscillations of constant amplitude were observed, and the parameters were recorded at this point.

Typical results of a stability study are shown in Fig. 36 for an overall density ratio of 80 and zero inlet subcooling, and in Fig. 37 for the same overall density ratio and 7% of the total heat input used to remove subcooling. Each curve shows the inlet fractional pressure drop y at the stability boundary versus τ/τ_d for the given values of r_1, b, and c. With a larger value of y than that at the stability boundary, the system is stable, with a smaller value the system is unstable. It is apparent from the curves that the inertia factor has some effect on stability, large values of τ_d tending to provide damping. However, for most practical systems the operating point is near the right hand end of the curve and the inertia of the liquid column can be doubled or halved without producing much effect on predicted stability. Comparison of Figs. 36 and 37 shows that an increase in subcooling exerts a substantial destabilizing effect when the overall density ratio is kept constant. This would, of course, require an increase in heat input to the fluid as the subcooling is increased. With constant heat input, increasing the subcooling produces a decrease in exit quality and hence in overall density ratio and this effect would counteract to some extent the destabilizing effect of increased subcooling.

Lowering the value of b corresponds to increasing the dependence of the heat transfer coefficient on mass flow rate, and it has a strong beneficial influence on stability.

A more detailed presentation of the analog results for partial boiling is given in a paper by Stenning and Veziroglu [5].

The qualitative effects of inertia, mass flow rate, and subcooling are all as one would expect from physical considerations. The fluid inertia appears as a damping factor in the equations, resisting changes in flow rate. High inertia (low τ/τ_d) is therefore desirable to suppress instability. Since the prime cause of instability is the interaction between flow rate and fluid density distribution within the heater, any effect which helps to keep the density constant as the flow varies is desirable, and vice-versa. Hence, a small value of b is helpful because a transient increase in flow is accompanied by a transient increase in heat input which offsets the reduction in exit quality that would occur if the heat input stayed constant. Subcooling produces the opposite effect, because an increase in flow requires an increase in the heat absorbed to remove subcooling. The exit quality drops, the density throughout the system rises, and the resulting changes in pressure drop distribution aid instability.

In the experimental studies of Type II oscillations with partial evaporation, the measured value of b appeared to be approximately 0.6 at the stability boundary for all experiments [22]. For this value of b, one would expect that with density ratios in the range of 25 to 250 and inlet subcooling absorbing up to 40% of the total heat input before boiling commences, the inlet pressure drop at the stability boundary might run as high as 60% of the total pressure drop from the surge tank to the exit. Instead, the system was extremely stable and the inlet pressure drop required for stability never exceeded 16% of the total. The experiments of Berenson with Freon-113 [13] show much better agreement with the analog study, with a y of

0.5 required to stabilize a system with a density ratio of 150.

For the analog study, a unity slip factor was assumed, and the frictional pressure drop was assumed to be proportional to the mass flow squared and inversely proportional to the mixture density. This is a fairly crude assumption, but should not be notably worse for Freon-11 than for Freon-113. For reasonable agreement between the analog predictions and the Freon-11 experiments, a value of b near 0.2 would be required during transients.

Comparison of the analog results with the subcooling experiments also raises some questions. Figure 38 shows the type of stability map that would be predicted by the analog study for varying inlet temperature, and this may be compared with Fig. 24. In both cases, the stability boundary is shifted to the right as power increases, and has a positive slope at low values of subcooling. The experiments, however, show an unexpected sharp S shaped bend in the stability boundary for which no explanation is available.

Time periods of Type II oscillations predicted by the analog studies were of the order of 1.5 to 2.0 times the residence time of a particle in the heater, and this result is in rough agreement with the experimental values shown in Fig. 19, for which a least squares fit is given by the relation $\tau_o = 2.29\ \tau_{ie}$. where τ_o is the time period of the oscillation and τ_{ie} is the computed residence time assuming that the liquid and vapor travel with equal velocity. The actual residence time would be larger than τ_{ie} due to real slip effects.

6.2.2. Analog computer study with superheat

This study was undertaken with the objective of developing some understanding of the additional variables which could be expected to have an effect on system stability when the vapor was superheated. At the time that the study was carried out, no experimental data had yet been taken on the test rig, and the only test results available with superheat were those presented by Ellerbrock for liquid hydrogen [23]. The analog study was therefore based on a geometry similar to that used in the hydrogen experiments, and the values of the parameters covered a range which was useful for comparison with hydrogen experiments and with Freon-11 experiments.

The system considered is shown in Figure 39. Liquid, subcooled or saturated, flows through an entrance duct and a valve to a heater. In the heater the liquid is completely evaporated and the vapor is superheated. Then the superheated gas flows into an exit plenum and out of a nozzle. The total pressure drop across the system is constant. Gravitational effects are neglected.

For analysis, the system is broken up into five segments or lumps - one for the inlet ducting including inlet valve, two equal segments for the boiler section of the heater, one for the superheater section of the heater, and one for the exit plenum. The number of segments was limited to five by the nonlinear components available in the analog computer used - an EAI TR-48 computer. It was felt that at least two segments would be necessary to evaluate the dynamics of the boiler section where instability originates. In addition, the number of available computer elements would only permit the study of a homogeneous and slipless flow.

The equations of continuity and heat transfer for the boiling section were set up in the same manner as the corresponding equations for the analysis of system stability with partial evaporation. Additional continuity equations were written for the superheat section and the exit plenum, and the effectiveness of the superheat section was assumed to be high so that the temperature leaving the superheat section could be considered constant [24].

For each set of operating conditions the inlet pressure drop was adjusted until the system was on the edge of instability, and the magnitude of the inlet pressure drop was then recorded. A typical set of outputs at the stability boundary is shown in Fig. 40. The symbol u is the ratio of the local velocity to steady state inlet velocity, and r is the ratio of local density to inlet density. The phase shift between the inlet mass flow rate and the pressure entering the heater was 180 degrees, in agreement with the experiments (Fig. 20).

The numerical results of the study were quite similar to those obtained with partial evaporation. To stabilize the system with overall density ratios in the range 200 to 400, and with an inlet pressure drop not greater than 20% of the overall pressure drop, a value of b of approximately 0.2 was required.

In both the NASA experiments with hydrogen [23] and the Freon-11 superheat experiments described in section 5.3, stable operation was obtained with the above density ratios and with very small inlet pressure drop. In both of these cases, therefore, it is necessary to assume a very low value for b during flow transients to match the analog predictions with the experiments.

6.2.3. Frequency response analysis

In the preceding sections, it was found that the analog computer results could be matched with the measured inlet pressure drop required for stability with Freon-11 only if a value of approximately 0.2 was assumed for the parameter b. The parameter b is in fact equal to $[1 - \frac{\dot{m}}{q} \frac{\partial q}{\partial \dot{m}}]$ where $\dot{m}$ is the mass flow rate and q is the heat flux, so that a small value of b corresponds to a strong dependence of heat transfer on flow rate. The steady state measurements of b near the stability boundary of Type II oscillations suggested that b could not be smaller than 0.6.

It was thought that two assumptions used in the analog simulation might lead to conservative predictions of instability and help to explain the discrepancy between theory and experiment. The subcooled region was represented by a very simple lumped parameter analysis, and the liquid and vapor velocities were assumed to be equal at each station in the heater. With the limited analog computer facilities available it was not possible to improve these two features of the simulations, but a linearized frequency response analysis could be made which would treat both the subcooled region and the vapor slip correctly, and would show whether these two factors could explain the failure of the analog results to match the experiments using the measured steady state value of b.

Consider a system consisting of an inlet restriction followed by a single tube heater in which boiling occurs. Let the pressure entering the restriction be p_a, the pressure between the restriction and the boiler be p_b, and the pressure after the boiler be p_c (constant). Let the flow rate through the restriction and into the boiler be $\dot{m}$ lbs./second.

If the pressure p_a undergoes a small perturbation δp_a, then the effects on the system can be understood from the block diagram shown in Figure 41. If the perturbation in p_b is δp_b, then a perturbation in flow rate $\delta\dot{m}$ is generated by the difference between δp_a and δp_b. In particular, if the pressure drop across the inlet restriction is given by the relation

$$p_a - p_b = K\dot{m}^2 \quad \ldots\ldots\ldots\ldots\ldots\ldots\ldots\ldots\ldots\ldots (1)$$

then for small perturbations away from steady state we have

$$2K\dot{m} \bullet \delta\dot{m} = \delta p_a - \delta p_b$$

or $$\delta\dot{m} = \frac{1}{2K\dot{m}} (\delta p_a - \delta p_b) \qquad (2)$$

The perturbation in $\delta\dot{m}$ generates a change in the pressure drop $(p_b - p_c)$ across the heater and hence, since p_c is constant, it also generates a perturbation in δp_b. The total effect on the system is shown in the feedback loop of the block diagram.

Now let δp_a undergo a small sinusoidal oscillation with frequency ω radians per second. δp_b and $\delta\dot{m}$ will also undergo sinusoidal oscillations of frequency ω, but with different amplitude and phase. $\delta\dot{m}$ is in phase with $(\delta p_a - \delta p_b)$. δp_b is related to $\delta\dot{m}$ through the transfer function of the heater $G(i\omega)$. If the phase difference between δp_b and $\delta\dot{m}$ is 180°, it then becomes possible for the oscillations to be self-sustaining even with δp_a equal to zero. If δp_a is zero, and the oscillations continue, then we must have

$$\delta\dot{m} = -\frac{1}{2K\dot{m}} \delta p_b \qquad (3)$$

that is to say, the phase difference between δp_b and $\delta\dot{m}$ must be 180° and

$$\left|\frac{\delta p_b}{\delta\dot{m}}\right| = |G(i\omega)| = 2K\dot{m} = \frac{2(p_a - p_b)}{\dot{m}} \qquad (4)$$

The frequency of the self-sustaining oscillations will correspond to the value of ω which produces 180° phase shift. If $|G(i\omega)|$ is less than $2K\dot{m}$, the oscillations will damp out and the system will be stable. If $|G(i\omega)|$ is greater than $2K\dot{m}$, the oscillations will grow in amplitude until they are limited in size by non-linear effects. We are interested in finding out whether self-excited oscillations can occur with p_a constant, and therefore wish to study the transfer function $G(i\omega)$, especially in the region where 180° phase shift occurs.

The heater is considered to be a single tube of constant diameter D and length L. Liquid enters in a subcooled state, and is brought to the saturation temperature in the length L_s. For the purposes of the analysis, the remainder of the tube $(L - L_s)$ is broken up into n equal lengths, and conditions calculated at each point (see Fig. 42). In the steady state, the heat input is assumed to be uniform along the tube. Average values for saturated liquid and vapor densities are used, and in the boiling region the fluid is treated as a mixture of saturated liquid and vapor with the liquid and vapor moving at different velocities (slip flow model).

The enthalpy increase h_t BTU/lb. in the heater is given by

$$h_t = \frac{H}{\dot{m}} \text{ BTU/lb.} \quad \ldots\ldots\ldots\ldots\ldots\ldots\ldots\ldots (5)$$

where H is the heat input BTU/sec.

The enthalpy increase to the boiling point h_s is found from

$$h_s = c_\ell(T_s - T_i) \quad \ldots\ldots\ldots\ldots\ldots\ldots\ldots\ldots (6)$$

where c_ℓ is the liquid specific heat, T_s is the saturation temperature and T_i is the inlet temperature.

The subcooled length is L_s, where

$$L_s = (\frac{h_s}{h_t}) \quad L \qquad \text{feet} \ldots\ldots\ldots\ldots\ldots\ldots\ldots\ldots (7)$$

The length of each boiling segment is ΔL.

$$\Delta L = \frac{L - L_s}{n} \qquad \text{feet} \ldots\ldots\ldots\ldots\ldots\ldots\ldots\ldots (8)$$

The enthalpy rise in each boiling segment is Δh.

$$\Delta h = (\frac{h_t - h_s}{n}) \quad \text{BTU/lb} \ldots\ldots\ldots\ldots\ldots\ldots\ldots\ldots (9)$$

The increment in quality in each boiling segment is Δx.

$$\Delta x = \frac{\Delta h}{h_{fg}} \ldots\ldots\ldots\ldots\ldots\ldots\ldots\ldots\ldots\ldots\ldots (10)$$

where h_{fg} is the latent heat of vaporisation.

The quality x_j at the end of the j^{th} boiling segment is obtained from the relation

$$x_j = j \ \Delta x \ldots\ldots\ldots\ldots\ldots\ldots\ldots\ldots\ldots\ldots\ldots (11)$$

Let A_o be the tube cross sectional flow area, let A_f be the liquid flow area and let A_g be the vapor flow area. Let $\beta = A_g/A_o$.

From Von Glahn's correlation for void fraction [25],

$$\frac{1}{x} = 1 - (\frac{\rho_f}{\rho_g})^{0.67} \left[1 - (\frac{1}{\beta})^{(\rho_f/\rho_g)^{0.1}}\right] \ldots\ldots\ldots (12)$$

where ρ_f is the saturated liquid density, ρ_g is the saturated vapor density.

Solving equation (12) for β, we obtain

$$\beta = [1 - (\frac{\rho_g}{\rho_f})^{0.67} \{1 - x^{-1}\}]^{-A} \quad \ldots\ldots\ldots\ldots\ldots (13)$$

where $A = (\rho_g/\rho_f)^{0.1}$

This equation can be used to obtain the void fraction β at the end of each boiling segment in the steady state.

The local mixture quality x is given by the equation

$$x = \frac{\rho_g\ v_g\ A_g}{\rho_f\ v_f\ A_f + \rho_g\ v_g\ A_g} \quad \ldots\ldots\ldots\ldots\ldots\ldots\ldots (14)$$

where v_f, v_g are the liquid and vapor velocities.
Let $s = v_g/v_f$.

$$A_o = A_f + A_g \quad \ldots\ldots\ldots\ldots\ldots\ldots\ldots\ldots\ldots\ldots\ldots (15)$$

Solving for s in terms of x, β, we obtain

$$s = \frac{x\ (\rho_f/\rho_g)[1 - \beta]}{\beta\ [1 - x]} \quad \ldots\ldots\ldots\ldots\ldots\ldots\ldots\ldots (16)$$

Equation (16) is used to calculate the slip ratio s at each station in the boiling region. The ratio s is assumed to remain constant at each point when oscillations occur. The liquid velocity v at inlet to the heater is given by the expression

$$v = \frac{\dot{m}}{0.785\ \rho_f D^2} \quad \ldots\ldots\ldots\ldots\ldots\ldots\ldots\ldots\ldots\ldots (17)$$

From continuity requirements, at each axial station in steady flow

$$\dot{m} = \rho_f \, v_f \, A_f + \rho_g \, v_g \, A_g \quad \ldots\ldots\ldots\ldots\ldots\ldots\ldots\ldots (18)$$

$$\rho_f \, v \, A_o = \rho_f \, v_f \, (A_o - A_g) + \rho_g \, s \, v_f \, A_g \quad \ldots\ldots\ldots (19)$$

Let $v_f/v = u$. Dividing by $\rho_f \, v \, A_o$ and solving for u, we obtain

$$u = [1 - \beta(1 - s\rho_g/\rho_f)]^{-1} \quad \ldots\ldots\ldots\ldots\ldots\ldots\ldots (20)$$

where u is the ratio of the liquid velocity at any point in the boiling region to the liquid velocity at the heater inlet. The ratio u is calculated at each station in the boiling region.

The objective of the analysis is to give a simple and general method for evaluating the stability of an evaporator using any fluid. In view of the uncertainties inherent in all schemes for computing pressure drop in two-phase flow, it was decided to use a simple method which could be made to fit the data for any given configuration fairly well by adjusting the coefficients.

The pressure drop in the heater can be regarded as the sum of the frictional pressure drop, the pressure drop required to increase the momentum of the mixture as it passes through the heater, and the pressure drop across the exit restriction (if any).

In single phase flow, the frictional pressure drop and the pressure drop through an orifice are proportional to the quantity ($\rho v^2/2$) which is equal to (Momentum/2A). The assumption is made in this analysis that the same relationship can be used in two-phase flow.

In any boiling flow segment, let the entry conditions be given the subscript (j-1) and the exit conditions the subscript j.

The frictional pressure drop across the element is found from the relation

$$\Delta p_f = 4f \frac{\Delta L}{D} \frac{(\text{Exit momentum + Inlet momentum})}{4\, A_o\, g_c} \quad \ldots\ldots (21)$$

where Δp_f is the frictional pressure drop

$$\text{Momentum} = \rho_f\, v_f^2\, A_f + \rho_g\, v_g^2\, A_g$$

$$\text{Momentum} = \rho_f\, v_f^2\, (A_o - A_g) + \rho_g\, s^2\, v_f^2\, A_g$$

$$\text{Momentum} = \rho_f\, v_f^2\, A_o\, [1 - \beta + \beta\, s^2\, \rho_g/\rho_f] \quad \ldots\ldots (22)$$

$$= \rho_f\, v^2\, A_o\, R \quad \ldots\ldots (23)$$

$$\text{where } R = u^2\, [1 - \beta\, (1 - \rho_g/\rho_f\, s^2)] \quad \ldots\ldots (24)$$

Substituting (23) in (21) we obtain

$$\Delta p_{fj} = f \frac{\Delta L}{D} \frac{\rho_f\, v^2}{g_c} [R_j + R_{j-1}] \quad \ldots\ldots (25)$$

The frictional pressure drop in the subcooled region Δp_{fs} is equal to $4f \frac{L_s}{D} \frac{\rho_f v^2}{2g_c}$.

Summing the frictional pressure drops for the entire heater, we obtain

$$(\Delta p_f)_{total} = f \frac{\Delta L}{D} \frac{\rho_f v^2}{g_c} [2 \frac{L_s}{\Delta L} + R_o + R_n + \sum_{j=1}^{n-1} 2R_j] \ldots\ldots (26)$$

where R_o is the value of R entering the first boiling segment and is equal to unity.

The pressure drop due to acceleration of the fluid from the heater inlet to the heater exit is given by the expression

$$\Delta p_a = \frac{1}{A_o g_c} [\text{Momentum leaving heater} - \text{momentum entering heater}] \ldots (27)$$

Substituting the expressions for momentum in equation (27) we obtain

$$\Delta p_a = \frac{\rho_f v^2}{g_c} [R_n - 1] \ldots\ldots (28)$$

The pressure drop across the exit restriction is also assumed to be proportional to momentum flux, and is written as

$$\Delta p_e = (z - 1) \frac{\rho_f v^2}{g_c} R_n \ldots\ldots (29)$$

where z is a number greater than or equal to unity.

Summing all these expressions, the total pressure drop Δp_t is obtained.

$$\Delta p_t = \frac{\rho_f v^2}{g_c} \{ f \frac{\Delta L}{D} [2 \frac{L_s}{\Delta L} + 1 + R_n + \sum_{j=1}^{n-1} 2R_j] + zR_n - 1\} \text{ pounds per square ft} \ldots\ldots (30)$$

The dynamic equations for the heater are linearized, and the response of the system to a sinusoidal fluctuation of inlet liquid velocity is obtained. The heater wall temperature is assumed to remain constant during the fluctuations (a reasonable assumption for the range of frequencies in which Type II oscillations are observed) and the heat transfer rate is assumed to vary linearly with mass flow rate for small perturbations away from steady state. The partial differential equation for the subcooled region can be solved exactly to give the enthalpy fluctuation entering the boiling region. A lumped parameter approach is used to analyze the dynamics of the boiling region. Pressure variations are assumed to be sufficiently small so that the vapor density can be considered to be constant during the oscillations.

The energy equation in the subcooled region is written below.

$$q b_p = \rho_f \, v \, A_o \frac{\partial h}{\partial x} + \rho_f \, A_o \frac{\partial e}{\partial t} \quad \text{......................(31)}$$

where q is the heat input rate per unit surface area, b_p is the perimeter of the tube, h is the liquid enthalpy and e is the internal energy of the liquid. For a liquid at low pressure, the internal energy is very nearly equal to the enthalpy. Hence equation (31) can be rewritten in the form

$$q b_p = \rho_f \, v \, A_o \frac{\partial h}{\partial x} + \rho_f \, A_o \frac{\partial h}{\partial t} \quad \text{.....................(32)}$$

For small perturbations δq, δv, δh superimposed on a steady condition q, v, h the equation becomes

$$\delta q\, b_p = \rho_f\, v\, A_o \frac{\partial \delta h}{\partial x} + \rho_f\, A_o \frac{\partial h}{\partial x} \cdot \delta v + \rho_f\, A_o \frac{\partial \delta h}{\partial t} \qquad \text{........(33)}$$

Assuming q is a function of mass flow rate

$$\delta q/q = a\, \delta v/v \qquad \text{........(34)}$$

where $a = \frac{\dot{m}}{q} \frac{\partial q}{\partial \dot{m}} = 1 - b$

Substituting (34) in (33), we obtain

$$\frac{\partial}{\partial x}(\delta h) + \frac{1}{v} \frac{\partial}{\partial t}(\delta h) + \frac{\delta v}{v}\left[\frac{\partial h}{\partial x} - \frac{aqb_p}{\rho A_o v}\right] = 0 \qquad \text{........(35)}$$

Now, since the steady state heat input is uniform along the tube, we have

$$\frac{\partial h}{\partial x} = \frac{h_s}{L_s} \qquad \text{........(36)}$$

Also, $q b_p L_s = h_s \rho_f A_o$ ....(37)

Substituting (36), (37) in (35) and dividing through by h_{fg}/L_s we find

$$\frac{\partial \left(\frac{\delta h}{h_{fg}}\right)}{\partial \left(\frac{x}{L_s}\right)} + \frac{L_s}{v} \frac{\partial}{\partial t}\left(\frac{\delta h}{h_{fg}}\right) + \frac{\delta v}{v}\left[\frac{h_s}{h_{fg}}\right](1 - a) = 0 \qquad \text{...(38)}$$

Let $\frac{x}{L_s} = x'$, $\frac{\delta v}{v} = u'$, $\frac{L_s}{v} = \tau$

$$\frac{\partial \left(\frac{\delta h}{h_{fg}}\right)}{\partial x'} + \tau \frac{\partial \left(\frac{\delta h}{h_{fg}}\right)}{\partial t} + u'\left[\frac{h_s}{h_{fg}}\right](1 - a) = 0 \qquad \text{........(39)}$$

Since the results of a linearised analysis are not affected by the amplitude of the input, it is convenient to set

$u' = e^{i\omega t}$. Then $\frac{\delta h}{h_{fg}} = h' \cdot e^{i\omega t}$ where h' is a complex function of x'. Substituting for $\delta h/h_{fg}$ in (39), then

$$\frac{\partial h'}{\partial x'} + h' i\omega\tau = -\left(\frac{h_s}{h_{fg}}\right)(1 - a) \quad \text{....................(40)}$$

with the boundary condition $h' = 0$ at $x = 0$. The solution of this equation is written below

$$h' = \frac{\left(\frac{h_s}{h_{fg}}\right)(1-a)}{i\omega\tau}\left[e^{-i\omega\tau x'} - 1\right] \quad \text{......................(41)}$$

whence, at the end of the subcooled region ($x' = 1$),

$$h' = \frac{\left(\frac{h_s}{h_{fg}}\right)(1 - a)}{\omega\tau}\left[-\sin\omega\tau + i\,(1 - \cos\omega\tau)\right] \quad \text{.........(42)}$$

Thus, the enthalpy leaving the subcooled region oscillates, and the fluid entering the first boiling zone is subcooled during half of the cycle and above the saturation enthalpy during the other half of the cycle. This perturbation in enthalpy affects the conditions leaving the first boiling zone.

Liquid at an enthalpy close to the saturation enthalpy enters the first boiling zone. A mixture of saturated liquid and vapor leaves the first boiling zone. We denote the conditions leaving the first boiling zone by the subscript 1.

The continuity requirement states that, Mass flow rate entering - mass flow rate leaving = Rate of change of mass within.

$$\rho_f\, v\, A_o - [\rho_f\, v_{f1} + \rho_g\, v_{g1} A_{g1}]$$
$$= \frac{\Delta L}{2}\, \frac{d}{dt}\, (\rho_f\, A_o + \rho_f\, A_{f1} + \rho_g\, A_{g1}) \qquad (43)$$

assuming a linear variation in gas and liquid area within the element

$$\rho_f\, v\, A_o - [\rho_f\, v_{f1}\, (A_o - A_{g1}) + \rho_g\, s_1\, v_{f1}\, A_{g1}]$$
$$= \frac{\Delta L}{2}\, \frac{d}{dt}\, [\rho_f (A_o - A_{g1}) + \rho_g\, A_{g1}]$$

Dividing through by $\rho_f\, A_o$,

$$v - v_{f1}\, [1 - \beta_1 + s_1 \frac{\rho_g}{\rho_f}\, \beta_1\,] = - \frac{\Delta L}{2}\, (1 - \frac{\rho_g}{\rho_f})\, \frac{d\beta_1}{dt} \qquad (44)$$

For small perturbations δv, δv_{f1}, $\delta\beta_1$ superimposed on a steady state v, v_{f1}, β_1, equation (44) becomes

$$\delta v - \delta v_{f1}\, [1 - \beta_1 + s_1 \frac{\rho_g}{\rho_f}\, \beta_1\,] + \delta\beta_1\, v_{f1}\, (1 - s_1 \frac{\rho_g}{\rho_f})$$
$$= - \frac{\Delta L}{2}\, (1 - \frac{\rho_g}{\rho_f})\, \frac{d\delta\beta_1}{dt} \qquad (45)$$

Dividing through by v, we obtain

$$\frac{\delta v}{v} - \frac{\delta v_{f1}}{v}\, [1 - \beta_1\, (1 - s_1 \frac{\rho_g}{\rho_f})\,] + \delta\beta_1\, u_1 (1 - s_1 \frac{\rho_g}{\rho_f})$$
$$= - \tau_b\, \frac{d\delta\beta_1}{dt} \quad \text{where } \tau_b = \frac{\Delta L}{2v}\, (1 - \rho_g/\rho_f)$$

or $$u' - D_1 \frac{\delta v_{f1}}{v} + F_1\, \delta\beta_1 = \tau_b\, \frac{d\delta\beta_1}{dt} \qquad (46)$$

Let $u' = e^{i\omega t}$, $\frac{\delta v_{f1}}{v} = u_1' \cdot e^{i\omega t}$, $\delta\beta_1 = B_1' \cdot e^{i\omega t}$.

Then (46) reduces to the form

$$1 - D_1 \; u_1' + F_1 \; B_1' = - \tau_b \; i \; \omega B_1' \quad \text{.......................(47)}$$

where $D_1 = 1 - \beta_1 \; (1 - s_1 \frac{\rho_g}{\rho_f}) = 1/u_1$ ....(48)

$$F_1 = u_1 \; (1 - s_1 \; \frac{\rho_g}{\rho_f}) \quad \text{..................................(49)}$$

Since the vapor is regarded as incompressible, the energy equation for a boiling zone reduces to the simple statement,

Volume flow rate out - volume flow rate in

$$= \frac{V_{fg}}{h_{fg}} \; \text{(heat available for vaporisation)} \quad \text{.................(50)}$$

where V_{fg} is the specific volume change in going from saturated liquid to saturated vapor.

For the first boiling zone, (50) becomes

$$v_{f1} \; A_{f1} + v_{g1} \; A_{g1} - v \; A_o = \frac{V_{fg}}{h_{fg}} \; [gb_p \; \Delta L + \rho_f A_o \; h_{ex} \;] \quad \text{..............(51)}$$

where h_{ex} is the excess enthalpy (above saturation enthalpy) leaving the subcooled region. Dividing through by A_o, equation (51) reduces to the form

$$v_{f1} [1 + \beta_1 \; (s_1 - 1)] - v = V_{fg} [\; \frac{qb_p \Delta L}{A_o h_{fg}} + \rho_f \; v \; \frac{h_{ex}}{h_{fg}} \;] \quad \text{...........(52)}$$

For small perturbations δv_{f1}, δv, δq, equation (52) reduces to

$$\delta v_{f1}[1 + \beta_1 (s_1 - 1)] + \delta\beta_1 V_{f1} (s_1 - 1) - \delta v$$

$$= V_{fg} [\frac{\delta q b_p \Delta L}{A_o h_{fg}} + \rho_f v \frac{\delta h}{h_{fg}}] \qquad (53)$$

where δh is the enthalpy fluctuation leaving the subcooled region.

Whence, dividing through by v, and setting $\delta q/q = a\delta v/v$

$$\frac{\delta v_{f1}}{v} G_1 + \delta\beta_1 H_1 - u' = V_{fg} [\frac{aqb_p \Delta L \ \delta v}{v^2 h_{fg} A_o} + \rho_f \frac{\delta h}{h_{fg}}] \qquad (54)$$

where $G_1 = 1 + \beta_1 (s_1 - 1)$

$H_1 = u_1 [s_1 - 1]$

Since $\frac{qb_p \Delta L}{\rho_f A_o v h_{fg}}$ is equal to Δx, the steady state increment in quality for the element, equation (54) can be further reduced to

$$\frac{\delta v_{f1}}{v} G_1 + \delta\beta_1 H_1 - u' = (\frac{\rho_f}{\rho_g} - 1) [a\Delta x \ u' + \frac{\delta h}{h_{fg}}] \qquad (55)$$

Since $u' = e^{i\omega t}$, let $\frac{\delta v_{f1}}{v} = u_1' \cdot e^{i\omega t}$, $\delta\beta_1 = B_1' \cdot e^{i\omega t}$,

$\frac{\delta h}{h_{fg}} = h' \cdot e^{i\omega t}$ where h' is given by equation (42). Then (55) becomes

$$u_1' G_1 + \beta_1' H_1 - 1 = (\frac{\rho_f}{\rho_g} - 1) [a\Delta x + \delta h'] \qquad (56)$$

Solving (47) and (56) simultaneously for u_1' and B_1', we obtain

$$B_1' = \frac{D_1\{(\rho_f/\rho_g - 1)\ (a\Delta x + h') + 1\} - G_1}{D_1\ H_1 + G_1[F_1 + i\tau_b w]} \quad \text{.................(57)}$$

$$u_1' = \frac{1 + B_1'\ [F_1 + i\tau_b w]}{D_1} \quad \text{..............................(58)}$$

All boiling zones after the first one receive a mixture of saturated liquid and saturated vapor at inlet. The method used is similar to that for the first zone. From continuity, assuming a linear variation in void fraction through the element, and using the subscript 1 for conditions entering the element and 2 for conditions leaving it, we obtain

$$[\rho_f\ v_{f1}\ A_{f1} + \rho_g\ v_{g1}\ A_{g1}] - [\rho_f\ v_{f2}\ A_{f2} + \rho_g\ v_{g2}\ A_{g2}]$$

$$= \frac{\Delta L}{2}\ \frac{d}{dt}\ [\rho_f\ A_{f1} + \rho_g\ A_{g1} + \rho_f\ A_{f2} + \rho_g\ A_{g2}] \text{.............(59)}$$

Substituting $v_g = sv_f$, $A_f = A_o - A_g$, $\beta = A_g/A_o$, the equation reduces to the form

$$v_{f1}\ [1 - \beta_1\ (1 - \frac{\rho_g}{\rho_f}\ s_1)] - v_{f2}\ [1 - \beta_2\ (1 - \frac{\rho_g}{\rho_f}\ s_2)]$$

$$= - \frac{\Delta L}{2}\ (1 - \frac{\rho_g}{\rho_f})\ \frac{d}{dt}\ (\beta_1 + \beta_2) \text{..........................(60)}$$

Linearizing the equation for small perturbations about a steady state, the perturbations obey the relation

$$\delta v_{f1}[1 - \beta_1\ (1 - \frac{\rho_g}{\rho_f}\ s_1)] - \delta\beta_1\ v_{f1}\ (1 - \frac{\rho_g}{\rho_f}\ s_1)$$

$$- \delta v_{f2}[1 - \beta_2\ (1 - \frac{\rho_g}{\rho_f}\ s_2)] + \delta\beta_2\ v_{f2}\ (1 - \frac{\rho_g}{\rho_f}\ s_2)$$

$$= -\frac{\Delta L}{2} \left(1 - \rho_g/\rho_f\right) \frac{d}{dt} \left(\delta\beta_1 + \delta\beta_2\right) \quad \text{.....................(61)}$$

Dividing through by v, we obtain

$$\frac{\delta v_{f1}}{v} D_1 - \delta\beta_1 F_1 - \frac{\delta v_{f2}}{v} + \delta\beta_2 F_2 + \tau_b \frac{d}{dt} \left(\delta\beta_1 + \delta\beta_2\right) = 0 \quad \text{..(62)}$$

where $$D_j = \left[1 - \beta_j \left(1 - \frac{\rho_g}{\rho_f} s_j\right)\right] \quad \text{.....................(63)}$$

$$F_j = u_j \left(1 - \frac{\rho_g}{\rho_f} s_j\right) \quad \text{..........................(64)}$$

$\frac{\delta v_{f1}}{v} = u_1' \cdot e^{i\omega t}$, $\delta\beta_1 = B_1' \cdot e^{iwt}$. Let $\frac{\delta v_{f2}}{v} = u_2' \cdot e^{i\omega t}$,

$\delta\beta_2 = B_2' \cdot e^{i\omega t}$. Then,

$$B_2' \left(F_2 + i\tau_b\omega\right) - u_2' D_2 = B_1' \left(F_1 - i\tau_b\omega\right) - u_1' D_1 \quad \text{.........(65)}$$

As in the case of the first boiling zone, the volume flow rate out of the zone minus the volume flow rate into the zone is equal to the volume equivalent of the heat input. Hence,

$$\left[v_{f2} A_{f2} + v_{g2} A_{g2}\right] - \left[v_{f1} A_{f1} + v_{g2} A_{g2}\right]$$

$$= \frac{v_{fg}}{h_{fg}} q b_p \Delta L \quad \text{.......................................(66)}$$

Linearizing this equation for small perturbations we obtain, setting $\frac{\delta q}{q} = a \frac{\delta \dot{m}_1}{\dot{m}_1}$

$$\frac{\delta v_{f2}}{v} \left[1 + \beta_2 \left(s_2 - 1\right)\right] + \delta\beta_2 \frac{v_{f2}}{v} \left(s_2 - 1\right)$$

$$- \frac{\delta v_{f1}}{v} [1 + \beta_1 \ (s_1 - 1)] - \delta\beta_1 \frac{v_{f1}}{v} (s_1 - 1)$$

$$= a\Delta x \ (\frac{\rho_f}{\rho_g} - 1) \frac{\delta \dot{m}_1}{\dot{m}_1} \quad \ldots\ldots\ldots\ldots\ldots\ldots\ldots\ldots\ldots\ldots\ldots (67)$$

$$\frac{\delta \dot{m}_1}{\dot{m}_1} = \frac{\delta v_{f1}}{v} D_1 - \delta\beta_1 F_1 \quad \ldots\ldots\ldots\ldots\ldots\ldots\ldots\ldots\ldots\ldots (68)$$

Hence, with $\frac{\delta v_{f1}}{v} = u_1' \cdot e^{i\omega t}$, $\delta\beta_1 = B_1' \cdot e^{i\omega t}$,

$\frac{\delta v_{f2}}{v} = u_2' \cdot e^{i\omega t}$, $\delta\beta_2 = B_2' \cdot e^{i\omega t}$, we obtain

$$u_2' G_2 + B_2' H_2 = u_1' [G_1 + T D_1] + B_1' [H_1 - T F_1] \ldots\ldots\ldots (69)$$

where $\quad T = a\Delta x \quad (\rho_f/\rho_g - 1)$

Solving (65) and (69) simultaneously for B_2' and u_2', we obtain

$$B_2' = \{[D_2(G_1 + TD_1) - G_2D_1] u_1' + [D_2(H_1 - TF_1)$$

$$+ G_2(F_1 - i\tau_b\omega)]B_1' \}/[D_2H_2 + G_2(F_2 + i\tau_b\omega)] \ldots\ldots\ldots (70)$$

$$u_2' = \frac{[G_1 + TD_1] u_1' + (H_1 - TF_1) B_1' - H_2 B_2'}{G_2} \quad \ldots\ldots\ldots\ldots (71)$$

In general, applying the above analysis to the j^{th} element, with conditions entering the element denoted by (j-1), and leaving the element denoted by j, we obtain,

$$B_j' = \{[D_j(G_{j-1} + TD_{j-1}) - G_j D_{j-1}] u_{j-1}' + [D_j(H_{j-1} - TF_{j-1})$$

$$+ G_j \ (F_{j-1} - i\tau_b\omega)]B'_{j-1}\}/[D_j \ H_j \ + G_j(F_j \ + i\tau_b\omega)] \quad \text{........(72)}$$

$$u'_j = \frac{[G_{j-1} + TD_{j-1}]u'_{j-1} + (H_{j-1} - TF_{j-1})B'_{j-1} - H_j B'_j}{G_j} \quad \text{.....(73)}$$

where $$D_j = \frac{1}{u_j} = [1 - B_j(1 - s_i \ \rho_g/\rho_f)] \quad \text{.............(74)}$$

$$F_j = u_j \ [1 - s_i \ \rho_g/\rho_f] \quad \text{........................(75)}$$

$$G_j = [1 + B_j \ (s_j - 1)] \quad \text{........................(76)}$$

$$H_j = u_j \ [s_j - 1] \quad \text{..............................(77)}$$

The overall pressure drop fluctuation is obtained from equations (21), (28), (29), by imposing a small perturbation on the steady flow and linearizing the resulting equations.

From equations (21) and (22)

$$\delta \ (\Delta p_{fj}) = \frac{f\Delta L}{D} \ \frac{\rho_f}{g_c} \ \{2v_{fj}[1 - \beta_j \ (1 - \frac{\rho_g}{\rho_f} \ s_j{}^2)]\delta v_{fj}$$

$$- v_{fj}^2 \ (1 - \frac{\rho_g}{\rho_f} \ s_j^2) \ \delta\beta_j + 2v_{f(j-1)}[1 - \beta_{j-1}(1 - \frac{\rho_g}{\rho_f} \ s_{j-1}^2)]$$

$$- v_f{}^2(j-1)(1 - \frac{\rho_g}{\rho_f} \ s_{j-1}^2) \ \delta\beta_{j-1}\} \quad \text{....................(78)}$$

$$\frac{\delta(\Delta p_{fj})}{\frac{\rho_f \ v^2}{g_c}} = \frac{f\Delta L}{D} \ \{ \ (XI)_j \ \frac{\delta v_{fj}}{v} - Y_j \ \delta\beta_j + (XI)_{j-1} \ \frac{\delta v_{f(j-1)}}{v}$$

$$- Y_{j-1} \ \delta\beta_{j-1} \ \} \quad \text{..................................(79)}$$

where $$(XI)_j = 2\, u_j \left[1 - \beta_j \left(1 - \frac{\rho_g}{\rho_f}\, s_j^2\right)\right] \qquad (80)$$

$$Y_j = u_j^2 \left[1 - \frac{\rho_g}{\rho_f}\, s_j^2\right] \qquad (81)$$

Hence, for sinusoidal fluctuations, let $\frac{\delta(\Delta p_{fj})}{\rho_f v^2/g_c} = P_{fj}' \cdot e^{i\omega t}$.

Then (79) reduces to

$$P_{fj}' = \frac{f\Delta L}{D} \{(XI)_j\, u_j' - Y_j\, B_j' + (XI)_{j-1}\, u_{j-1}' - Y_{j-1}\, B_{j-1}'\} \qquad (82)$$

Similarly, the perturbations in Δp_{fs}, Δp_a and Δp_e may be obtained as follows.

$$P_{fs}' = 4f\, \frac{L_s}{D} \qquad (83)$$

$$P_a' = [(XI)_n\, u_n' - Y_n\, B_n' - 2] \qquad (84)$$

$$P_e' = (z-1)\, [(XI)_n\, u_n' - Y_n\, B_n'] \qquad (85)$$

where $\frac{\delta(\Delta p_a)}{\rho_f v^2/g_c} = P_a' \cdot e^{i\omega t}$, $\frac{\delta(\Delta p_e)}{\rho_f v^2/g_c} = P_e' \cdot e^{i\omega t}$, $\frac{\delta(\Delta P_{fs})}{\rho_f v^2/g_c} = P_{fs}' \cdot e^{i\omega t}$

Summing all the pressure drop perturbations, including the frictional pressure drop in the subcooled region,

$$P' = \left(\frac{f\Delta L}{D} + z\right)[(XI)_n\, u_n' - Y_n\, B_n'] + \frac{f\Delta L}{D}\left[4\, \frac{L_s}{\Delta L} + 2\right] - 2$$

$$+ 2\, \frac{f\Delta L}{D} \sum_{j=1}^{n-1} [(XI)_j\, u_j' - Y_j\, B_j'] \qquad (86)$$

P' is evaluated as a complex number with real and imaginary parts P'R, P'I. The pressure amplitude $|P'| = \sqrt{(P'R)^2 + (P'I)^2}$, and the phase angle $\phi = \arctan\left(\frac{P'I}{P'R}\right)$ (see Figure 43). If the phase angle ϕ reaches a value of 180° at any frequency the system is unstable unless a suitable inlet restriction is applied. From equation (4) marginal stability exists when

$$(p_a - p_b) = \frac{1}{2} \left| \frac{\delta(\Delta p_t)}{\delta\dot{m}/\dot{m}} \right| \quad \ldots\ldots (87)$$

$$|\delta(\Delta p_t)| = \frac{\rho_f v^2}{g_c} \left| P' \right|_{180°} \quad \ldots\ldots (88)$$

$$\left|\frac{\delta\dot{m}}{\dot{m}}\right| = \left|\frac{\delta v}{v}\right| = 1 \quad \ldots\ldots (89)$$

Hence, for marginal stability,

$$(p_a - p_b) = \frac{1}{2} \frac{\rho_f v^2}{g_c} \left| P' \right|_{180°} \quad \ldots\ldots (90)$$

A Fortran listing for the frequency response analysis is given in Appendix B.

Frequency response characteristics were obtained for a number of typical Freon-11 operating conditions. In Figure 44, three frequency response plots are shown for a mass flow rate of 0.54 pounds per minute, with an inlet temperature of 70.4°F and a power input of 1230 BTU/hr. The boiling length was broken up into 20 segments. The solid line illustrates the locus of P'I, P'R for a value of a of 0.4 (equivalent to b = 0.6). A phase shift of 180°does occur, and using equation 90 it is found that 49% of the total pressure drop should take place at the inlet to give marginal stability. Comparing this result with typical test data for this flow rate and power level, we see that in actuality a very small inlet pressure drop was sufficient to stabilise the system. The only parameter which can possibly achieve the desired effect is a, and the broken line in Figure 44 shows the effect of changing a to 0.7. A phase shift of 180° now occurs with a much smaller value of P', and an inlet pressure drop of only 18% of the total is sufficient to stabilise the system.

With a value of a equal to 0.8, the system is completely stable and no inlet pressure drop is needed. This trend is shown by all the operating points which have been examined using the frequency response analysis, and it suggests that the analog simulation was accurate in predicting that small values of b (large values of a) were necessary for stability. Failing any other explanation for the high stability of the system using Freon-11, it seems to be necessary to conclude that the heat transfer rate during transients was probably strongly dependent on flow rate, and that this effect could not be predicted from the steady flow heat transfer data for flows in the range 0.4 to 1.0 pounds per minute.

6.3. Type III Oscillations.

The key to these oscillations lies in a study of the wall temperature recordings in combination with the pressure recordings (Fig. 6(b)).

From the known power input, and the mass and specific heat of the tube, it is possible to convert the temperature record into a plot of heat flux minus electrical input flux ($q - q_o$) versus wall temperature throughout the cycle. This information is plotted in Figure 45 for the point on the tube where the maximum temperature fluctuations occurred in the test at 2390 BTU/hr. The input flux q_o was 19,850 BTU/hr.ft.^{2}. In the region ABC the pressure traces are smooth, and the tube wall was apparently operating at the bottom of the valley in the boiling curve (See Fig. 8). The heat flux out of the wall was less than the power input to this portion of the tube, and so the wall temperature rose steadily until, at C, density wave oscillations commenced and built up to full amplitude at D. The flow disturbances associated with the density wave oscillations apparently broke up the vapor film next to the tube wall, and raised the heat flux from the wall above the power input to the tube, which now started to cool off. At E, the density waves attenuated and at A they had disappeared. However, A is on the statically unstable portion of the boiling curve and so the cycle recommenced. The general shape of the steady boiling curve is shown as a broken line in Figure 45.

To stabilize the flow completely, it is necessary to reduce the power (or increase the flow rate) until the power input q_o lies below q_c. To obtain fully developed density waves as in 6(c) it is necessary to raise the power (or reduce the flow rate) until the power input q_o is above q_E. With $q_C < q_o < q_E$, no fixed operating condition is possible, and the heater continuously cycles around the loop. Although it has not yet been possible to define clearly all the conditions required for thermal oscillations, a clue may be obtained from Figure 45. For thermal oscillations to occur, the density wave oscillations must quench (at E) at a higher flux than they start (at C). This could only happen if the flow at E was greater than the flow at C, so that the exit quality at E was less than the exit quality at C. Observation of the rotameter during the cycle showed that this requirement was fulfilled (the differential pressure transducer had not yet been installed). It appears, then that a relatively rare combination of flow and heat transfer characteristics may be necessary to permit thermal oscillations to occur. However, although they may be rare they are also exceedingly dangerous. Pressure pulses of 50 to 100 psi were observed during the experiments with thermal oscillations, and several pressure gages were damaged. Since the thermal oscillations require density wave oscillations during part of their cycle, they can also be eliminated by inlet orificing.

The period of the thermal oscillations can be predicted only if the flux-temperature loop is known for the cycle. For unit area of the tube, at any point in the cycle,

$$Mc_m \frac{dT_w}{dt} = q_o - q \qquad \text{.......................(1)}$$

where M is the mass of unit surface area of the tube, c_m is the specific heat of the metal, q_o is the power input flux and q is the flux from the tube to the fluid. Integrating for one cycle.

$$\tau = Mc_m \oint \frac{dT_w}{(q_o - q)} \quad \ldots\ldots\ldots\ldots\ldots\ldots\ldots\ldots\ldots (2)$$

where τ is the time period. For a given flux-temperature loop, the period is proportional to the tube mass per unit heat transfer area.

7. CONCLUSIONS

Type I and Type II oscillations have been identified in both Freon-11 and water, and analyses have been developed which reproduce the main features of these oscillations, although the analyses have not yet reached the point where accurate prediction of the onset and frequency of the oscillations is always possible.

When operating with water, the system was much less stable than when operating with Freon-11. The steam within the heater apparently behaved as a non-condensible gas during Type I oscillations, providing an internal gas spring which made the upstream flow restriction ineffective as a source of damping. There was a marked lack of thermal equilibrium between vapor and liquid in the water leaving the heater which could have been responsible for this effect, since the steam persisted long after it should have condensed.

Analysis of the Type II oscillations in Freon-11 suggests that boiling heat transfer during transients may differ substantially from steady state heat transfer, and that the transient effects can be extremely beneficial in stabilizing the system.

It appears that experiments which are limited to the observation of self-induced oscillations cannot provide all the information needed for accurate prediction of stability boundaries. Controlled transient experiments of either the pulse or frequency response type would be extremely useful for generating additional information about dynamic effects.

ACKNOWLEDGEMENTS

The work described in this report was sponsored by the National Aeronautics and Space Administration and directed by the authors. However, many other individuals made substantial contributions to the project. The principal participants were Mr. L. Arrondo, Mr. T. C. Wang, Mr. G. Callahan and Mr. D. Mayer.

REFERENCES

1. Ledinegg, M. "Instability of Flow During Natural and Forced Convection", Die Warme, 61, # 8, pp 891-8, 1938; AEC - tr - 1861, 1954.

2. Gouse, S.W., "Two-Phase Gas-Liquid Flow Oscillations: Preliminary Survey", Engineering Projects Laboratory, Department of Mechanical Engineering, MIT Report DSR 8734-5, July 1964.

3. Blatt, T.A., and Adt, R.R., "An Experimental Investigation of Boiling Heat Transfer and Pressure-Drop Characteristics of Freon-11 and Freon 113 Refrigerants", A.I.Ch.E. Journal, May 1964, pp. 369-373.

4. Callahan, G.M., "Two-Phase Flow Pressure Drop Oscillations" M.S. Thesis, Mechanical Engineering Department, University of Miami, February 1966.

5. Stenning, A.H., and Veziroglu, T.N., "A Parametric Study of Boiling Instability", ASME paper 64-WA/FE-28, presented at the Annual Meeting, Dec. 1964.

6. Stenning, A.H., "Instabilities in the Flow of a Boiling Liquid," Journal of Basic Engineering, Trans. ASME, Series D, Vol. 86, June 1964, pp. 213-217.

7. Gouse, S.W., and Andrysiak, C.D., "Flow Oscillations in a Closed Loop with Transparent, Parallel, Vertical Heated Channels", M.I.T., NSF Grants G11355 and G19771 Report No. 8973-2, June 1963.

8. Mayer, D. "Instabilities in Boiling Water Flow" M.S. Thesis, Mechanical Engineering Department, University of Miami, October, 1966.

9. Maulbetsch, J.S., and Griffith, P., "System-Induced Instabilities in Forced Convection Flows with Subcooled Boiling", Third International Heat Transfer Conference, August 1966.

10. Stenning, A.H. and Veziroglu, T.N., "Flow Oscillation Modes in Forced-Convection Boiling," Proceedings of the 1965 Heat Transfer and Fluid Mechanics Institute, June 1965, pp. 301-316. Stanford University Press.

11. Lockhart, R.W., and Martinelli, R.D., "Proposed Correlation of Data for Isothermal Two-Phase, Two-Component Flow in Pipes", Chemical Engineering Progress, Vol. 45, p.39, 1949.

12. Fauske, H.K., "Contribution to the Theory of Two-Phase, One-Component Critical Flow", NASA Report No. N63-11025, October 1962.

13. Berenson, P.J., "Flow Stability in Multitube Forced-Convection Vaporizers," Technical Documentary Report No. APL TOR 64-117, AIResearch Manufacturing Division. The Garrett Corporation, October 1964, pp. 1-79.

14. Davidov, A.A., "Investigation of Flow Pulsations in Tubes of the Evaporation Section of Radiant Boilers", AEC-tr-4490, pp. 141-160, 1961, (Moscow 1955).

15. Semenovker, I.E., "The Occurrence of Pulsations in the Evaporation Tubes of Steam Boilers, AEC-tr-4490, pp.161-181, June 1961, (Moscow 1955).

16. Wallis, G.B., and Heasley, J.H., "Oscillations in Two-Phase Flow Systems", Journal of Heat Transfer, Trans. ASME Series C, Vol. 83, August 1961, pp.363-369.

17. Quandt, E.R., "Analysis and Measurements of Flow Oscillations," Chemical Engineering Progress, Monograph and Symposium Series # 32-S, Heat Transfer, Buffalo, N.Y. August 1960, pp. 111-126.

18. Meyer, J.E., and Rose, R.P., "Application of a Momentum Integral Model to the Study of Parallel Channel Boiling Flow Oscillations", Journal of Heat Transfer, Trans. ASME Series C, Vol. 85, February 1963, pp. 1-9.

19. Jones, A.B., "Hydrodynamic Stability of a Boiling Channel", KAPL-2170, Knolls Atomic Power Laboratory, October 1961.

20. Worsøe-Schmidt, P., "Some Characteristics of Flow Pattern and Heat Transfer of Freon-12 Evaporating in Horizontal Tubes," Ingeniøren, Denmark, No. 3, September 1959.

21. Rounthwaite, C., and Clouston, M., "Heat Transfer During Evaporation of High Quality Water-Steam Mixtures Flowing in Horizontal Tubes," ASME International Developments in Heat Transfer, Part I, 1961, pp. 200-211.

22. Wang, T.C., "Boiling Flow Oscillations in Freon-11", M.S. Thesis, Mechanical Engineering Department, University of Miami, October 1965.

23. Ellerbrock, H.H., Livingood, J.N.B., and Straight, D.M., "Fluid Flow and Heat Transfer Problems in Nuclear Rockets," Proceedings of the NASA-University Conference on the Science and Technology of Space Exploration, Vol. 2, November 1962, pp. 87-116.

24. Stenning, A.H., and Veziroglu, T.N., "Semi-Annual Status Report on Boiling Flow Instability," Department of Mechanical Engineering, University of Miami, NASA Grant NsG-424, Report No. 3, May 1964.

25. von Glahn, U.H., "An Empirical Relation for Predicting Void Fraction with Two-Phase Steam-Water Flow", NASA Tech. Note D-1189, January, 1962.

NOMENCLATURE

Symbols:

$a = 1-b$	Dimensionless derivative of heat transfer with respect to flow
A	Area
$b = 1-a$	Fraction of heat transfer independent of flow
b_p	Perimeter of tube
c	Heat input to remove subcooling as fraction of heat into first lump
c'	Heat input to remove subcooling as fraction of total heat input
c_ℓ	Specific heat of liquid
c_m	Specific heat of metal
D	Tube diameter
e	Stability parameter (6.1); internal energy (6.2.3)
f	Friction factor
h	Heat transfer coefficient (6.1); enthalpy (6.2.3)
H	Heat input
i	$\sqrt{-1}$
j	Lump number
K	Pressure drop proportionality factor
L	Tubing length
$\dot{m}$	Mass flow rate
M	Mass
p	Pressure
P	Pressure
q	Heat flux
Q	Volume flow rate
r	Density ratio
s	Slip ratio
t	Time
T	Temperature
u	Velocity ratio
U	Velocity
v	Velocity
V_{fg}	Specific volume change from liquid to vapor
x	Fraction of vapor by mass
y	Inlet pressure drop as fraction of overall pressure drop
z	Loss Factor

Greek Symbols:

β	Void fraction
ρ	Density
τ	Time constant; period of oscillation
ω	Radian frequency

Subscripts:

a	air; system inlet; acceleration
b	boiler inlet
be	bulk boiling inception to system exit
bs	bulk boiling inception
c	boiler exit
d	dynamic
e	exit
ev	liquid evaporated
ex	excess
f	saturation; liquid; frictional
fg	liquid to vapor change
g	gas; vapor
he	heater exit
hi	heater inlet
i	inlet; imaginary
ie	heater inlet to system exit
j	segment number; station number
l	liquid
m	metal
n	lump number; station number
o	oscillation; steady state; total
p	perimeter
r	real
s	subcooling; saturation; steady flow
se	system exit
si	system inlet
sub	subcooling
t	heater; total
v	saturated vapor
w	wall

APPENDIX A

TABULATION OF PARAMETERS USED FOR LINEARIZED STABILITY ANALYSIS FOR HEATER POWER INPUT OF 1170 BTU/HR.

$\dot{m}$ lbs/min	e	τ_1 min	τ_2 min	m_1	m_2	n_1	n_2	Behavior	ω rad/min	Period min
2.53	1.720	2.17	0.0106	0.0544	0.700	27.7	4.78	Stable	-	-
2.40	1.710	2.14	0.0130	-0.0886	0.760	22.4	4.80	Stable	-	-
2.30	1.700	2.10	0.0148	-0.1580	0.916	19.0	3.14	Unstable	-	-
2.35	1.705	2.12	0.0385	-0.1480	0.800	21.1	4.70	Near Onset	3.04	2.10

APPENDIX B

FORTRAN PROGRAM FOR FREQUENCY RESPONSE ANALYSIS OF TYPE II OSCILLATIONS

```
      COMPLEX CN1,CN,HP,CPV1,CPV2,CPV3,CPV4,BP(100),UP(100),PP(100)
      DIMENSION X(100),B(100),S(100),U(100),D(100),
     1R(100),DP(100),TBW(1001),F(100),G(100),
     2H1(100),X1(100),Y(100),DELTA(10)
    1 FORMAT(4E14.6)
    2 FORMAT(6I5)
    3 FORMAT(4H1A1=,E14.6,4X4H AM=,E14.6,
     14X4H AL=,E14.6,/3H C=,E14.6,4X5H DIA=,
     2E14.6,4X7H DELTA=,E14.6,/4H FF=,E14.6,
     34X5H HFG=,E14.6,4X3H Q=,E14.6,/
     46H RHOF=,E14.6,4X6H RHOG=,E14.6,
     54X4H TS=,F14.6,/4H TI=,E14.6,4X
     63H Z=,E14.6,4X7H DELT1=,E14.6)
    4 FORMAT(4H NN=,I5,4X4H N1=,I5)
    5 FORMAT(///5X20H PRESSURE DROP (DP)=,E14.6,4X4H VL=,E14.6/5H ALS=,
     1E14.6)
    6 FORMAT(/4H XJ=,4E14.6)
    7 FORMAT(/4H BJ=,4E14.6)
    8 FORMAT(/4H SJ=,4E14.6)
    9 FORMAT(/4H UJ=,4F14.6)
   10 FORMAT(/4H RJ=,4E14.6)
   11 FORMAT(29H PHASE ANGLE GREATER THAN 180)
   12 FORMAT(/30H PRESSURE TO STABILIZE SYSTEM=,E14.6)
   13 FORMAT(/5H PPX=,E14.6,4X5H PPY=,E14.6,
     14X5H PHI=,E14.6,/4H TB=,
     2E14.6,4X5H TBW=,E14.6)
   14 FORMAT(/4H J1=,I5,4X3H I=,I5,/)
   15 FORMAT(4H BP=,2E14.6,2X,2E14.6,2X,2E14.6,2X,2E14.6)
   16 FORMAT(4H UP=,2E14.6,2X,2E14.6,2X,2E14.6,2X,2E14.6)
   17 FORMAT(4H X1=,2E14.6,2X,2E14.6,2X,2E14.6,2X,2E14.6)
   18 FORMAT(3H Y=,2E14.6,2X,2E14.6,2X,2E14.6,2X,2E14.6)
  400 READ (5,1) A1,AM,AL,C,DIA,DELTA(1),FF,HFG,Q,RHOF,RHOG,TS,TI,Z,
     1DELTA(2)
      READ (5,2) NN,N1
      WRITE (6,3) A1,AM,AL,C,DIA,DELTA(1),FF,HFG,Q,RHOF,RHOG,TS,TI,Z,
     1DELTA(2)
      WRITE (6,4) NN,N1
C     THE VALUE OF THE INDEX I CORRESPONDES TO THE NUMBER OF SEGMENTS OF
C     SATURATED LIQUID AND/OR VAPOR
  300 DO 200 I=20,NN
      AN=I
  301 N=I
```

```
      H=Q/AM
      HS=C*(TS-TI)
  302 ALS=AL*HS/H
      A=(RHOG/RHOF)**0.1
  303 VL=AM/(0.785*RHOF*DIA*DIA)
      TAU=ALS/VL
  304 DL=(AL-ALS)/AN
      DH=(H-HS)/AN
  305 DX=DH/HFG
      TB=(1.-RHOG/RHOF)*DL/(2.*VL)
  306 T1=(RHOF/RHOG-1.)*A1*DX
      RZ=0.
  307 DO 196 J=1,N
      AJ=J
  308 X(J)=AJ*DX
  309 B(J)=1./(1.-(RHOG/RHOF)**0.67*(1.-1./X(J)))**A
  310 S(J)=X(J)*(RHOF/RHOG)*(1.-B(J))/(B(J)*(1.-X(J)))
  311 D(J)=1.-B(J)*(1.-RHOG*S(J)/RHOF)
  312 U(J)=1./D(J)
  313 R(J)=U(J)*U(J)*(1.-B(J)*(1.-S(J)*S(J)*RHOG/RHOF))
      RZ=2.*R(J)+RZ
  196 CONTINUE
      IF(X(I))201,200,201
  201 RZ=RZ-2.*R(I)
  314 DP(I)=(RHOF*VL*VL/32.2)*(FF*DL/DIA*(2.*ALS/DL+1.+R(I)+RZ)+Z*R(I)-1
     1.)
      WRITE (6,5) DP(I),VL,ALS
      WRITE (6,6) (X(J),J=1,N)
      WRITE (6,7) (B(J),J=1,N)
      WRITE (6,8) (S(J),J=1,N)
      WRITE (6,9) (U(J),J=1,N)
      WRITE (6,10) (R(J),J=1,N)
      IF(N1)200,200,500
  500 ASSIGN 504 TO LUVB
  501 W=0.0001/TB
      IA=1
      TW=TAU*W
      TBW(1)=TB*W
  315 DO 199 J1=1,N1
      CPV1=CMPLX(-SIN(TW),1.-COS(TW))
  317 HP=HS*(1.-A1)/(HFG*TW)* CPV1
  318 DO 197 J=1,N
  319 F(J)=U(J)*(1.-S(J)*RHOG/RHOF)
  320 G(J)=(1.+B(J)*(S(J)-1.))
```

```
321 H1(J)=U(J)*(S(J)-1.)
197 CONTINUE
    CPV2=CMPLX(F(1),TBW(J1))
322 BP(1)=(D(1)*((RHOF/RHOG-1.)*(A1*DX+HP)+1.)-G(1)
   1/(D(1)*H1(1)+G(1)*CPV2)
323 UP(1)=(1.+BP(1)*CPV2)/D(1)
324 DO 328 J=2,N
    CPV3=CMPLX(F(J-1),-TBW(J1))
    CPV4=CMPLX(F(J),TBW(J1))
325 BP(J)=((D(J)*(G(J-1)+T1*D(J-1))-G(J)*D(J-1))
   1*UP(J-1)+(D(J)*(H1(J-1)-T1*F(J-1))+G(J)*CPV3)
   2*BP(J-1))/(D(J)*H1(J)+G(J)*CPV4)
326 UP(J)=((G(J-1)+T1*D(J-1))*UP(J-1)+(H1(J-1)-T1*F(J-1))*BP(J-1)
   1-H1(J)*BP(J))/G(J)
327 X1(J)=2.*U(J)*(1.-B(J)*(1.-S(J)*S(J)*RHOG/RHOF))
    Y(J)=U(J)*U(J)*(1.-S(J)*S(J)*RHOG/RHOF)
328 CONTINUE
329 CN=(FF*DL/DIA+Z)*(X1(I)*UP(I)-Y(I)*BP(I))-2.+FF*DL/DIA*(4.*ALS
   1/DL+2.)
    NM1=I-1
    PP(1)=X1(1)*UP(1)-Y(1)*BP(1)
330 DO 198 J=2,NM1
331 CN1=X1(J)*UP(J)-Y(J)*BP(J)
332 PP(J)=PP(J-1)+CN1
198 CONTINUE
333 PP(I)=CN+2.*FF*DL/DIA*PP(I-1)
334 PPX=REAL(PP(I))
335 PPY=AIMAG(PP(I))
336 PHI=ATAN(PPY/PPX)
    IF(PHI-3.14)340,337,337
337 WRITE (6,11)
338 PDSS=1./64.4*RHOF*VL*VL*SQRT(PPX*PPX+PPY*PPY)
339 WRITE (6,12) PDSS
    GO TO 346
340 WRITE (6,13) PPX,PPY,PHI,TB,TBW(J1)
341 WRITE (6,14) J1,I
342 WRITE (6,15) (BP(J),J=1,N)
343 WRITE (6,16) (UP(J),J=1,N)
344 WRITE (6,17) (X1(J),J=1,N)
345 WRITE (6,18) (Y(J),J=1,N)
    GO TO LUVB,(504,346)
504 IF(TBW(J1)-0.00011)505,506,506
505 W=0.01/TB
    TW=TAU*W
```

```
    TBW(1)=0.
506 IF(TBW(J1)-0.1)346,507,507
507 IA=2
    ASSIGN 346 TO LUVB
346 TBW(J1+1)=TBW(J1)+DELTA(IA)
199 CONTINUE
200 CONTINUE
    GO TO 400
401 CALL EXIT
    END
```

TABLE I

SOME DATA AND CALCULATED PARAMETERS FOR FREON-11 EXPERIMENTS
WITH PARTIAL BOILING AT ONSET OF DENSITY-WAVE TWO-PHASE FLOW OSCILLATIONS
(TEST SYSTEM EXTENT: FREON-11 CONTAINER TO EXIT VALVE - NO SURGE TANK)

Exp. No.	P_{si} psia	P_{hi} psia	P_{he} psia	T_{hi} °F	T_{bs} °F	T_{he} °F	$\dot{m}$ $\frac{lbs.}{min.}$	q $\frac{Btu}{hr.ft.^2}$	c'	$\frac{\rho_{hi}}{\rho_{se}}$	y
A001	45.24	41.72	37.42	74.7	134.4	125.5	0.510	20496	0.157	110	0.115
A002	56.37	51.90	46.04	74.8	148.9	136.2	0.832	20701	0.315	51	0.107
A003	69.50	51.82	46.17	75.5	148.7	136.9	0.729	20701	0.273	60	0.323
A004	69.30	52.60	46.80	75.4	149.7	137.5	0.814	20906	0.307	52	0.306
A005	69.30	54.37	48.36	75.7	151.9	139.9	0.810	21653	0.303	53	0.274
A006	54.65	51.49	45.98	75.7	148.3	137.0	0.622	21674	0.221	76	0.079
A007	46.57	40.25	38.91	75.2	132.1	133.0	0.483	17391	0.167	87	0.198
A008	50.98	46.14	43.92	75.6	141.1	137.1	0.569	17484	0.225	64	0.133
A009	53.24	50.08	47.06	75.7	146.5	140.4	0.531	17580	0.227	66	0.082
A010	56.57	53.99	50.30	75.3	151.4	143.4	0.685	17580	0.315	45	0.062
A011	59.90	56.44	53.65	75.5	154.4	149.1	0.732	21664	0.284	49	0.076
A012	71.46	68.16	64.64	75.5	171.8	163.3	0.623	24659	0.250	58	0.058
A013	52.94	50.52	48.02	75.5	147.0	141.9	0.531	15375	0.262	54	0.063
A014	54.41	52.03	48.93	75.5	149.0	142.8	0.643	15375	0.326	42	0.060
A015	58.33	54.96	51.73	75.5	152.6	146.0	0.780	16688	0.384	33	0.077
A016	60.19	57.49	54.28	75.5	155.6	149.7	0.660	17778	0.317	43	0.060
A017	61.03	54.99	53.69	75.5	152.6	151.1	0.552	20709	0.219	64	0.130
A018	68.52	63.31	60.23	75.5	163.2	157.4	0.835	20666	0.376	33	0.097
A019	68.77	65.49	62.05	75.5	166.6	158.2	0.758	20634	0.352	37	0.061
A020	51.37	50.38	48.49	70.5	146.8	144.6	0.430	13508	0.257	57	0.027

TABLE I (continued)

Exp. No.	P_{si} psia	P_{hi} psia	P_{he} psia	T_{hi} °F	T_{bs} °F	T_{he} °F	$\dot{m}$ $\frac{lbs.}{min.}$	q $\frac{Btu}{hr.ft.^2}$	c'	$\frac{\rho_{hi}}{\rho_{se}}$	Y
A021	53.23	51.80	49.73	72.2	148.7	146.1	0.522	13508	0.313	44	0.037
A022	53.13	49.17	47.31	71.8	145.3	142.0	0.687	12839	0.415	29	0.103
A023	59.16	55.27	53.66	75.2	153.0	151.7	0.647	13138	0.408	28	0.088
A024	58.43	55.83	54.32	75.7	153.7	152.5	0.485	13138	0.307	42	0.058
A025	46.13	44.24	42.04	76.1	138.3	135.3	0.380	13291	0.187	79	0.060
A026	40.25	39.03	36.06	76.9	130.1	124.7	0.409	13160	0.175	87	0.048
A027	44.61	42.96	39.96	76.8	136.3	130.6	0.454	13423	0.213	70	0.056
A028	35.32	33.30	26.54	75.7	120.2	102.6	0.450	17013	0.124	165	0.098
A029	44.34	42.29	38.43	76.4	135.3	128.8	0.427	16965	0.156	105	0.069
A030	53.65	51.72	48.19	76.7	148.6	143.7	0.558	16917	0.251	58	0.050
A031	64.13	61.54	59.08	76.7	160.7	158.6	0.627	16917	0.332	38	0.053
A032	68.45	66.42	64.44	77.3	168.2	165.3	0.533	16917	0.300	43	0.038
A033	73.25	71.23	69.37	77.8	179.6	170.6	0.519	17013	0.306	41	0.034
A034	39.83	37.36	27.53	78.0	127.3	102.4	0.587	19738	0.155	158	0.098
A035	39.83	37.31	27.86	78.4	127.3	103.6	0.573	19819	0.149	157	0.100
A036	39.73	37.41	28.20	78.6	127.4	104.4	0.561	19768	0.146	156	0.093
A037	39.54	37.41	28.51	79.0	127.4	105.6	0.593	20190	0.150	147	0.086
A038	21.18	19.66	17.86	77.4	90.0	85.4	0.357	5947	0.074	95	0.237
A039	40.19	37.43	28.03	78.5	127.5	104.1	0.566	19846	0.147	158	0.108
A040	39.65	37.04	28.12	78.8	126.8	104.6	0.529	19846	0.135	165	0.105
A041	48.87	46.18	40.33	79.3	141.1	131.3	0.593	19846	0.195	86	0.079
A042	25.54	25.50	21.57	74.8	104.6	96.2	0.828	10908	0.235	65	0.003
A043	24.31	24.15	20.45	75.3	101.5	92.8	0.638	11059	0.156	91	0.017

TABLE I (continued)

Exp. No.	P_{si} psia	P_{hi} psia	P_{he} psia	T_{hi} °F	T_{bs} °F	T_{he} °F	$\dot{m}$ lbs./min.	q Btu/hr.ft.^{2}	c'	ρ_{hi}/ρ_{se}	y
A044	19.29	18.44	16.78	78.5	86.6	83.9	0.498	5522	0.064	69	0.188
A045	19.36	17.98	16.50	79.4	85.2	82.7	0.419	5452	0.036	82	0.300
A046	26.00	24.91	21.49	76.2	103.4	96.2	1.092	8881	0.343	39	0.096
A047	22.69	21.84	18.76	77.7	95.8	89.1	0.558	8846	0.116	91	0.106
A048	20.39	19.36	17.40	78.1	89.2	84.0	0.306	8846	0.037	172	0.181
A049	27.79	27.63	25.98	78.1	109.1	106.2	0.492	8846	0.181	64	0.012
A050	27.49	27.38	25.75	77.9	108.6	105.5	0.449	8916	0.162	72	0.008
A051	25.38	25.12	21.09	76.2	103.7	91.0	0.676	11176	0.172	85	0.024
A052	21.56	20.63	18.75	79.4	92.7	85.3	0.354	11215	0.042	173	0.135
A053	29.81	29.74	27.64	80.0	113.4	109.1	0.458	11395	0.141	87	0.005
A054	29.34	28.92	23.63	74.5	111.9	100.4	0.857	13820	0.242	76	0.029
A055	27.78	27.18	22.26	75.5	108.2	96.2	0.675	13820	0.167	103	0.046
A056	26.45	25.67	21.23	76.0	104.9	93.4	0.544	13777	0.119	132	0.066
A057	24.35	23.27	19.71	76.6	99.3	89.7	0.421	13820	0.072	180	0.111
A058	24.03	22.27	19.11	77.7	96.9	87.9	0.377	14222	0.052	212	0.187
A059	41.50	40.97	38.31	76.6	133.3	129.8	0.841	14470	0.347	37	0.020
A060	41.21	40.50	37.85	76.6	132.5	128.5	0.727	14103	0.303	44	0.027
A061	41.28	40.36	37.76	76.8	132.3	128.4	0.620	14425	0.252	56	0.035
A062	40.40	39.08	36.82	77.3	130.2	126.5	0.471	14381	0.182	79	0.051
A063	38.12	36.23	34.73	78.5	125.4	124.4	0.356	14337	0.123	113	0.080
A064	49.41	49.11	47.39	78.6	145.2	143.8	0.820	14204	0.406	27	0.009
A065	48.39	48.10	46.30	79.2	143.8	142.6	0.670	14238	0.322	38	0.009
A066	48.34	48.01	46.23	79.3	143.7	142.1	0.565	14268	0.279	47	0.010

TABLE II

SOME DATA AND CALCULATED PARAMETERS FOR FREON-11 EXPERIMENTS WITH PARTIAL BOILING AT ONSET OF DENSITY-WAVE TWO-PHASE FLOW OSCILLATIONS (TEST SYSTEM EXTENT: SURGE TANK TO EXIT VALVE)

Exp. No.	P_{si} psia	P_{hi} psia	P_{he} psia	T_{hi} °F	T_{bs} °F	T_{he} °F	$\dot{m}$ $\frac{lbs.}{min.}$	q $\frac{Btu}{hr.ft.^2}$	τ_o sec.	τ_{ie} sec.	τ_{be} sec.	c'	$\frac{\rho_{hi}}{\rho_{se}}$	Y
B001	19.53	19.40	17.51	74.2	89.3	82.7	0.554	5902	1.75	1.48	0.96	0.140	61	0.026
B002	19.19	19.04	17.30	75.0	88.3	81.8	0.482	5890	1.70	1.31	0.87	0.105	71	0.034
B003	19.10	18.92	17.19	75.4	87.9	81.7	0.473	5862	1.51	1.28	0.86	0.097	73	0.042
B004	18.94	18.43	16.89	75.6	86.5	80.5	0.408	5890	1.54	1.11	0.76	0.070	87	0.119
B005	21.05	20.94	19.20	75.6	93.5	87.8	0.645	5890	1.85	1.79	1.16	0.198	46	0.018
B006	21.34	19.80	17.75	69.3	90.4	81.8	0.565	6973	1.67	1.38	0.76	0.171	68	0.232
B007	21.92	19.66	17.66	70.1	90.0	81.0	0.476	6973	1.76	1.25	0.67	0.136	82	0.313
B008	23.71	23.71	22.88	71.1	100.4	94.9	0.464	6523	1.96	1.91	0.96	0.216	52	0.001
B009	23.22	23.15	22.34	71.8	99.0	93.7	0.391	6448	2.00	1.72	0.83	0.171	66	0.008
B010	23.15	22.62	22.23	72.5	97.7	93.7	0.371	6417	1.82	1.63	0.80	0.151	69	0.062
B011	22.22	22.20	19.91	69.0	96.7	87.5	0.604	7788	2.17	1.48	0.73	0.222	62	0.003
B012	27.16	27.03	25.68	71.5	107.9	101.6	0.559	7681	2.50	1.92	0.91	0.277	45	0.010
B013	25.40	25.24	24.34	73.0	103.9	98.4	0.352	7526	2.42	1.48	0.61	0.151	80	0.015
B014	23.50	23.47	20.05	72.3	99.9	87.9	0.618	9962	1.60	1.05	0.47	0.176	84	0.003
B015	23.25	23.08	19.75	73.9	98.9	87.1	0.569	9896	1.50	0.97	0.44	0.149	93	0.020
B016	25.12	24.80	21.85	72.3	102.9	93.9	0.492	9964	1.82	1.08	0.43	0.158	93	0.031
B017	24.26	23.19	21.37	68.2	99.1	92.7	0.296	9984	1.70	0.94	0.29	0.095	156	0.113
B018	29.72	29.67	27.29	70.4	113.3	106.0	0.767	10212	2.94	1.61	0.72	0.337	41	0.003
B019	30.59	30.28	28.26	67.9	114.5	105.2	0.607	10210	2.79	1.60	0.63	0.291	51	0.020
B020	27.34	26.71	24.84	68.5	107.1	98.5	0.408	9999	2.27	1.24	0.42	0.165	93	0.050
B021	33.92	33.91	32.26	69.7	121.4	114.7	0.818	10014	5.20	2.06	0.97	0.443	27	0.000
B022	35.95	35.18	33.72	69.4	123.6	118.0	0.706	9800	5.00	2.11	0.94	0.410	30	0.036

TABLE II (continued)

Exp. No.	P_{si} psia	P_{hi} psia	P_{he} psia	T_{hi} °F	T_{bs} °F	T_{he} °F	$\dot{m}$ lbs./min.	q Btu/hr.ft.^{2}	τ_o sec.	τ_{ie} sec.	τ_{be} sec.	c'	ρ_{hi}/ρ_{se}	y
B023	34.39	34.01	32.35	67.7	121.5	115.4	0.644	9867	4.46	1.97	0.82	0.370	36	0.019
B024	33.49	33.47	31.87	68.6	120.5	113.9	0.517	9970	4.16	1.75	0.64	0.284	51	0.001
B025	34.34	34.19	32.64	71.5	121.8	114.8	0.392	9920	2.60	1.59	0.51	0.209	70	0.008
B026	34.95	34.61	33.15	73.8	122.5	116.0	0.247	10043	2.06	1.37	0.34	0.126	119	0.017
B027	38.61	38.58	37.38	71.9	129.3	123.1	0.238	9966	1.76	1.59	0.37	0.145	107	0.001
B028	26.50	26.44	21.94	71.2	106.7	91.5	0.786	11212	2.08	1.14	0.48	0.259	70	0.005
B029	25.68	25.45	21.24	65.8	104.4	85.5	0.670	11292	2.20	1.15	0.42	0.239	83	0.021
B030	24.97	24.72	20.59	70.1	102.8	86.1	0.552	11609	1.94	0.93	0.34	0.162	110	0.024
B031	23.57	23.06	19.40	67.8	98.8	84.4	0.438	11252	1.68	0.87	0.29	0.125	142	0.056
B032	22.10	21.20	18.25	72.0	94.1	81.8	0.306	11356	1.40	0.61	0.20	0.061	216	0.121
B033	30.29	30.22	27.33	69.1	114.4	103.9	0.693	10942	2.43	1.46	0.59	0.301	52	0.004
B034	29.90	29.61	26.82	72.1	113.2	102.6	0.560	10908	2.25	1.28	0.48	0.221	69	0.019
B035	29.63	29.31	26.56	70.3	112.5	102.6	0.480	11187	2.27	1.21	0.41	0.190	84	0.022
B036	28.11	27.70	25.44	71.7	109.2	99.8	0.366	11593	1.95	0.98	0.29	0.124	123	0.031
B037	36.87	36.79	34.48	72.3	126.4	117.1	0.658	11600	2.69	1.61	0.62	0.323	43	0.003
B038	37.78	36.59	25.88	67.82	126.0	114.6	0.568	11656	2.69	1.43	0.37	0.299	117	0.009
B039	36.90	36.64	34.51	73.0	126.1	116.7	0.489	11656	2.59	1.44	0.47	0.235	62	0.012
B040	33.96	33.61	31.78	66.3	120.7	111.1	0.379	11283	1.77	1.41	0.39	0.192	87	0.019
B041	29.93	29.84	24.41	70.3	113.7	96.2	0.815	14354	2.00	0.99	0.35	0.258	79	0.006
B042	28.71	28.21	23.03	69.4	110.4	93.1	0.687	14310	1.60	0.90	0.30	0.206	99	0.036
B043	28.24	27.62	22.47	72.0	109.1	91.9	0.547	14837	1.59	0.76	0.23	0.143	135	0.046
B044	24.66	24.18	20.14	70.9	101.5	87.0	0.400	14284	1.38	0.63	0.18	0.089	194	0.049
B045	33.10	32.41	28.14	75.6	118.6	104.4	0.760	14310	1.75	1.01	0.38	0.240	67	0.038
B046	31.45	30.67	26.77	76.1	115.2	102.2	0.630	14398	1.87	0.89	0.31	0.180	87	0.047
B047	29.40	28.63	25.02	74.7	112.2	99.2	0.487	14310	1.81	0.78	0.24	0.130	122	0.052

TABLE II (continued)

Exp. No.	P_{si} psia	P_{hi} psia	P_{he} psia	T_{hi} °F	T_{bs} °F	T_{he} °F	$\dot{m}$ $\frac{lbs.}{min.}$	q $\frac{Btu}{hr.ft.^2}$	τ_o sec.	τ_{ie} sec.	τ_{be} sec.	c'	$\frac{\rho_{hi}}{\rho_{se}}$	Y
B048	38.49	38.38	34.78	77.4	129.1	118.0	0.977	14398	2.50	1.30	0.55	0.369	37	0.005
B049	37.90	37.56	34.34	68.1	127.7	117.1	0.848	14310	2.85	1.40	0.56	0.372	41	0.015
B050	38.00	37.53	34.33	68.9	127.7	117.1	0.716	14310	2.63	1.32	0.45	0.309	51	0.020
B051	36.78	36.25	33.49	70.1	125.5	115.4	0.704	14310	2.22	1.25	0.43	0.287	53	0.024
B052	34.79	33.94	31.82	71.3	121.4	112.9	0.711	14310	1.92	1.16	0.42	0.261	55	0.043
B053	38.94	38.66	31.76	72.1	129.7	109.4	1.363	19950	2.00	0.94	0.34	0.412	49	0.012
B054	37.61	36.64	29.44	73.0	126.2	105.1	1.104	19950	1.60	0.84	0.28	0.309	69	0.042
B055	32.03	31.12	24.82	73.0	116.1	96.6	0.773	19950	1.43	0.65	0.19	0.176	119	0.053
B056	37.99	37.03	29.73	69.4	126.9	106.1	1.027	20053	1.82	0.87	0.27	0.309	73	0.041
B057	41.11	40.84	35.07	67.7	133.2	116.4	1.109	19660	1.90	1.05	0.35	0.387	48	0.010
B058	40.24	39.41	33.78	70.7	130.9	114.2	0.994	19683	1.62	0.95	0.31	0.319	58	0.032
B059	38.28	37.22	31.96	71.5	127.2	111.3	0.860	19660	1.77	0.86	0.26	0.256	72	0.045
B060	35.80	34.26	29.73	72.1	122.0	108.2	0.733	19629	1.58	0.76	0.22	0.196	92	0.073
B061	45.24	45.01	40.47	66.9	139.6	128.5	1.194	20053	3.15	1.18	0.42	0.454	34	0.008
B062	46.53	45.78	41.44	68.1	140.7	126.8	1.098	20053	1.75	1.16	0.40	0.418	37	0.024
B063	45.50	44.76	40.50	68.5	139.2	125.6	0.988	2053	2.14	1.10	0.36	0.366	43	0.024
B064	44.60	43.75	39.65	69.0	137.6	124.7	0.878	20001	1.89	1.04	0.32	0.317	52	0.028
B065	42.31	41.19	37.74	69.5	133.6	122.2	0.753	19950	1.60	0.95	0.27	0.255	65	0.041
B066	37.10	35.16	32.24	70.2	123.5	110.7	0.596	20053	1.59	0.76	0.20	0.167	102	0.087
B067	45.85	45.36	37.78	66.8	140.2	118.6	1.587	25312	2.14	0.90	0.29	0.481	43	0.016
B068	45.14	44.28	36.45	67.8	138.6	116.3	1.471	25312	1.90	0.86	0.27	0.431	49	0.028
B069	44.08	43.38	35.17	68.6	137.2	114.6	1.344	25312	1.85	0.81	0.25	0.382	58	0.024
B070	42.98	41.76	33.54	69.4	134.7	112.0	1.201	25312	1.47	0.76	0.22	0.325	70	0.043
B071	41.39	39.74	31.48	70.3	131.4	108.7	1.073	25428	1.30	0.69	0.19	0.271	86	0.062
B072	37.96	36.13	28.31	71.7	1253	103.5	0.937	25428	1.35	0.60	0.16	0.208	112	0.079

TABLE III

SOME DATA AND CALCULATED PARAMETERS FOR FREON-11 EXPERIMENTS WITH SUPERHEAT AT ONSET OF DENSITY-WAVE TWO-PHASE FLOW OSCILLATIONS (TEST SYSTEM EXTENT: SURGE TANK TO EXIT PLENUM)

Exp. No.	P_{si} psia	P_{hi} psia	P_{he} psia	P_{ep} psia	T_{hi} °F	T_{bs} °F	T_{he} °F	T_{ep} °F	$\dot{m}$ $\frac{lbs.}{min.}$	q $\frac{Btu}{hr.ft.^2}$	c'	$\frac{\rho_{hi}}{\rho_v}$	$\frac{\rho_{hi}}{\rho_{se}}$	y
C001	32.83	30.31	24.47	20.59	75.2	114.5	324.3	270.8	0.393	23267	0.101	140	251	0.139
C002	34.57	32.22	25.50	20.99	75.4	118.2	256.5	179.1	0.418	23267	0.110	135	213	0.118
C003	36.38	33.92	26.78	21.91	75.7	121.3	199.8	132.4	0.456	23267	0.117	132	187	0.114
C004	38.34	35.90	28.30	22.98	75.9	124.8	145.4	104.2	0.510	23267	0.126	130	169	0.104
C005	39.05	36.78	28.99	23.48	76.5	126.3	85.0	71.8	0.549	23267	0.128	132	154	0.093
C006	39.21	35.29	28.01	22.80	69.9	123.8	105.9	81.5	0.540	23109	0.137	137	163	0.159
C007	37.96	34.77	27.20	21.88	71.2	122.8	142.1	95.4	0.497	23185	0.131	135	175	0.137
C008	37.17	34.37	26.86	21.60	72.1	122.1	167.7	157.9	0.467	21278	0.128	137	200	0.125
C009	36.39	32.85	25.76	20.94	72.9	119.3	219.4	137.4	0.435	23467	0.119	135	199	0.163
C010	29.55	27.93	22.88	19.08	71.0	109.7	94.7	74.9	0.394	16807	0.099	167	194	0.110
C011	28.64	26.60	21.84	18.65	73.0	106.9	149.5	124.7	0.376	17013	0.087	168	219	0.147
C012	28.32	26.16	21.53	18.45	73.0	105.9	160.9	110.3	0.354	17013	0.085	168	215	0.160
C013	45.04	40.52	32.09	26.01	73.0	132.6	152.4	121.2	0.624	28334	0.151	117	154	0.149
C014	44.01	38.95	30.73	24.92	73.4	130.0	193.5	142.8	0.573	28334	0.143	118	167	0.173
C015	41.02	37.14	29.07	23.54	73.9	127.0	264.1	165.5	0.489	28334	0.135	118	185	0.148
C016	55.61	49.77	39.36	31.42	72.3	146.1	127.1	109.3	0.803	34570	0.184	100	123	0.143
C017	54.04	48.16	38.05	30.54	72.5	143.9	161.1	125.7	0.751	34887	0.178	99	131	0.150
C018	53.61	47.42	37.40	30.05	73.0	142.9	191.0	150.4	0.722	35187	0.174	99	140	0.159
C019	52.18	46.35	36.78	29.86	73.4	141.4	219.1	175.5	0.687	34887	0.170	99	147	0.156
C020	50.36	45.02	35.64	28.97	73.9	139.5	247.8	182.1	0.650	35274	0.164	100	154	0.150
C021	32.41	31.02	26.12	22.73	73.0	115.9	102.6	81.6	0.408	17117	0.110	147	163	0.079
C022	31.30	29.59	24.96	21.81	73.0	113.1	101.8	71.6	0.377	17126	0.103	150	167	0.103
C023	29.91	28.46	24.12	21.20	73.4	110.8	129.3	73.9	0.346	17114	0.096	151	173	0.095

TABLE III (continued)

Exp. No.	P_{si} psia	P_{hi} psia	P_{he} psia	P_{ep} psia	T_{hi} °F	T_{bs} °F	T_{he} °F	T_{ep} °F	$\dot{m}$ $\frac{lbs.}{min.}$	q $\frac{Btu}{hr.ft.^2}$	c'	$\frac{\rho_{hi}}{\rho_v}$	$\frac{\rho_{hi}}{\rho_{se}}$	y
C024	29.22	27.78	23.64	20.91	73.9	109.4	172.4	83.4	0.314	17114	0.091	151	179	0.099
C025	29.07	27.58	23.49	20.81	74.7	109.0	183.7	68.4	0.273	17114	0.088	149	174	0.104
C026	39.32	36.59	30.26	25.82	73.0	126.0	147.3	92.3	0.482	23009	0.135	123	146	0.111
C027	38.17	35.46	29.50	25.38	73.4	124.0	189.2	116.2	0.448	23009	0.129	123	156	0.115
C028	36.08	33.70	27.86	23.89	73.9	120.9	238.0	154.2	0.418	23009	0.120	128	179	0.111
C029	48.68	45.67	37.57	31.50	74.1	140.4	124.3	119.4	0.650	27291	0.167	105	125	0.089
C030	47.48	43.85	36.24	30.68	74.7	137.7	153.8	138.6	0.614	27289	0.159	106	133	0.110
C031	46.20	42.43	35.00	29.69	75.2	135.6	186.6	140.6	0.566	27471	0.152	106	139	0.120
C032	45.03	41.65	34.27	29.04	75.2	134.3	203.7	148.0	0.545	27455	0.149	107	144	0.111
C033	44.14	40.67	33.41	28.34	75.2	132.8	225.7	145.3	0.510	27465	0.145	108	147	0.118
C034	59.78	53.66	44.85	38.02	70.5	151.0	138.9	123.5	0.795	34887	0.198	88	103	0.136
C035	58.60	52.68	44.14	37.63	70.7	149.8	169.4	146.5	0.751	34887	0.195	88	109	0.135
C036	56.79	51.26	42.51	35.98	71.6	148.0	200.2	171.3	0.714	34887	0.189	89	120	0.131
C037	55.51	48.66	40.32	34.25	72.1	144.6	244.1	200.5	0.660	34887	0.179	92	133	0.168
C038	54.44	47.49	39.04	33.00	72.5	143.0	286.4	238.4	0.620	34887	0.174	93	148	0.175
C039	35.10	33.47	29.23	26.25	72.1	120.5	110.5	80.7	0.393	17089	0.123	132	140	0.080
C040	32.99	31.27	27.69	25.27	73.9	116.3	193.5	117.8	0.330	17089	0.109	134	157	0.095
C041	46.86	43.98	38.37	34.25	74.7	137.9	127.3	103.7	0.538	23267	0.159	102	110	0.090
C042	45.93	43.05	37.74	33.91	75.0	136.5	145.2	98.9	0.502	23267	0.155	102	110	0.092
C043	44.95	41.77	36.71	33.12	75.2	134.5	182.7	120.1	0.467	23267	0.149	103	118	0.105
C044	42.45	39.66	35.07	31.89	75.4	131.1	251.0	163.8	0.415	23267	0.141	106	134	0.101
C045	54.63	50.09	44.21	39.77	71.2	146.5	150.8	124.3	0.620	28087	0.185	89	98	0.114
C046	53.46	48.72	43.17	39.08	71.9	144.7	195.7	148.7	0.566	28087	0.179	89	105	0.122
C047	51.10	46.86	41.45	37.59	72.3	142.1	241.2	146.1	0.496	28087	0.172	91	109	0.117
C048	47.38	43.33	37.72	33.84	73.0	136.9	311.6	186.2	0.441	28087	0.159	97	132	0.124
C049	64.09	56.13	49.27	44.09	70.5	154.0	226.1	198.8	0.673	34119	0.204	78	102	0.161
C050	61.00	54.71	47.96	42.94	69.6	152.3	248.2	195.5	0.634	34119	0.201	80	104	0.136

TABLE IV

SOME DATA AND CALCULATED PARAMETERS FOR FREON-11 SUBCOOLING EXPERIMENTS AT ONSET OF DENSITY-WAVE TWO-PHASE FLOW OSCILLATIONS (TEST SYSTEM EXTENT: SURGE TANK TO EXIT VALVE)

Exp. No.	P_{si} psia	P_{hi} psia	P_{he} psia	T_{hi} °F	T_{bs} °F	T_{he} °F	$\dot{m}$ $\frac{lbs.}{min.}$	q $\frac{Btu}{hr.ft.^2}$	c'	$\frac{\rho_{hi}}{\rho_{se}}$	y
D001	43.77	43.52	37.89	73.9	137.3	126.2	1.151	19950	0.384	43	0.009
D002	43.55	43.44	37.40	80.2	137.2	124.7	0.899	19950	0.270	60	0.004
D003	43.33	43.25	37.20	84.2	136.9	124.7	0.841	19950	0.234	66	0.003
D004	44.00	43.96	37.70	86.8	137.9	125.5	0.771	19950	0.209	72	0.001
D005	44.59	44.53	38.14	90.54	138.8	126.4	0.719	19950	0.184	78	0.002
D006	45.89	45.71	39.42	89.4	140.5	128.3	0.937	20053	0.252	56	0.006
D007	45.94	45.86	39.50	93.6	140.7	128.5	0.883	20053	0.220	61	0.003
D008	48.83	48.60	41.61	102.6	144.6	131.4	0.983	20053	0.219	53	0.007
D009	51.28	51.09	43.87	110.3	147.9	135.6	1.052	20053	0.211	48	0.005
D010	52.09	51.90	44.54	115.6	148.9	136.4	1.078	20053	0.192	47	0.005
D011	30.79	30.68	24.62	76.7	115.3	99.3	0.790	14398	0.222	85	0.007
D012	37.38	37.31	33.58	82.23	127.3	118.0	0.657	14398	0.217	64	0.003
D013	39.19	39.11	35.14	87.0	130.3	121.1	0.700	14398	0.222	57	0.003
D014	40.36	40.24	36.24	90.8	132.1	123.0	0.732	14544	0.220	54	0.005
D015	41.47	41.34	37.06	94.4	133.9	124.7	0.784	14691	0.223	50	0.005
D016	42.86	42.68	37.91	105.6	136.0	126.8	0.828	14485	0.185	48	0.006
D017	44.53	44.35	39.35	110.4	138.5	128.9	0.880	14485	0.182	44	0.006
D018	46.98	46.69	41.49	119.0	141.9	132.2	0.962	14485	0.163	40	0.009
D019	48.64	48.25	42.84	123.1	144.1	134.9	1.059	14485	0.164	35	0.012
D020	24.61	24.46	21.76	72.2	102.2	94.7	0.531	8528	0.194	72	0.015
D021	24.54	24.46	21.91	76.6	102.1	95.3	0.496	8528	0.155	78	0.007

TABLE IV (continued)

Exp. No.	P_{si} psia	P_{hi} psia	P_{he} psia	T_{hi} °F	T_{bs} °F	T_{he} °F	$\dot{m}$ lbs./min.	q Btu/hr.ft.^{2}	c'	ρ_{hi}/ρ_{se}	y
D022	25.25	25.16	22.21	84.5	103.7	95.8	0.438	8528	0.103	92	0.008
D023	26.21	26.12	22.98	91.8	105.9	97.9	0.510	8528	0.088	79	0.008
D024	26.65	26.52	23.21	95.7	106.7	99.2	0.408	8528	0.056	99	0.011
D025	24.95	24.87	22.06	96.6	103.1	94.9	0.362	8385	0.029	114	0.008
D026	45.69	45.40	40.25	79.6	140.1	130.5	1.084	19575	0.353	41	0.009
D027	45.32	45.22	39.96	85.1	139.8	129.3	0.852	19575	0.251	57	0.003
D028	45.86	45.69	40.30	89.7	140.5	129.8	0.822	19575	0.226	60	0.005
D029	46.69	46.52	40.96	94.7	141.7	131.4	0.841	19575	0.214	58	0.005
D030	53.75	53.12	46.64	110.8	150.5	140.5	1.318	19575	0.287	33	0.016
D031	38.85	38.65	33.92	74.3	129.6	118.4	0.880	14926	0.342	47	0.008
D032	39.54	39.36	34.37	80.7	130.7	118.9	0.739	15225	0.255	60	0.007
D033	42.48	42.29	36.81	91.6	135.4	123.4	0.867	15225	0.263	49	0.007
D034	43.80	43.61	37.84	99.2	137.4	125.6	0.908	15225	0.242	46	0.006
D035	47.72	47.36	41.13	110.3	142.9	131.4	1.104	14926	0.256	35	0.011
D036	51.88	51.48	44.97	118.8	148.4	137.0	1.162	14987	0.246	31	0.011
D037	52.67	52.26	45.51	123.0	149.4	138.0	1.201	14987	0.227	31	0.011
D038	55.02	54.71	47.64	128.9	152.4	141.3	1.240	14987	0.211	29	0.008
D039	49.73	49.53	44.39	80.3	145.8	135.5	0.822	19982	0.285	52	0.006
D040	50.17	50.02	44.86	83.5	146.4	135.7	0.809	19982	0.270	53	0.004
D041	51.55	51.39	46.05	87.7	148.2	137.6	0.867	19982	0.279	48	0.004
D042	53.36	53.05	47.80	93.6	150.3	139.8	0.905	19982	0.274	44	0.008
D043	56.15	55.84	50.11	99.8	153.7	143.4	0.982	19982	0.284	39	0.007
D044	58.60	58.33	52.40	109.1	156.7	146.5	1.072	19950	0.276	35	0.006
D045	60.76	60.39	54.30	113.9	159.3	148.9	1.110	19950	0.273	33	0.008

TABLE V

SOME DATA AND CALCULATED PARAMETERS FOR FREON-11 SUBCOOLING EXPERIMENTS AT ONSET OF DENSITY-WAVE TWO-PHASE FLOW OSCILLATIONS (TEST SYSTEM EXTENT: SURGE TANK TO EXIT TUBING - NO EXIT VALVE)

Exp. No.	P_{si} psia	P_{hi} psia	P_{he} psia	T_{hi} °F	T_{bs} °F	T_{he} °F	$\dot{m}$ $\frac{lbs.}{min.}$	q $\frac{Btu}{hr.ft.^2}$	c'	$\frac{\rho_{hi}}{\rho_{se}}$	Y
E001	48.82	48.44	38.42	71.6	144.5	123.0	1.490	25257	0.451	52	0.011
E002	48.97	48.75	37.23	82.3	144.8	120.1	1.198	25257	0.313	72	0.006
E003	56.02	55.69	42.00	110.7	153.6	126.4	1.369	25621	0.247	61	0.008
E004	53.85	53.63	40.53	102.4	151.1	126.4	1.311	25621	0.266	65	0.006
E005	59.05	58.41	43.94	118.2	156.9	132.2	1.471	25806	0.239	56	0.014
E006	40.45	40.21	31.01	73.9	132.2	110.5	1.136	19846	0.350	70	0.009
E007	41.28	41.06	30.88	85.5	133.5	110.0	1.037	19846	0.264	82	0.008
E008	44.00	43.63	32.55	97.5	137.5	114.2	1.097	19846	0.234	76	0.012
E009	48.44	47.86	35.94	107.8	143.7	120.5	1.341	19846	0.257	59	0.017
E010	50.08	49.70	36.66	120.2	146.1	121.8	1.259	19846	0.176	64	0.011
E011	33.07	32.97	25.54	74.1	119.7	100.3	0.937	14514	0.309	75	0.006
E012	33.48	33.38	25.12	87.9	120.4	99.4	0.784	14719	0.183	98	0.005
E013	38.43	38.19	28.80	96.5	128.9	107.8	1.080	14808	0.264	63	0.010
E014	38.73	38.51	28.28	107.8	129.4	106.7	0.969	14808	0.151	79	0.009
E015	39.66	39.45	28.58	115.0	130.9	107.8	0.943	14808	0.108	83	0.008
E016	26.82	26.70	21.57	73.9	107.2	92.3	0.746	11215	0.231	80	0.010
E017	26.97	26.87	21.18	82.2	107.5	90.1	0.566	11215	0.134	113	0.008
E018	30.64	30.53	23.27	93.1	115.0	95.7	0.777	11215	0.160	83	0.007
E019	29.47	29.38	22.21	97.9	112.7	93.1	0.552	11215	.078	120	0.006
E020	29.61	29.53	22.21	100.9	113.0	92.3	0.503	11215	.058	132	0.005
E021	35.89	35.70	27.73	69.4	124.6	104.3	1.048	16792	0.361	71	0.009

TABLE V (continued)

Exp. No.	P_{si} psia	P_{hi} psia	P_{he} psia	T_{hi} °F	T_{bs} °F	T_{he} °F	$\dot{m}$ $\frac{lbs.}{min.}$	q $\frac{Btu}{hr.ft.^2}$	c'	$\frac{\rho_{hi}}{\rho_{se}}$	y
E022	36.79	36.60	27.82	81.4	126.1	104.4	0.937	16792	0.263	83	0.009
E023	39.02	38.85	29.28	90.2	129.9	107.8	1.023	16792	0.255	75	0.007
E024	43.43	43.13	32.42	103.7	136.8	114.7	1.269	16792	0.264	59	0.010
E025	41.77	41.53	30.56	108.8	134.3	111.2	1.168	16792	0.188	69	0.009
E026	43.38	43.12	31.44	113.5	136.7	112.9	1.072	17013	0.155	75	0.009
E027	40.45	40.20	31.38	70.4	132.2	112.0	1.227	19846	0.400	63	0.010
E028	40.70	40.48	30.77	78.6	132.6	110.5	1.052	19846	0.301	78	0.008
E029	42.36	42.15	31.52	89.0	135.2	112.0	1.062	19846	0.261	80	0.008
E030	43.54	43.32	32.65	94.0	137.0	113.7	1.072	19846	0.245	76	0.007
E031	50.01	49.66	37.35	110.0	146.1	122.4	1.350	19846	0.261	56	0.010
E032	52.85	52.42	38.45	128.7	149.6	125.1	1.305	19846	0.148	60	0.011
E033	51.28	50.87	37.14	131.0	147.6	123.3	1.227	19846	0.110	66	0.011
E034	44.38	44.04	34.02	75.2	138.1	115.8	1.227	22642	0.358	67	0.011
E035	44.87	44.65	33.92	82.5	139.0	115.4	1.117	22642	0.294	77	0.007
E036	46.19	45.89	34.70	88.1	140.8	117.1	1.065	22642	0.261	79	0.010
E037	48.99	48.57	36.79	98.3	144.6	120.5	1.220	22642	0.264	67	0.012
E038	49.67	49.25	37.29	103.5	145.5	121.8	1.240	22752	0.243	66	0.012
E039	55.75	55.06	24.03	111.3	152.9	131.0	1.638	22752	3.077	45	0.017
E040	59.67	59.04	43.51	137.0	157.7	133.9	1.446	22752	0.144	55	0.014
E041	23.07	23.00	18.94	71.0	98.7	85.4	0.607	8496	0.205	82	0.008
E042	23.26	23.17	19.10	75.5	99.1	85.7	0.464	8496	0.133	107	0.012
E043	24.86	24.77	19.85	80.8	102.9	88.0	0.657	8496	0.177	79	0.009
E044	24.49	24.39	19.28	88.8	102.0	87.2	0.505	8496	0.081	108	0.010
E045	23.51	23.42	18.88	91.0	99.7	85.3	0.393	8564	0.041	138	0.010

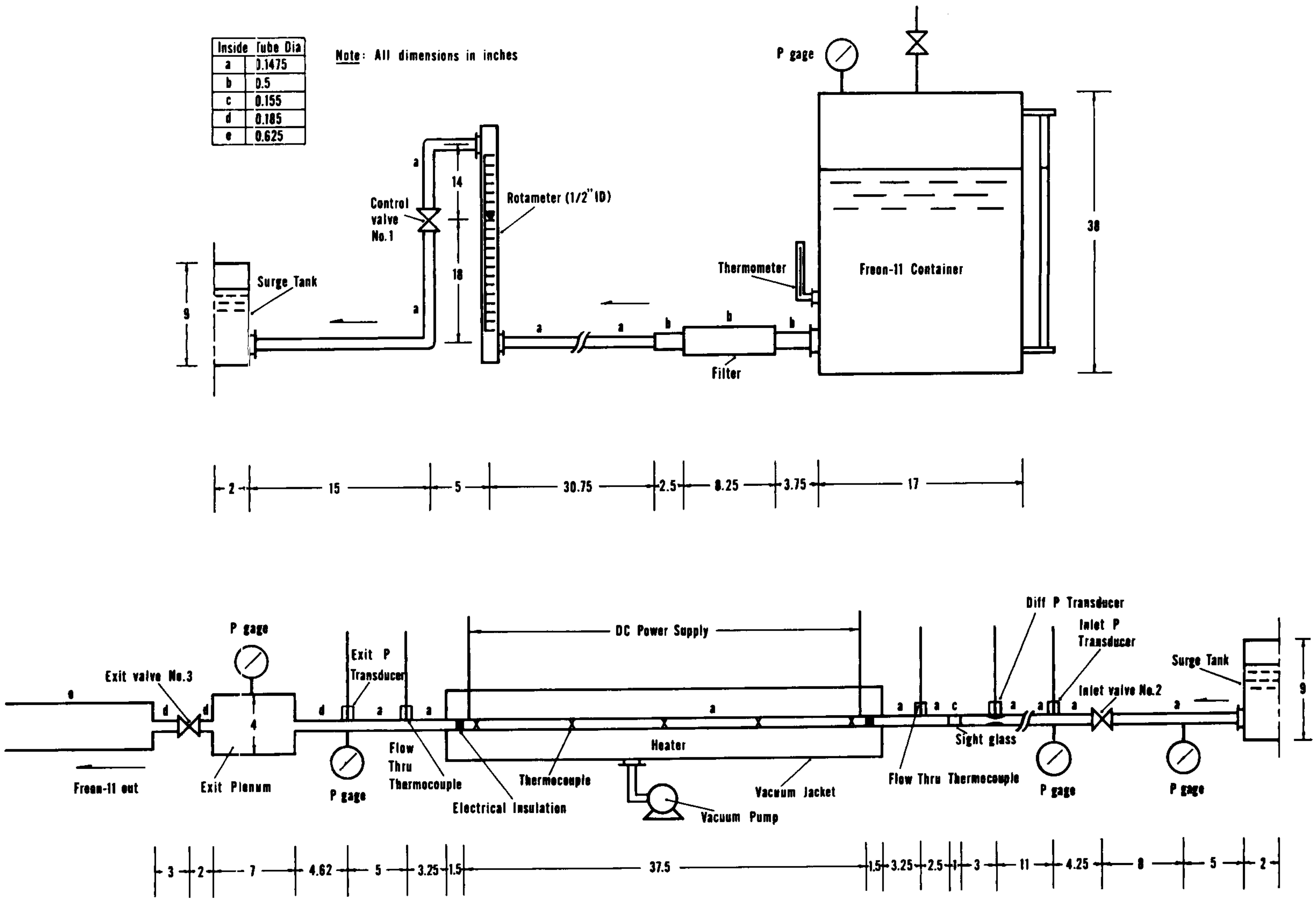

FIG. 1.- SCHEMATIC DIAGRAM OF FREON-II BOILING FLOW APPARATUS

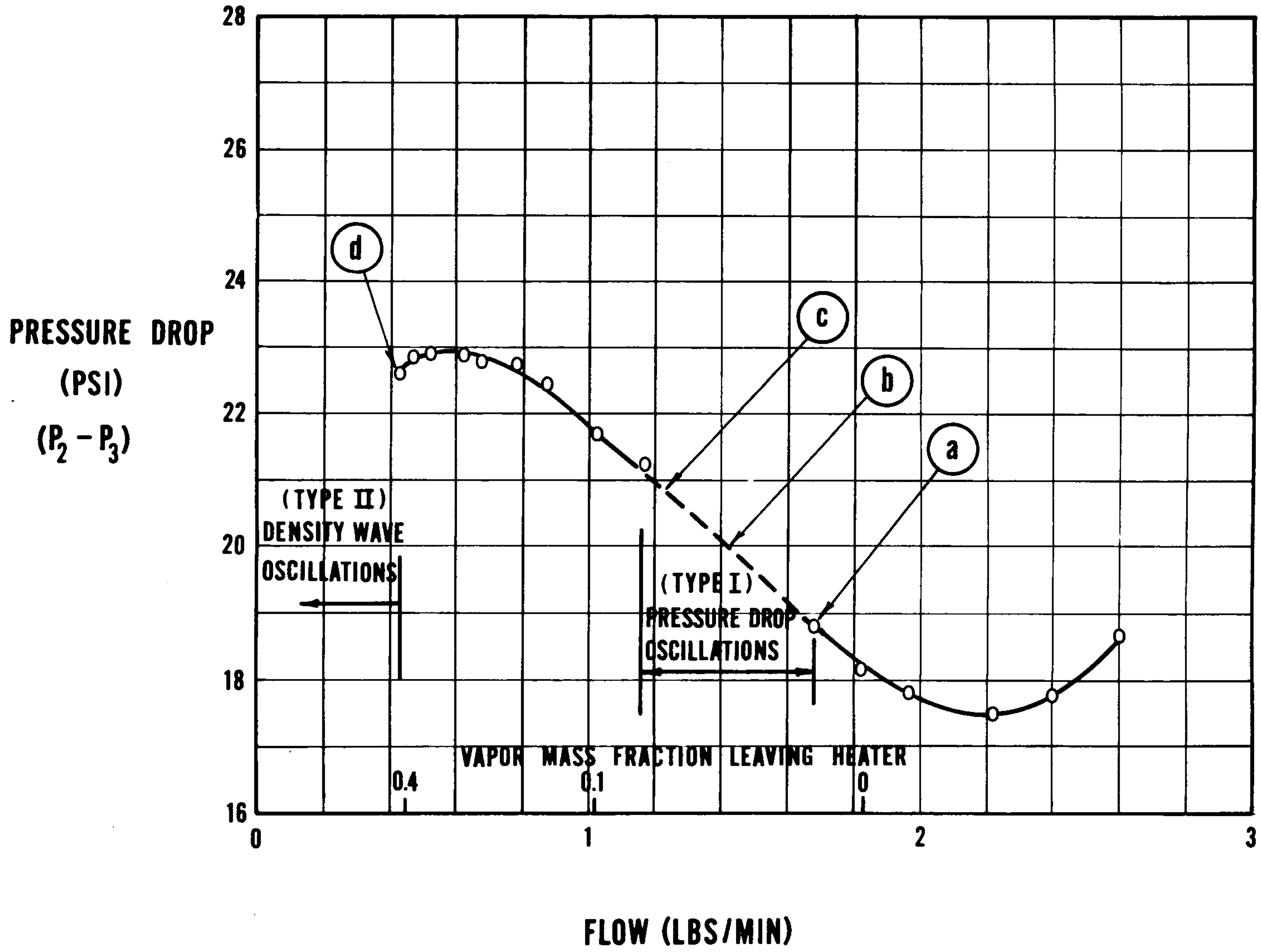

FIG. 2.—PRESSURE DROP VERSUS FLOW FOR TEST SECTION AT 344 WATTS

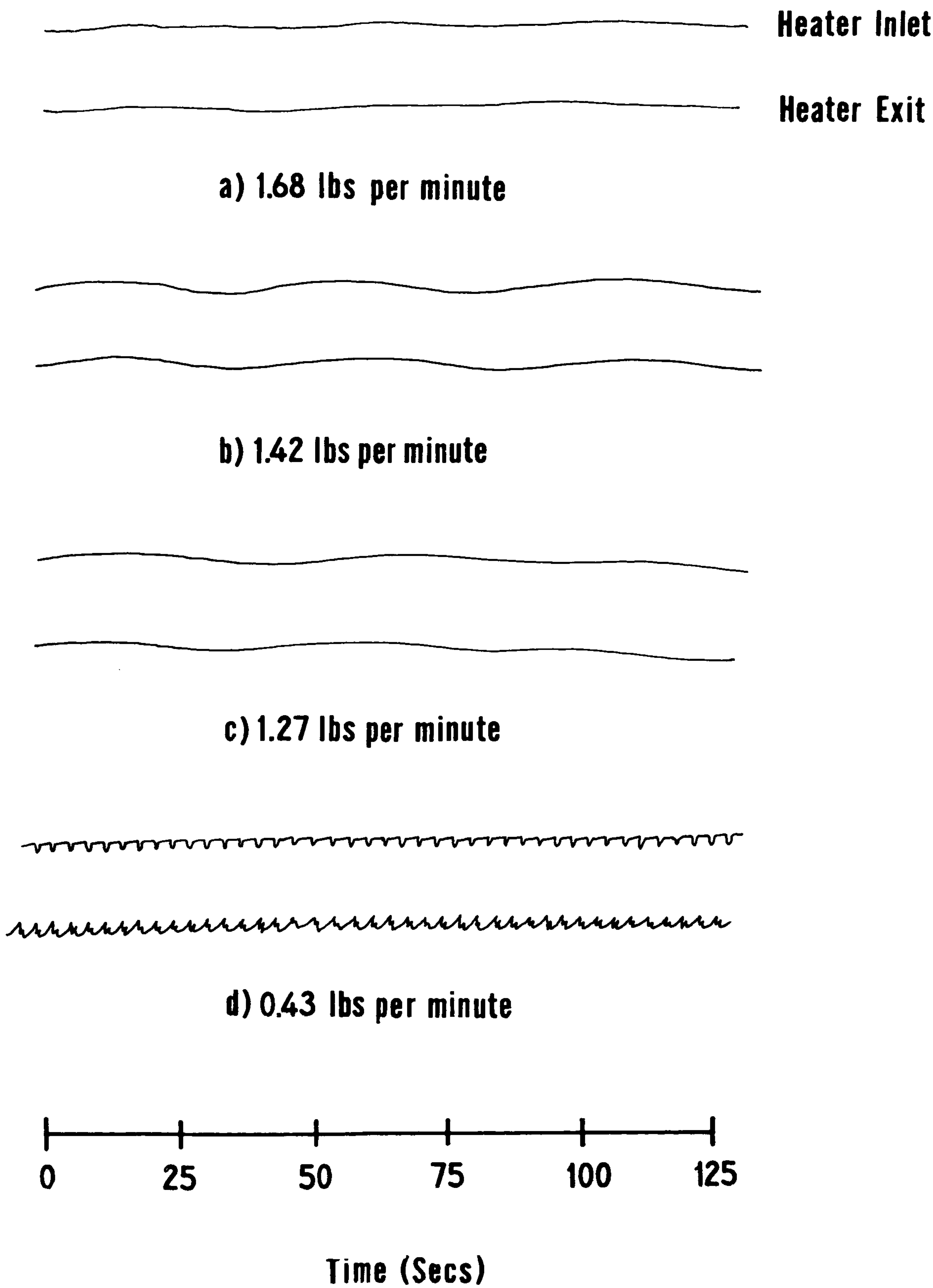

FIG. 3.– PRESSURE OSCILLATIONS AT 344 WATTS

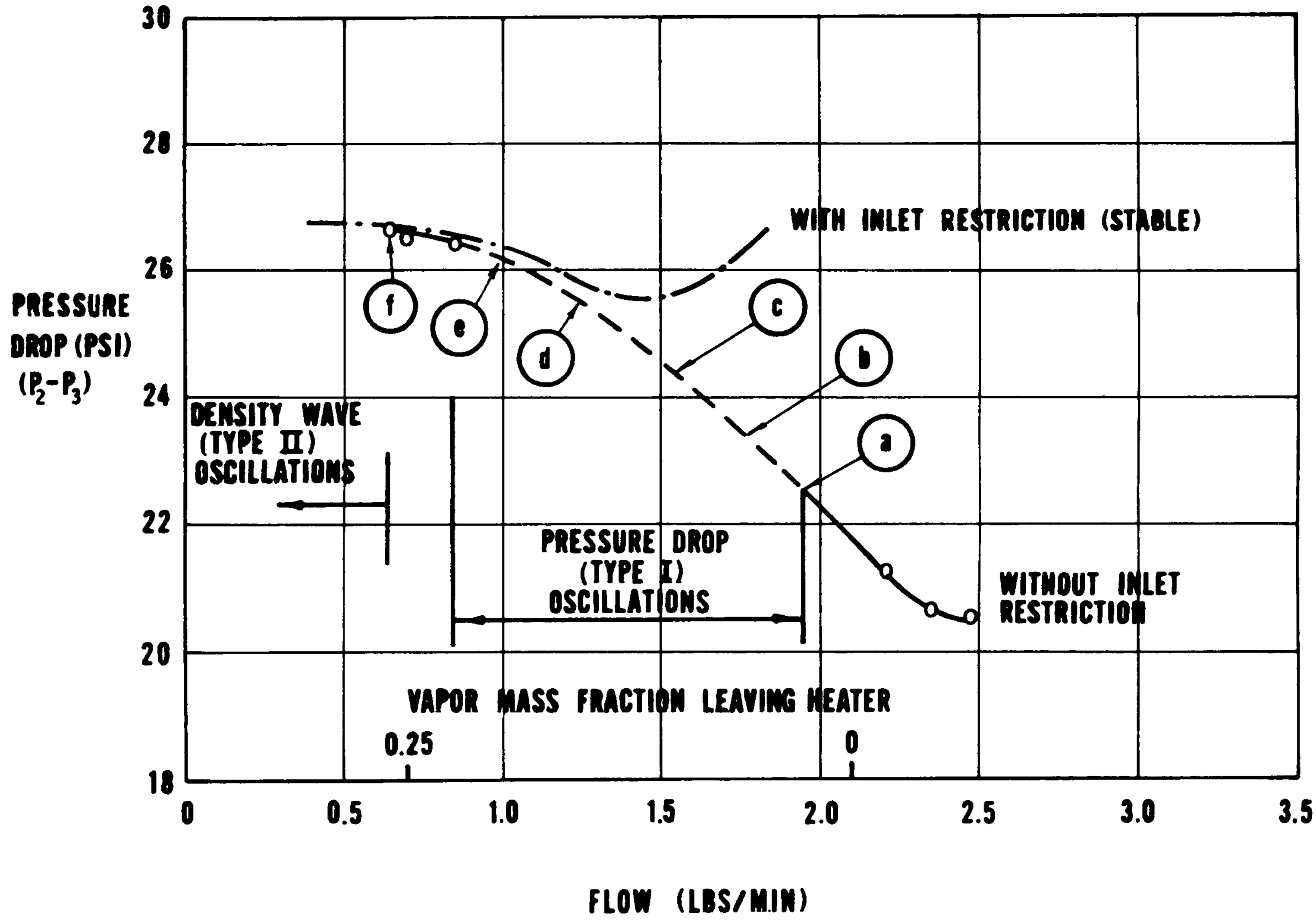

FIG. 4.—PRESSURE DROP VERSUS FLOW FOR TEST SECTION AT 389 WATTS

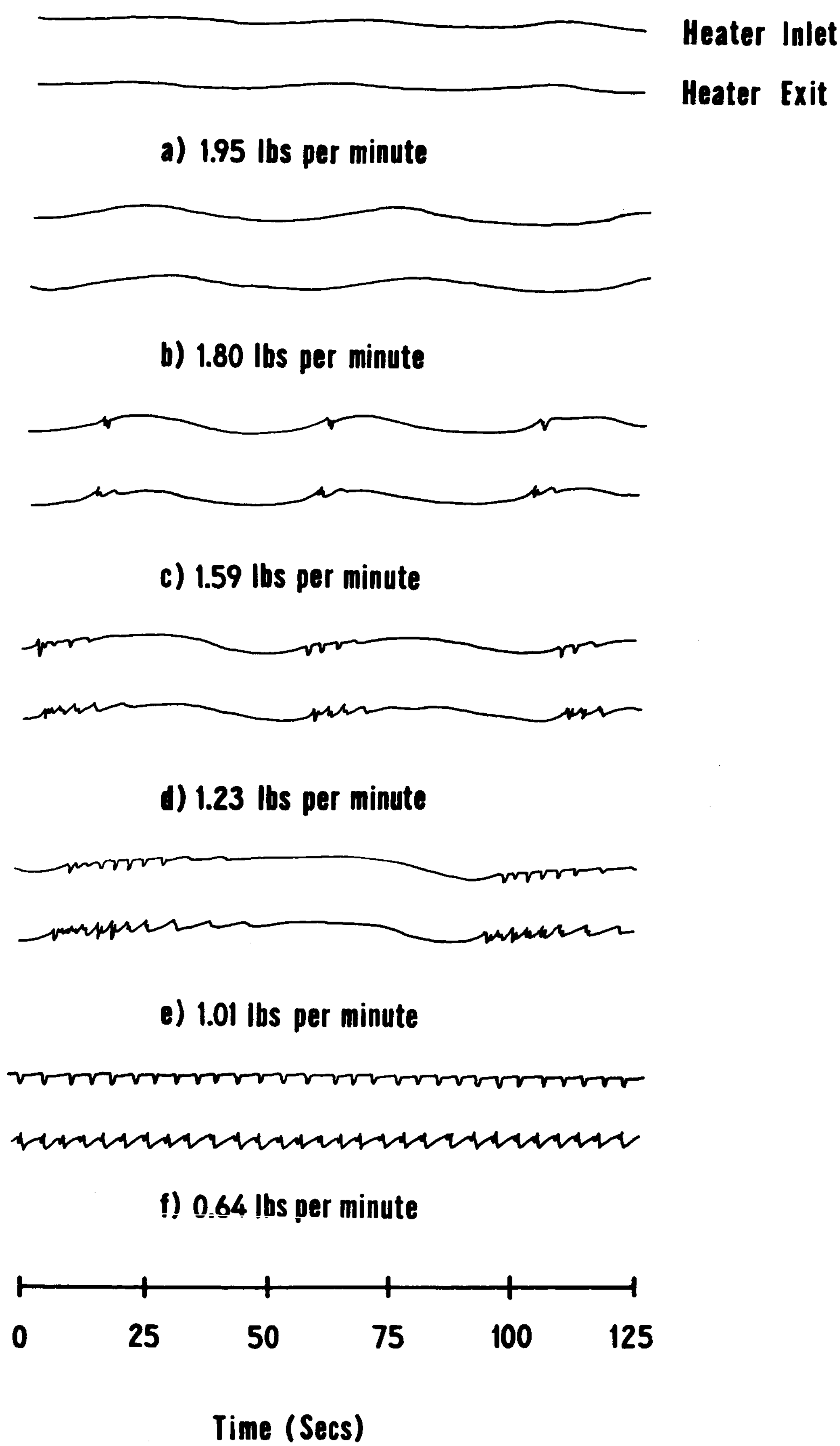

FIG 5.—PRESSURE OSCILLATIONS AT 389 WATTS

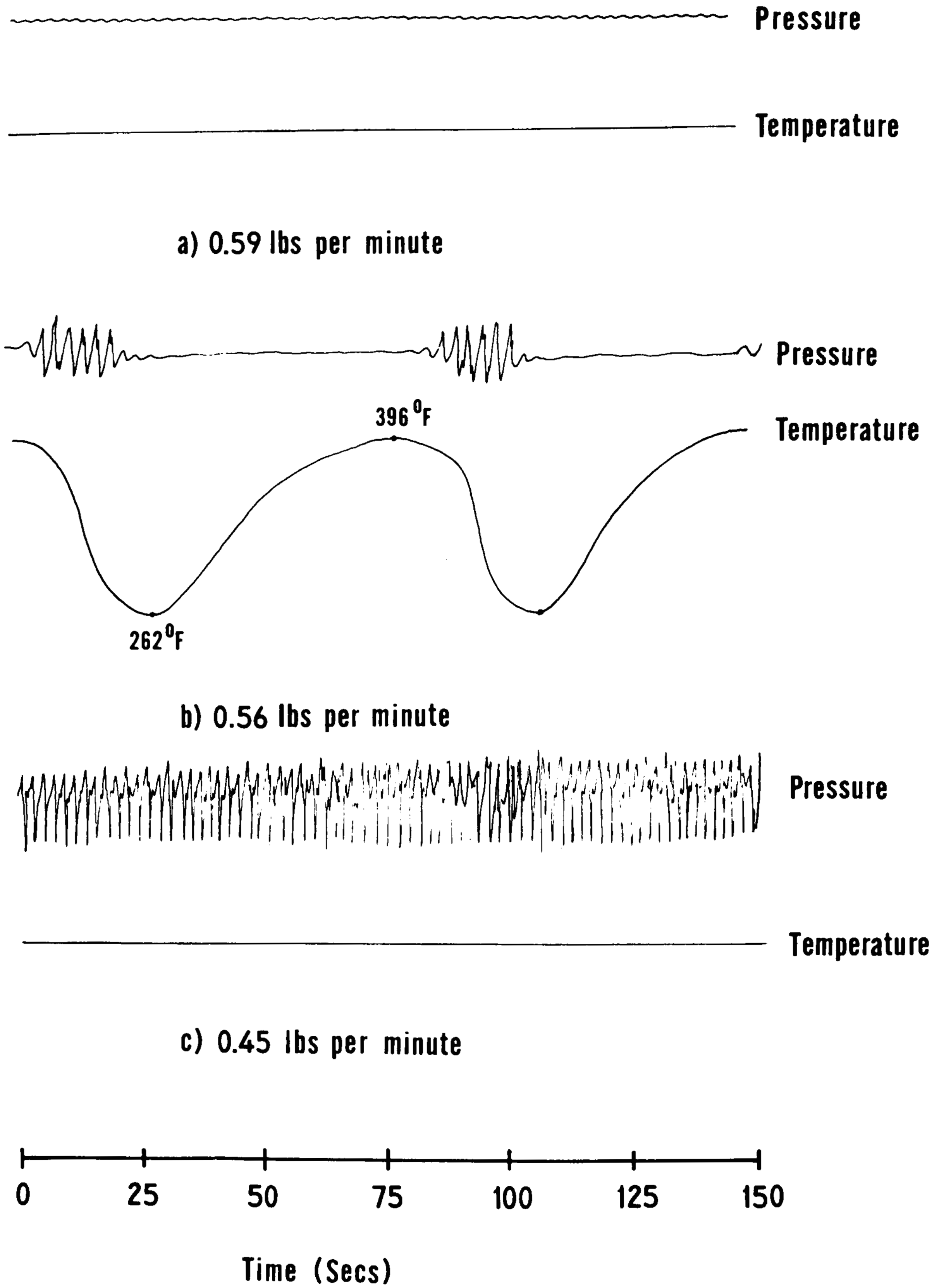

FIG. 6.—PRESSURE AND TEMPERATURE OSCILLATIONS AT 700 WATTS

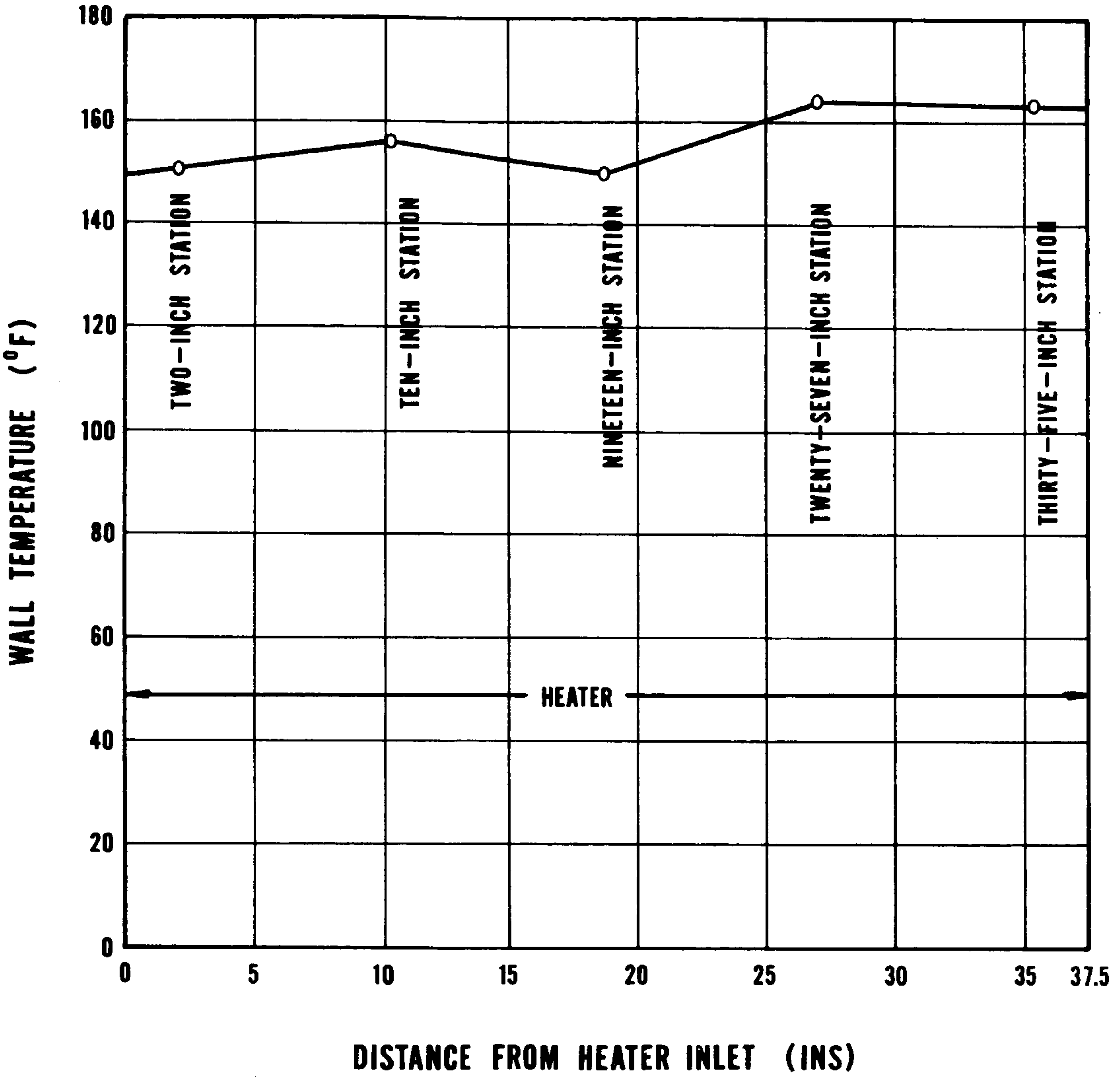

FIG. 7.—HEATER WALL TEMPERATURE AT 700 WATTS BEFORE OSCILLATIONS

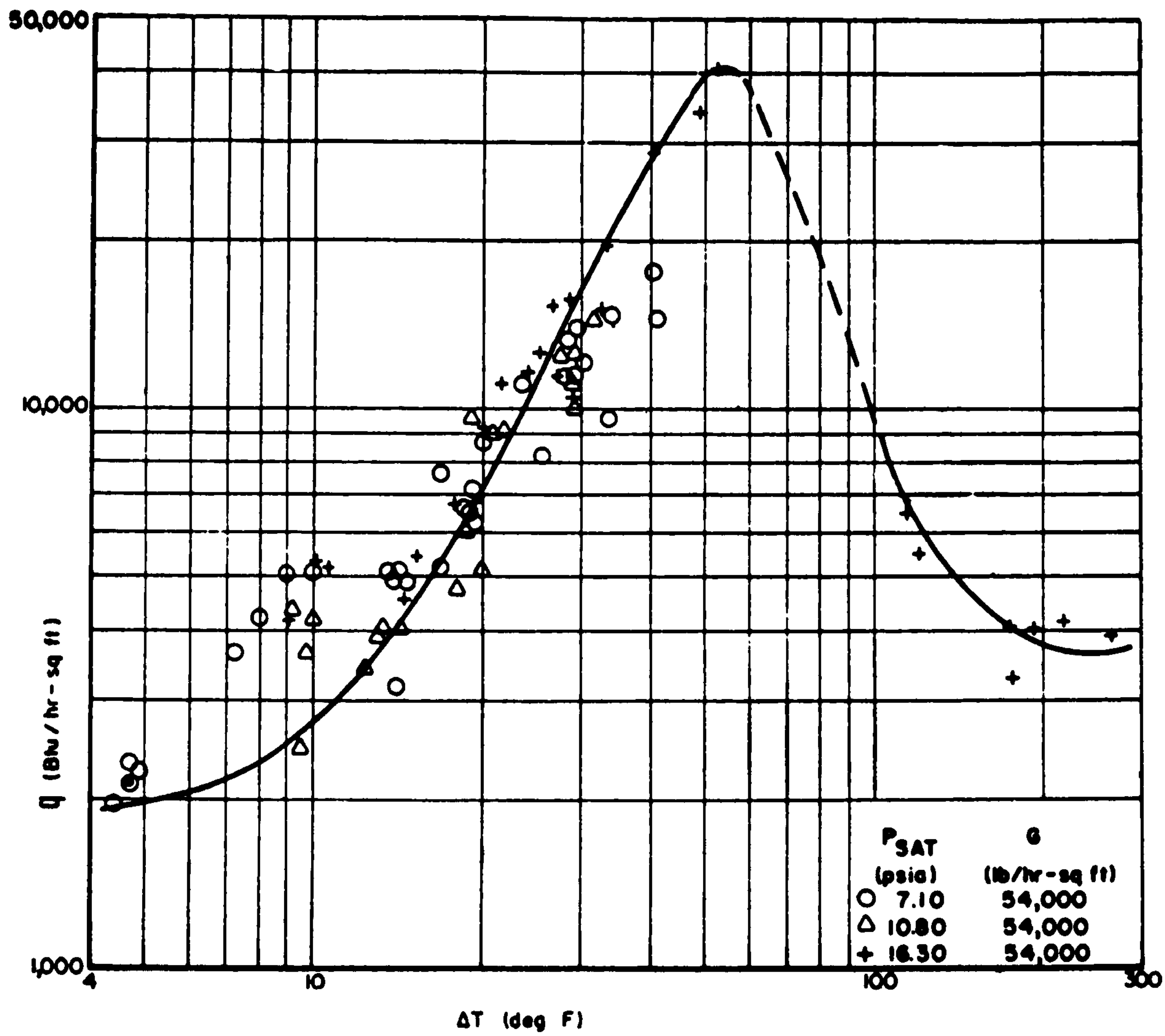

FIG. 8.— TYPICAL BOILING CURVE FOR FREON-11 (REPRODUCED FROM [3])

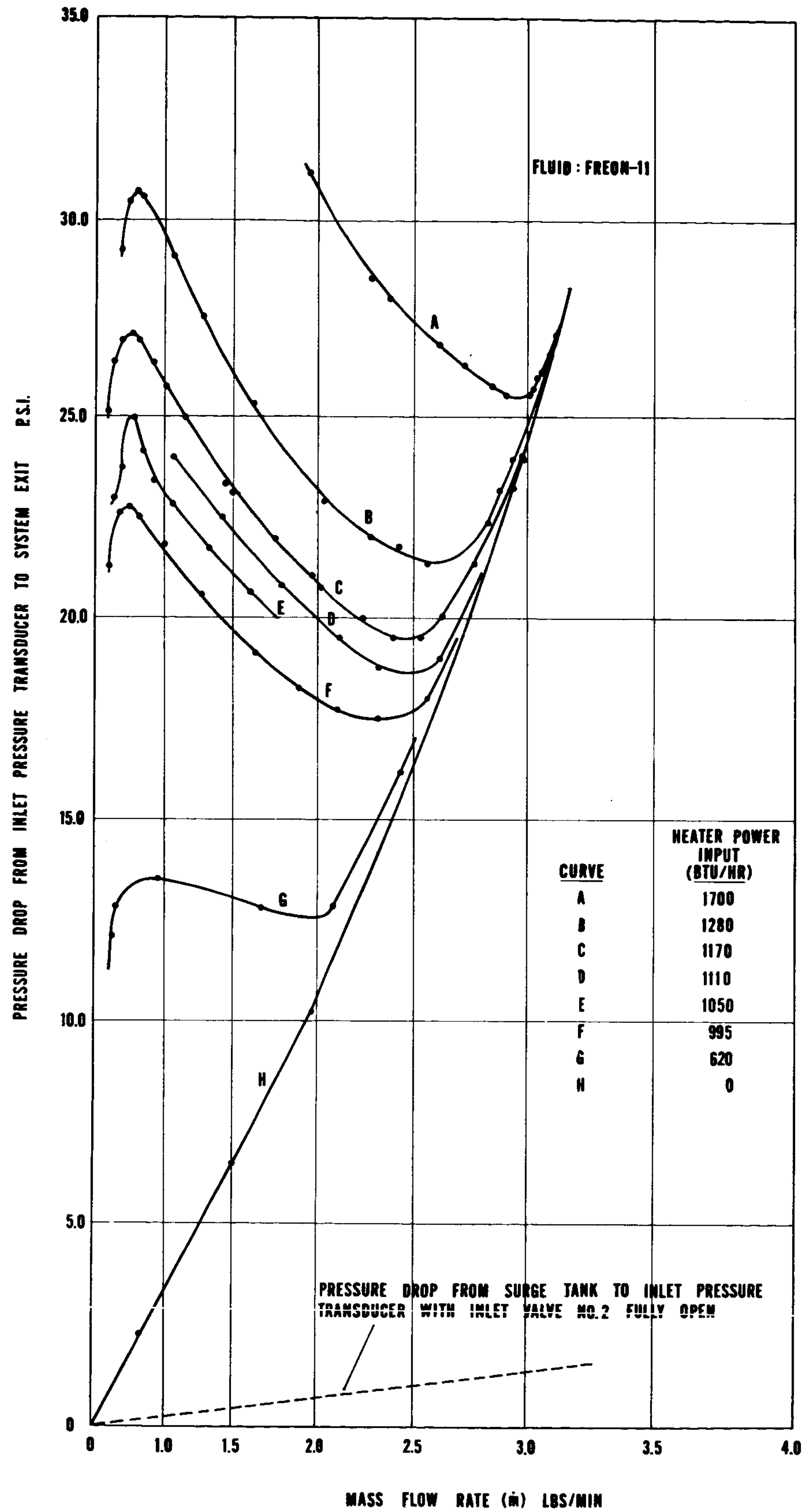

FIG. 9.—PRESSURE DROP VS MASS FLOW RATE STEADY STATE RELATIONSHIP

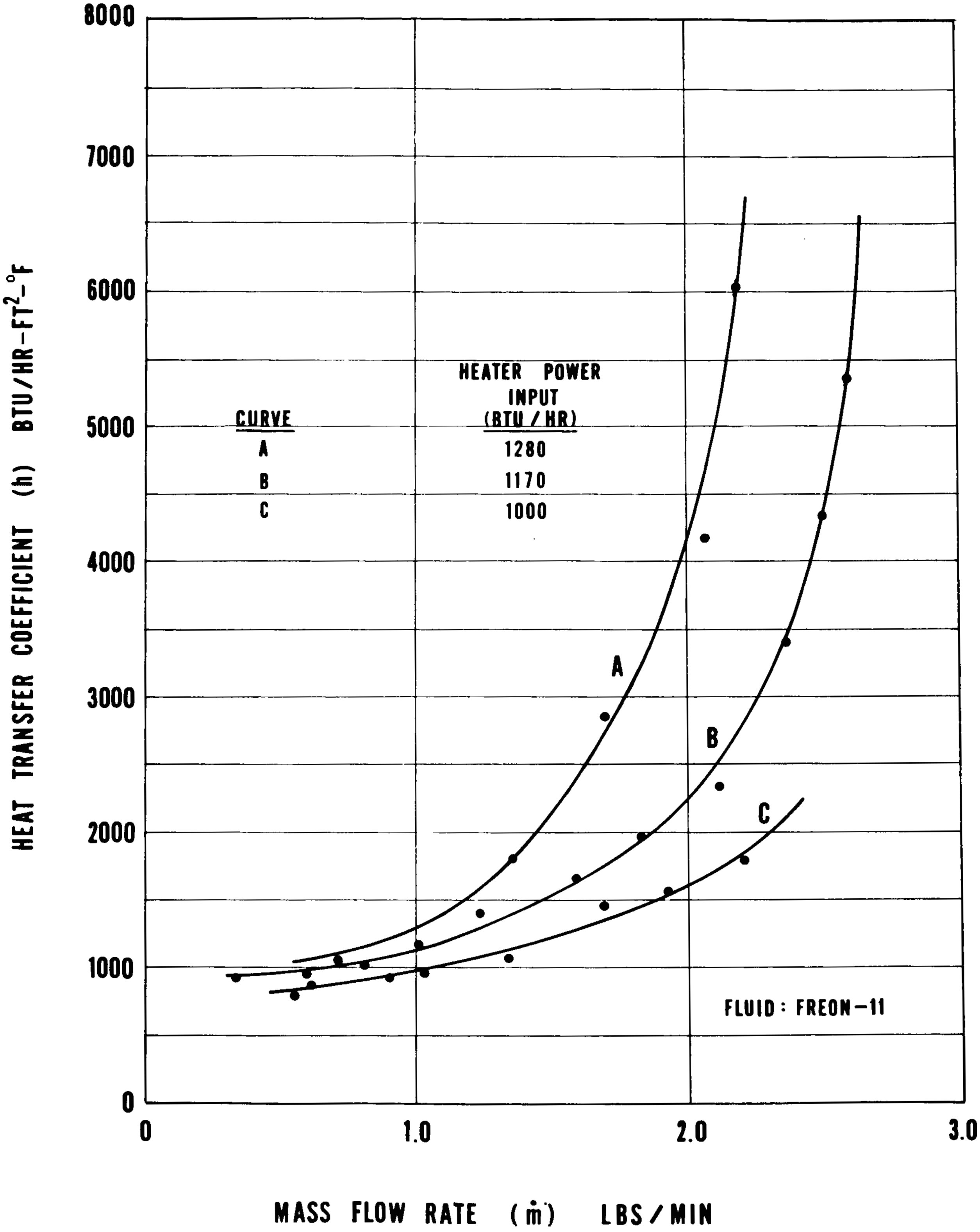

FIG. 10.- HEAT TRANSFER COEFFICIENT VS MASS FLOW RATE

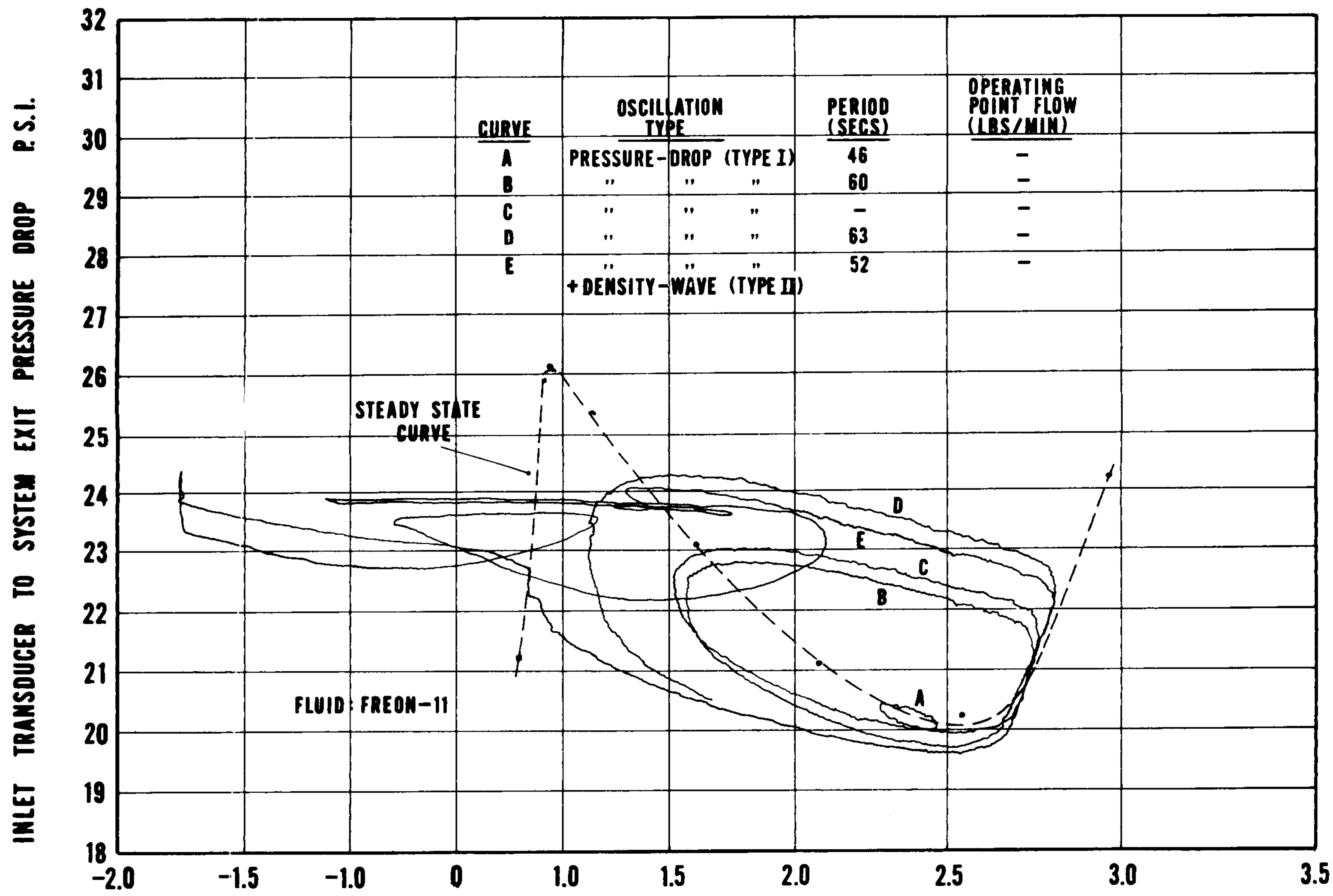

FIG. 11.- PRESSURE DROP VS MASS FLOW RATE LIMIT CYCLES FOR HEAT INPUT OF 1170 BTU/HR

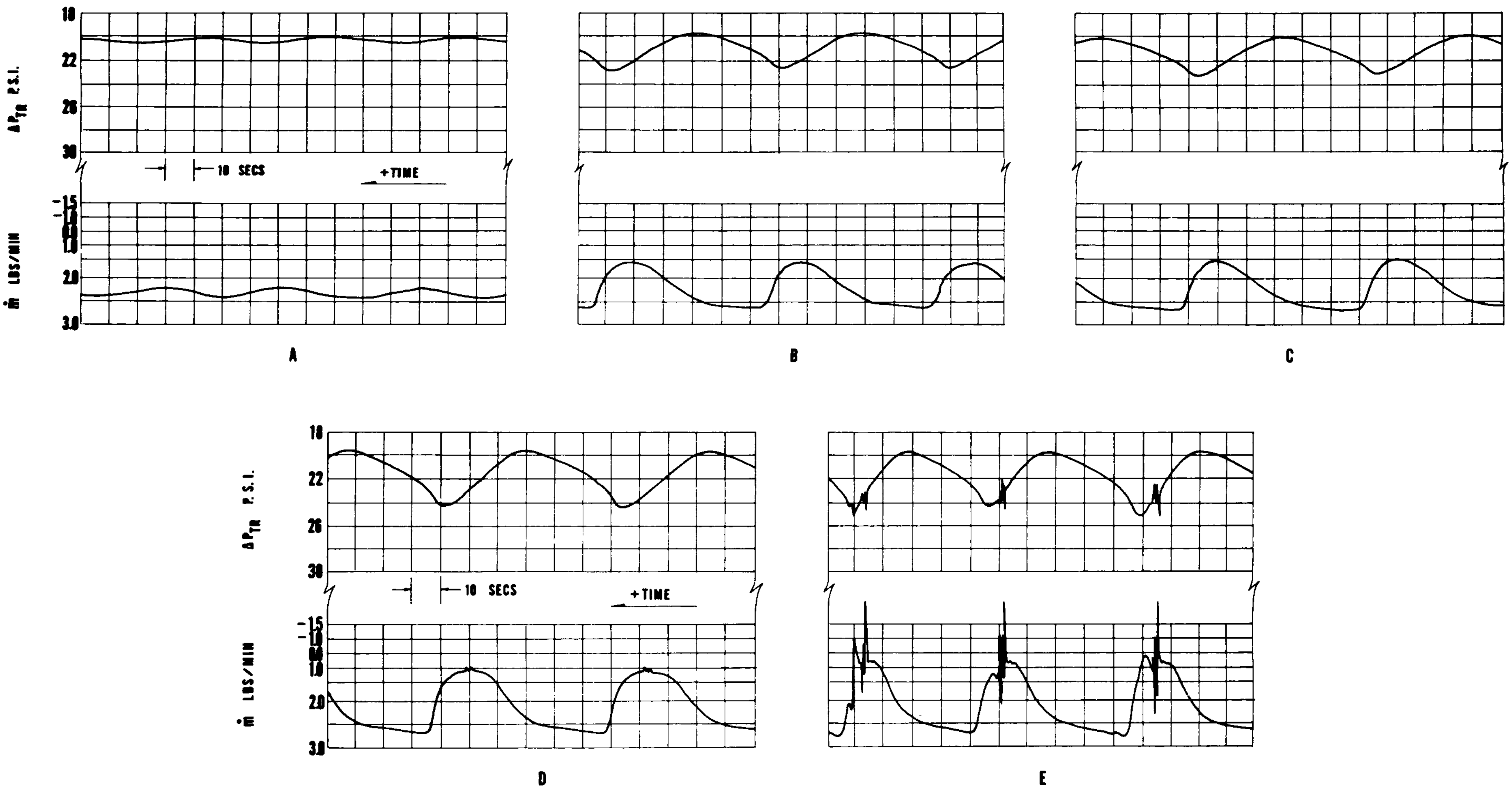

FIG.12.- PRESSURE DROP AND MASS FLOW RATE OSCILLATIONS FOR HEAT INPUT OF 1170 BTU/HR CORRESPONDING TO LIMIT CYCLES OF FIG.11

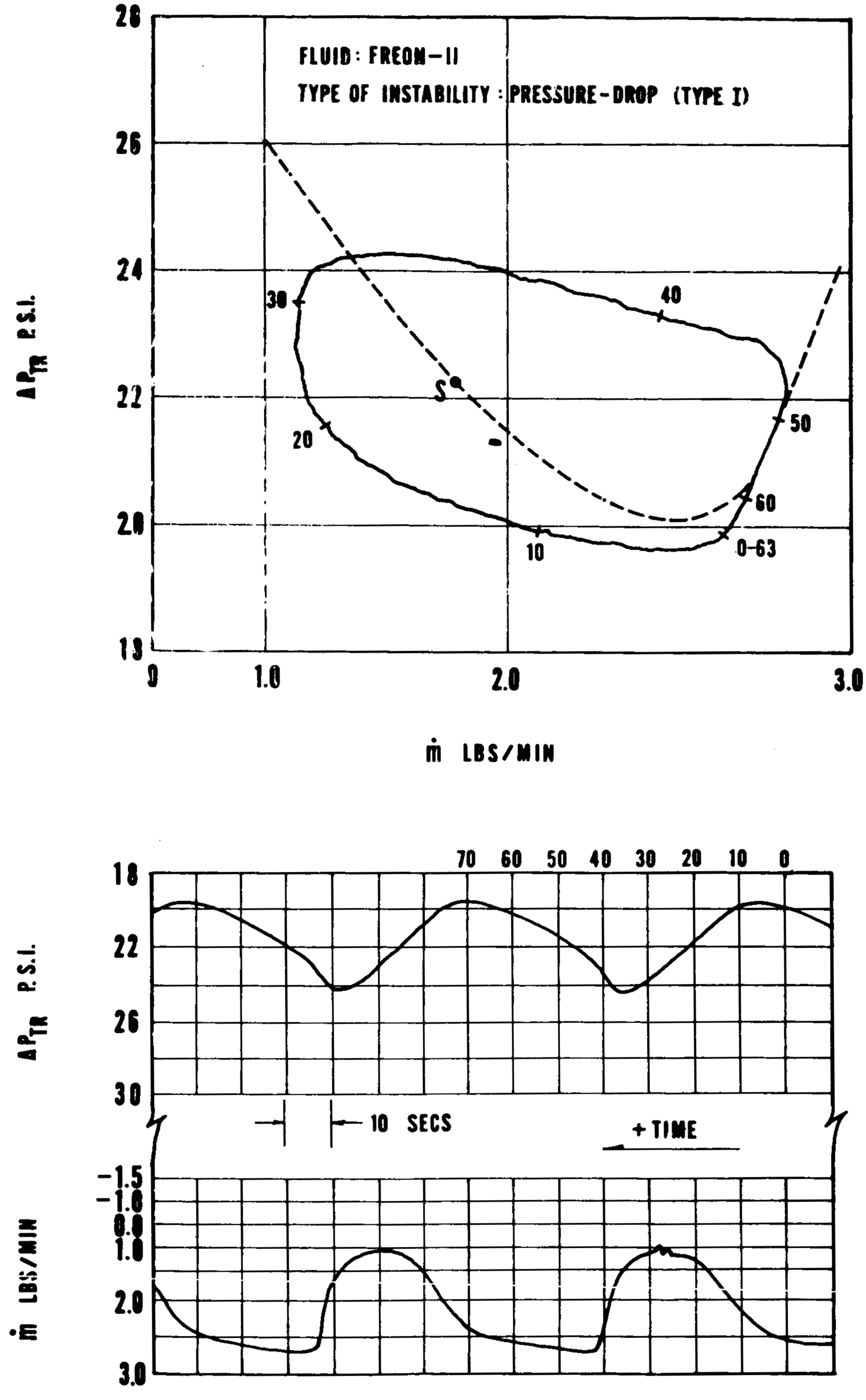

FIG. 13.— TYPICAL PRESSURE DROP VS MASS FLOW RATE
LIMIT CYCLE AND CORRESPONDING TIME RECORDING

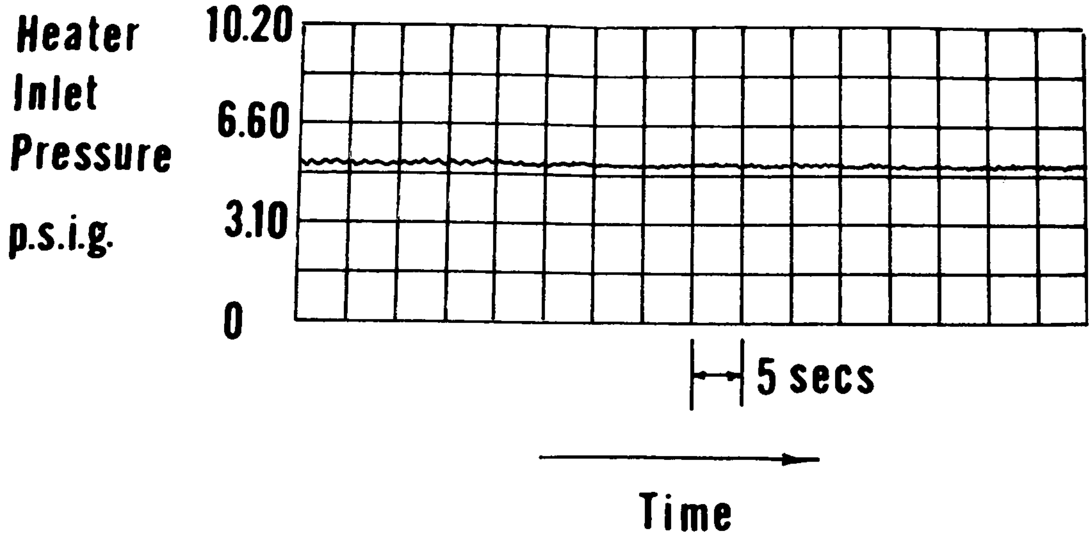

FIG.14(a).- A PRESSURE RECORDING AT STABILITY BOUNDARY

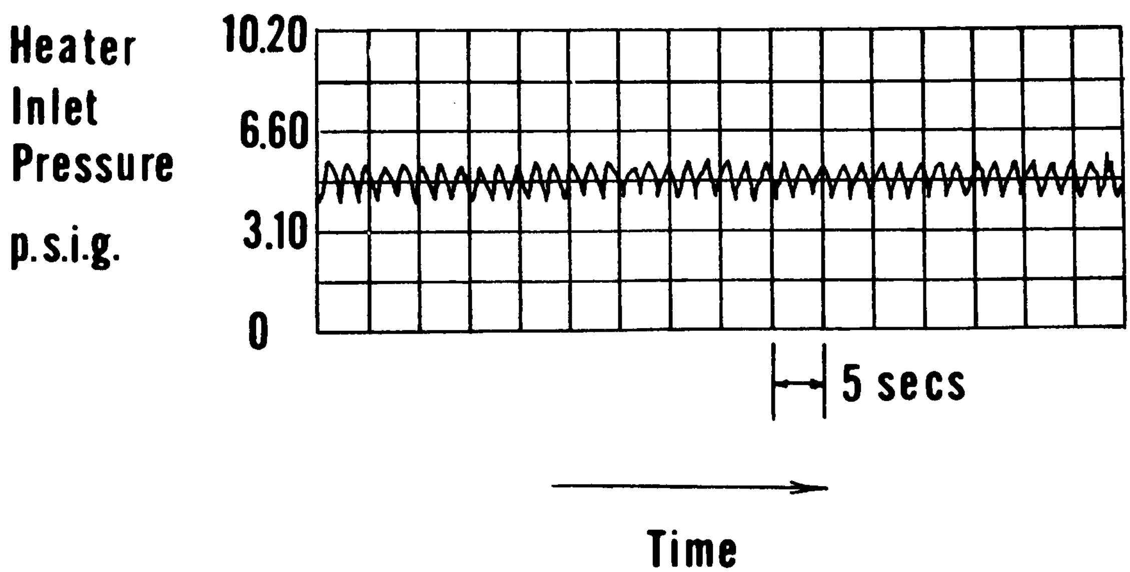

FIG.14(b).- A PRESSURE RECORDING IN UNSTABLE REGION

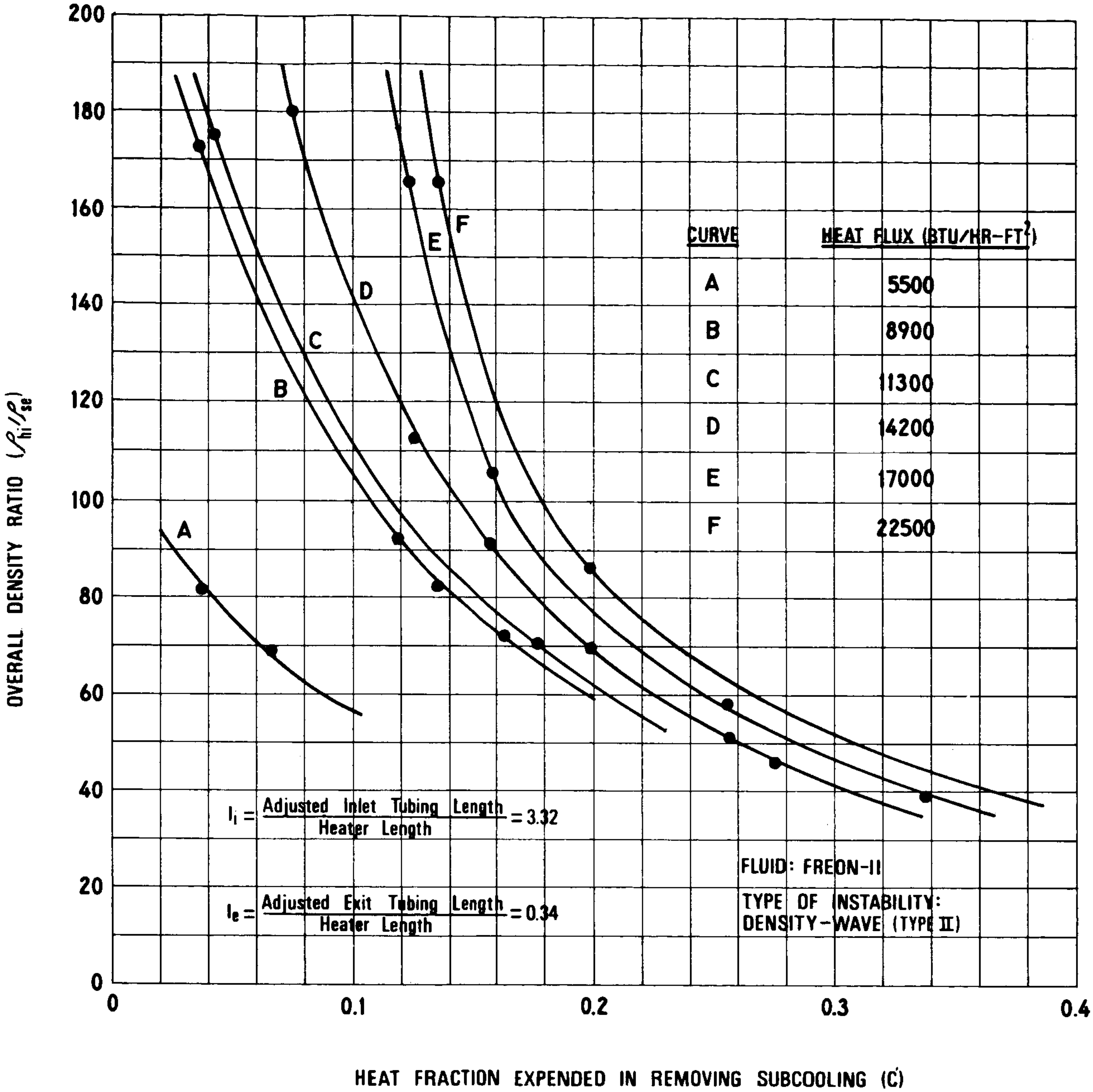

FIG.15 – OVERALL DENSITY RATIO VS HEAT FRACTION EXPENDED IN REMOVING SUBCOOLING FOR PARTIAL BOILING EXPERIMENTS (SYSTEM WITHOUT SURGE TANK)

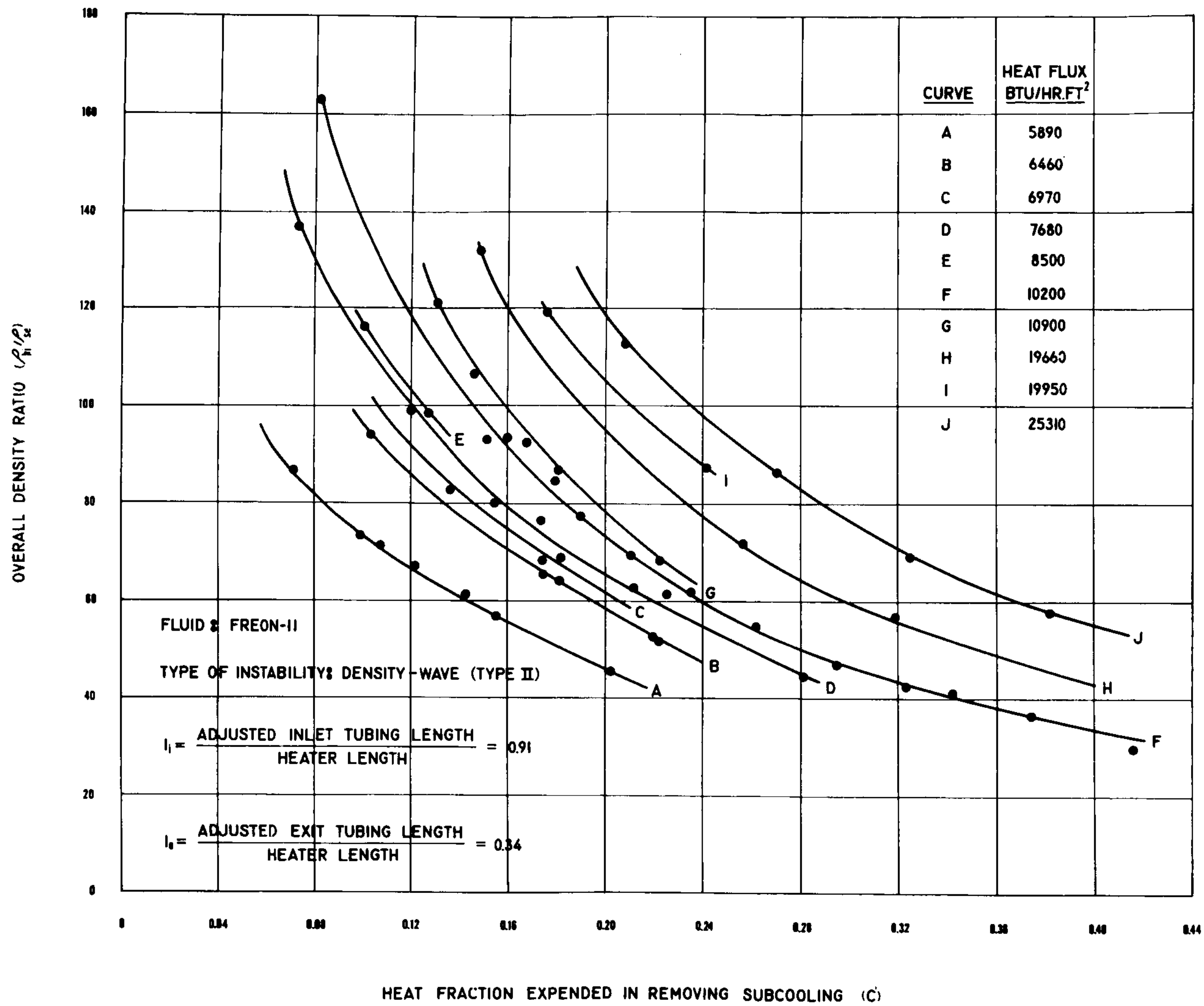

FIG.16.- OVERALL DENSITY RATIO VS HEAT FRACTION EXPENDED IN REMOVING SUBCOOLING FOR PARTIAL BOILING EXPERIMENTS (SYSTEM WITH SURGE TANK)

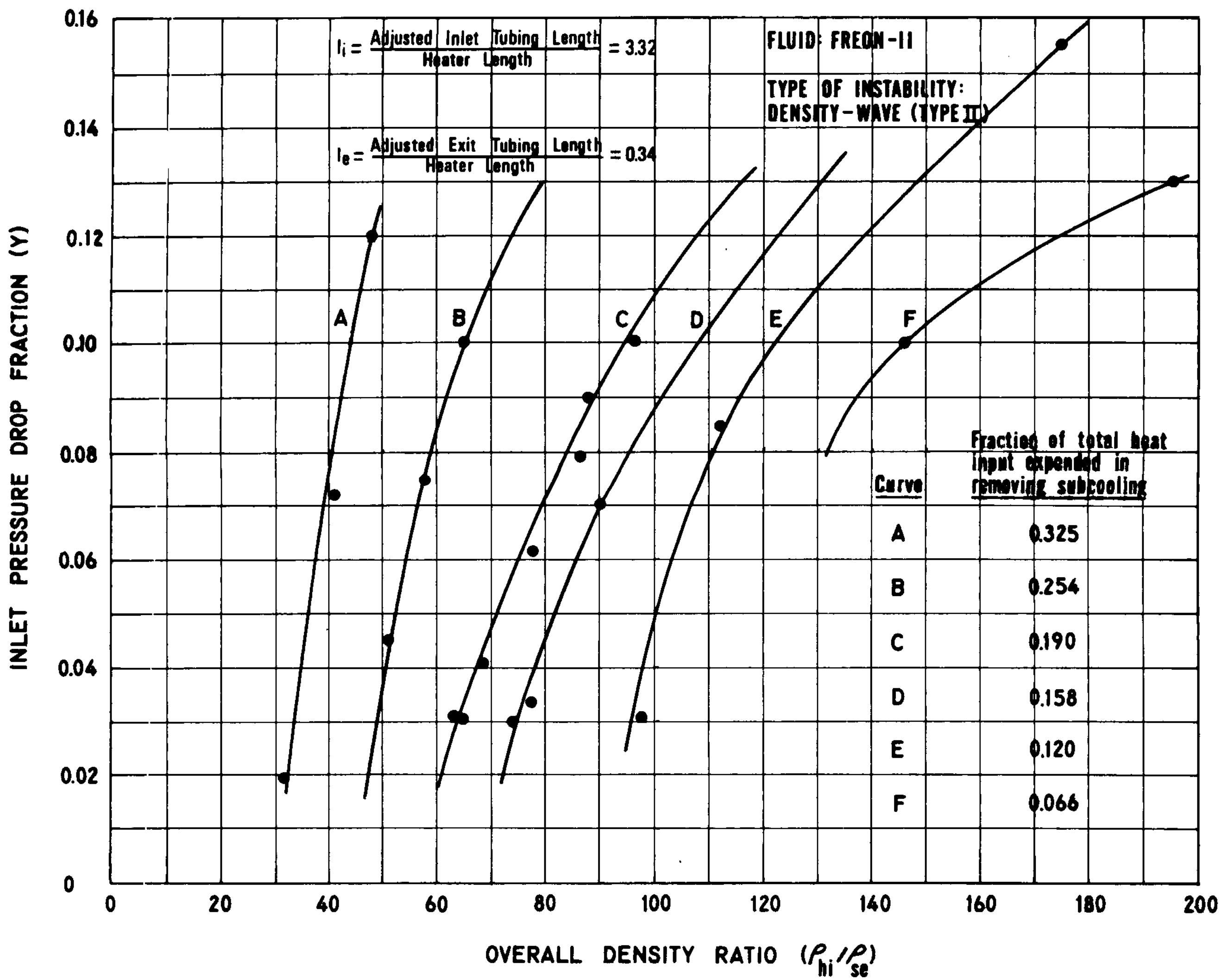

FIG.17.— INLET PRESSURE DROP FRACTION VS OVERALL DENSITY RATIO AT STABILITY BOUNDARY FOR PARTIAL BOILING EXPERIMENTS (SYSTEM WITHOUT SURGE TANK)

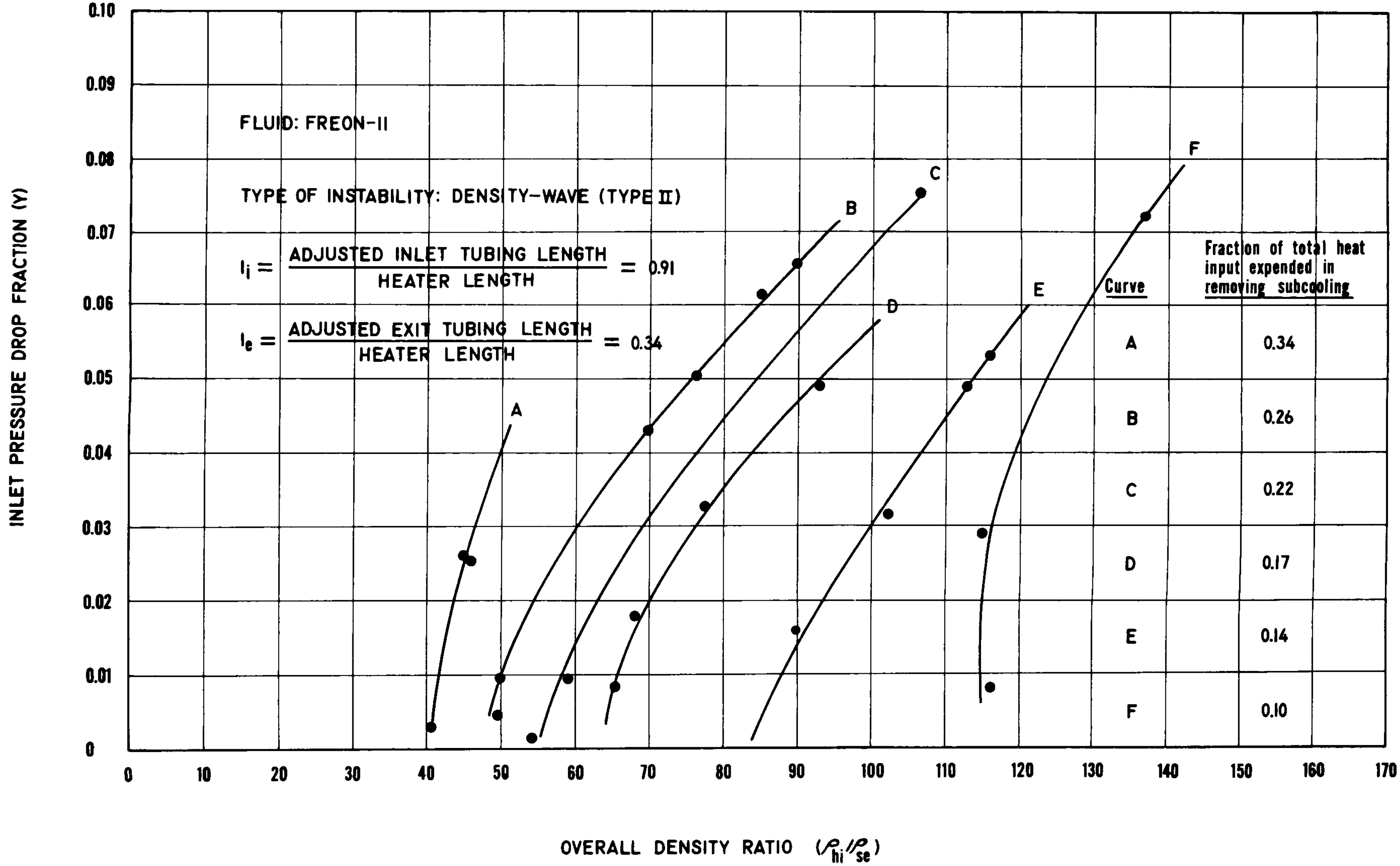

FIG.18.- INLET PRESSURE DROP FRACTION VS OVERALL DENSITY RATIO AT STABILITY BOUNDARY FOR PARTIAL BOILING EXPERIMENTS (SYSTEM WITH SURGE TANK)

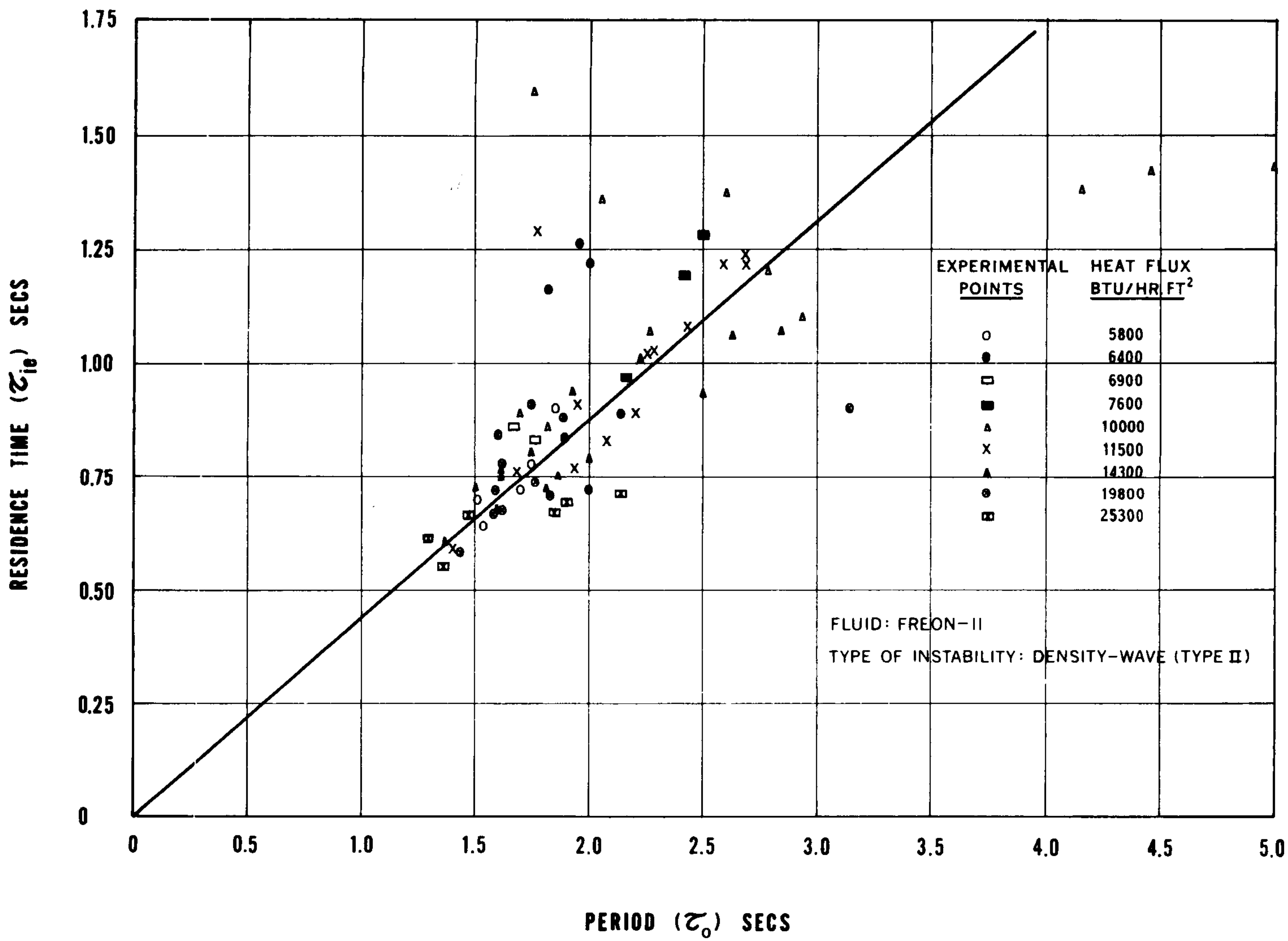

FIG.19. – RESIDENCE TIME FROM HEATER INLET TO SYSTEM EXIT VS TIME PERIOD OF OSCILLATIONS

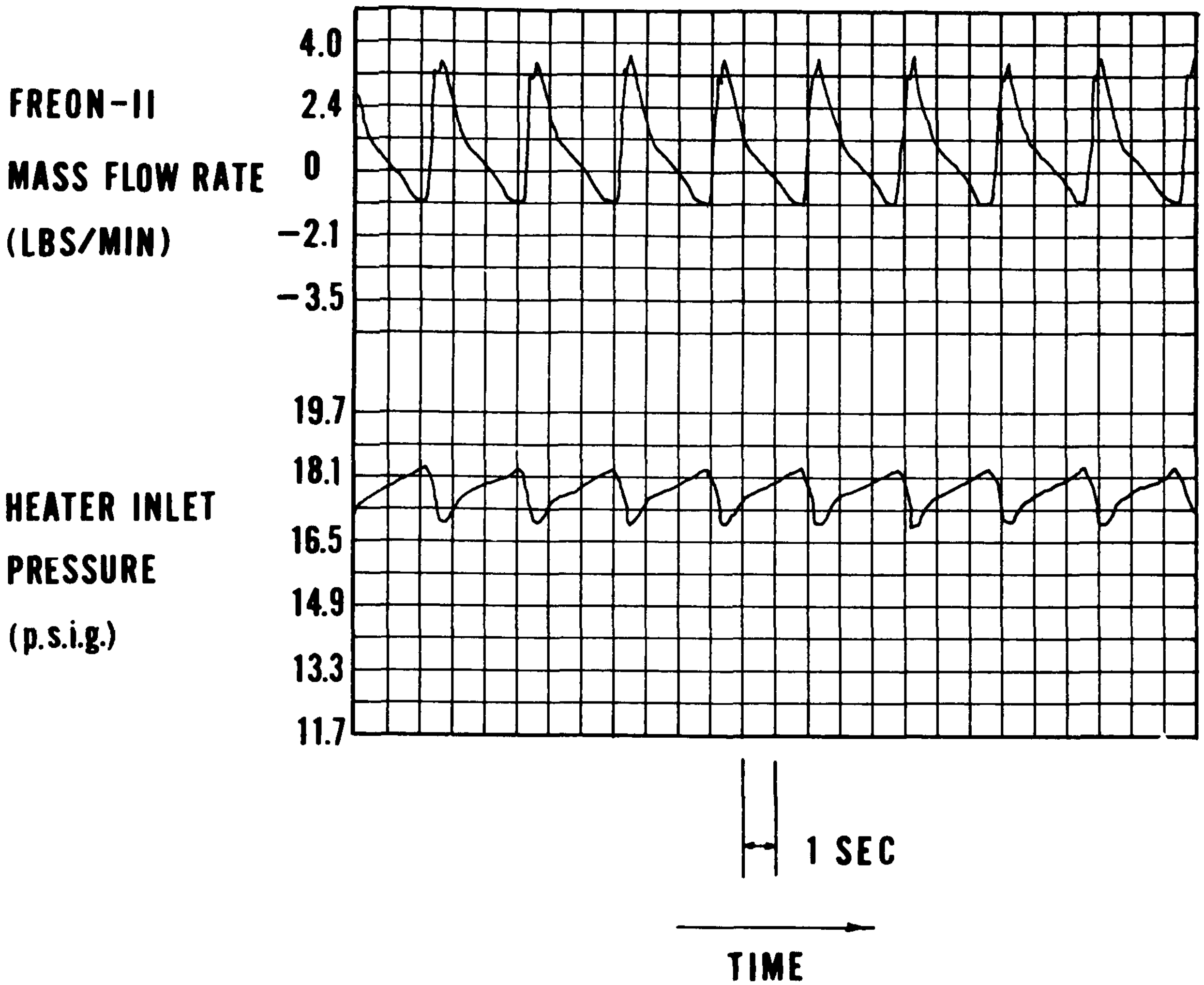

FIG.20.– MASS FLOW RATE AND PRESSURE RECORDING OF DENSITY-WAVE (TYPE II) OSCILLATIONS

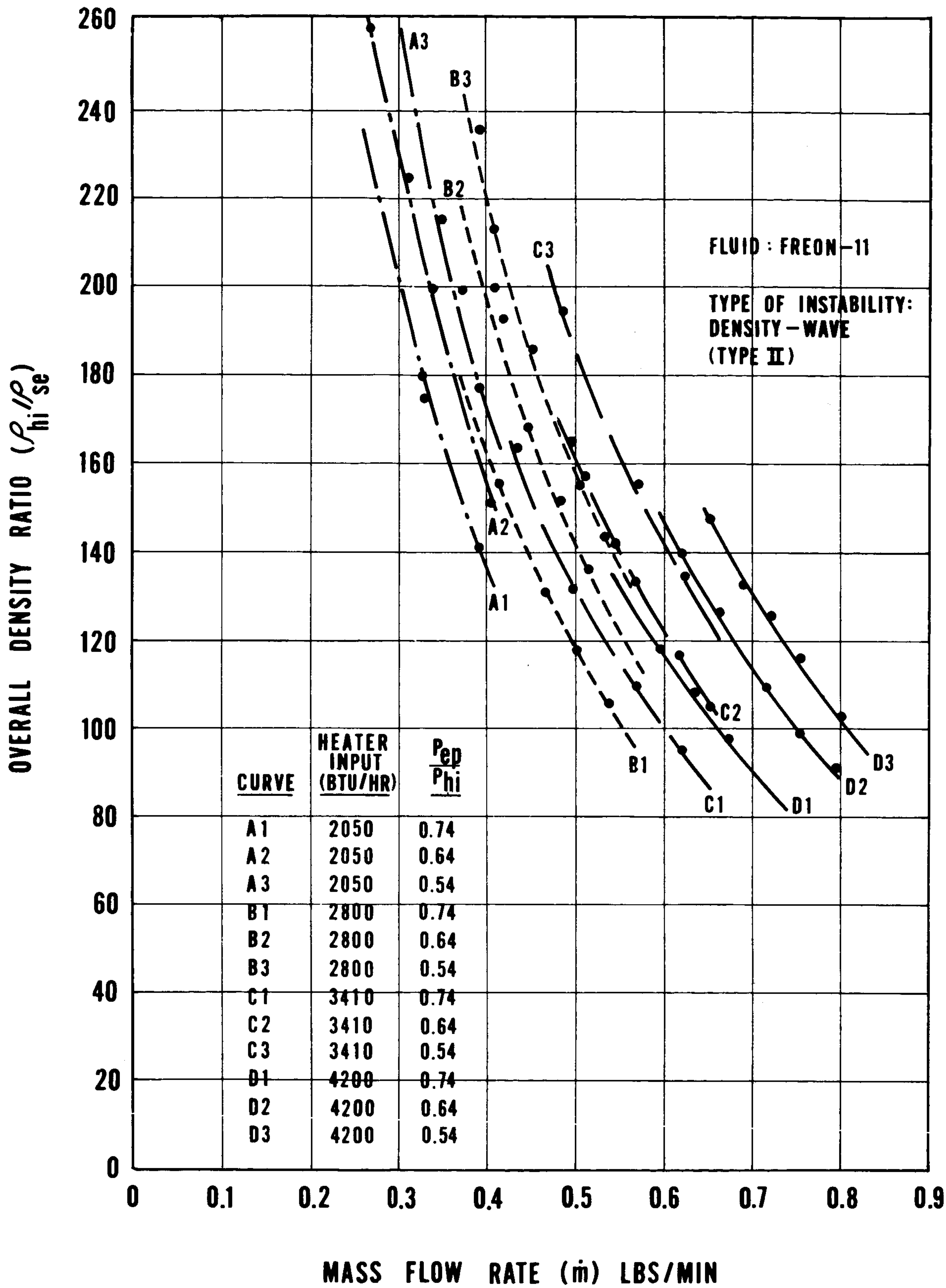

FIG.21.– OVERALL DENSITY RATIO VS MASS FLOW RATE FOR SUPERHEAT EXPERIMENTS

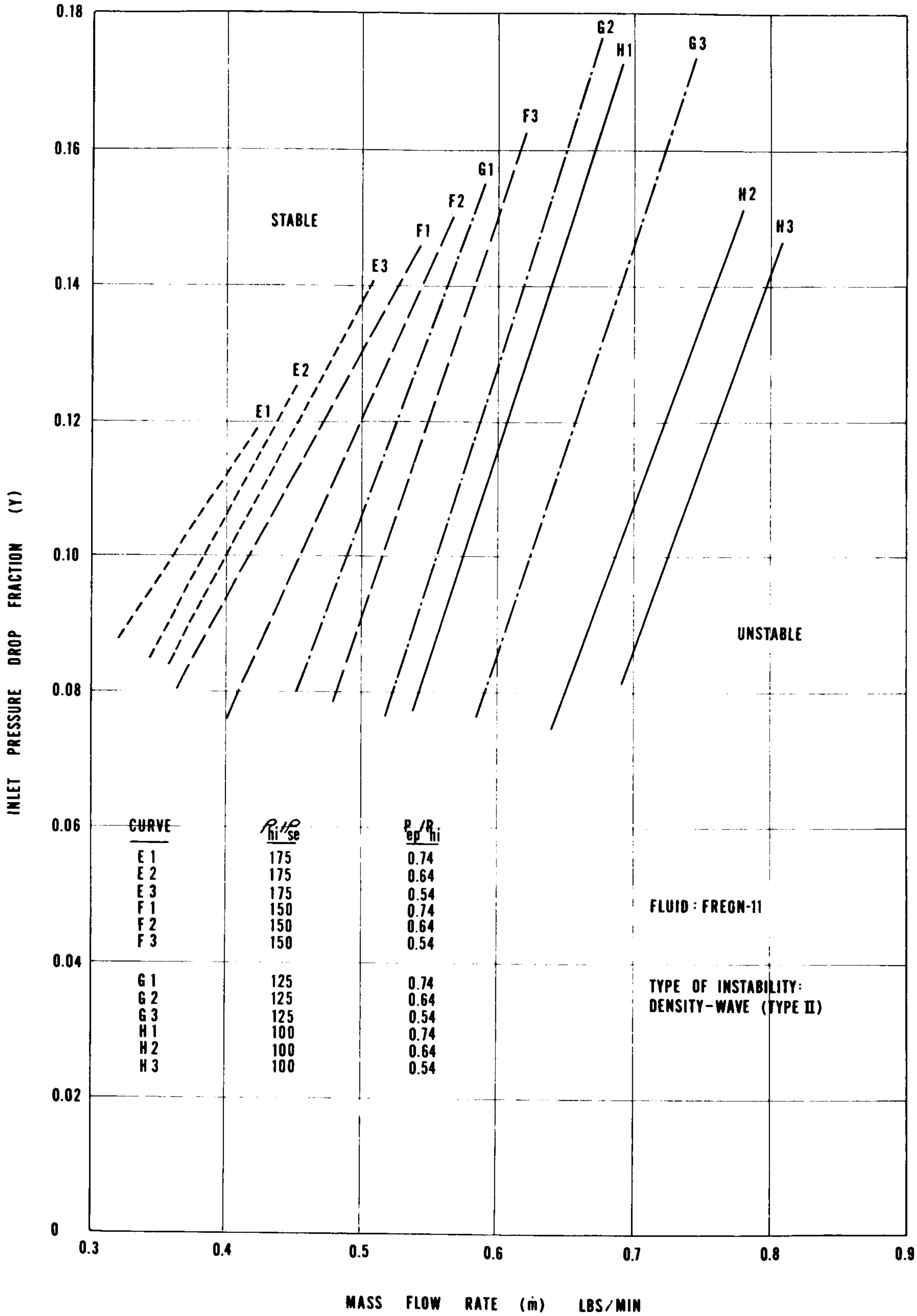

FIG.22- INLET PRESSURE DROP FRACTION VS MASS FLOW RATE AT STABILITY BOUNDARY FOR SUPERHEAT EXPERIMENTS

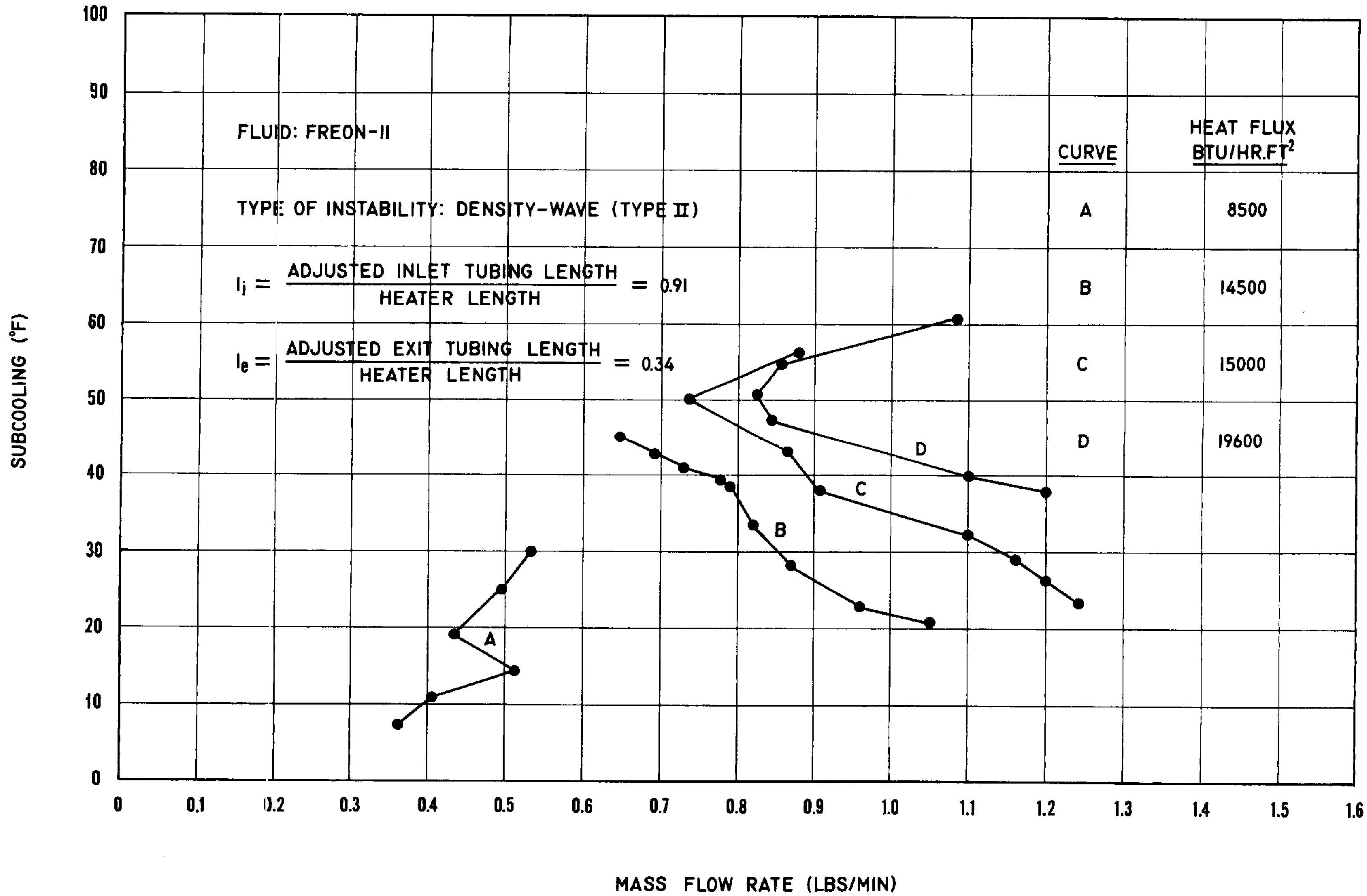

FIG.23.- SUBCOOLING VS MASS FLOW RATE AT STABILITY BOUNDARY FOR FIXED GEOMETRY (EXIT VALVE PARTLY CLOSED)

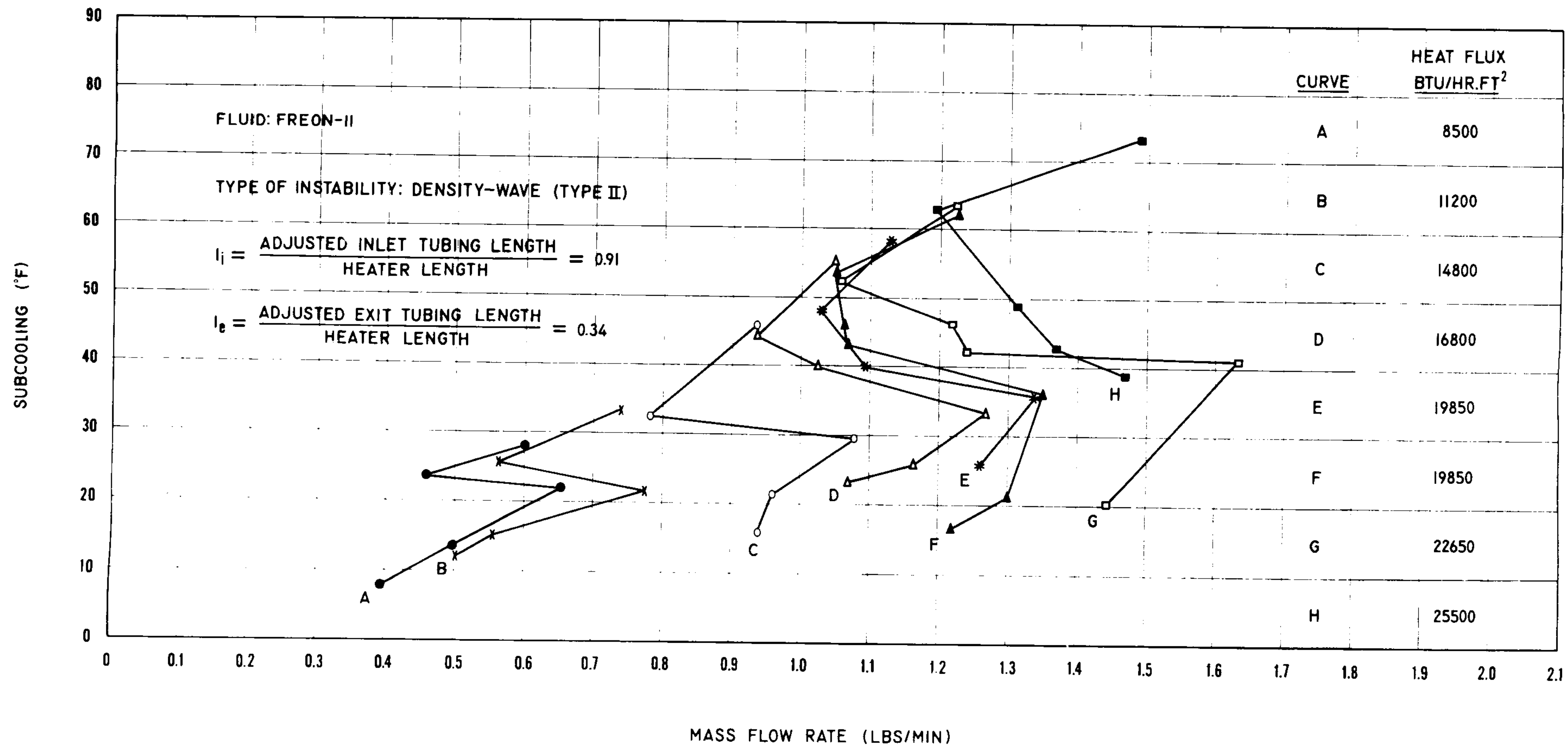

FIG.24.- SUBCOOLING VS MASS FLOW RATE AT STABILITY BOUNDARY FOR FIXED GEOMETRY (NO EXIT VALVE)

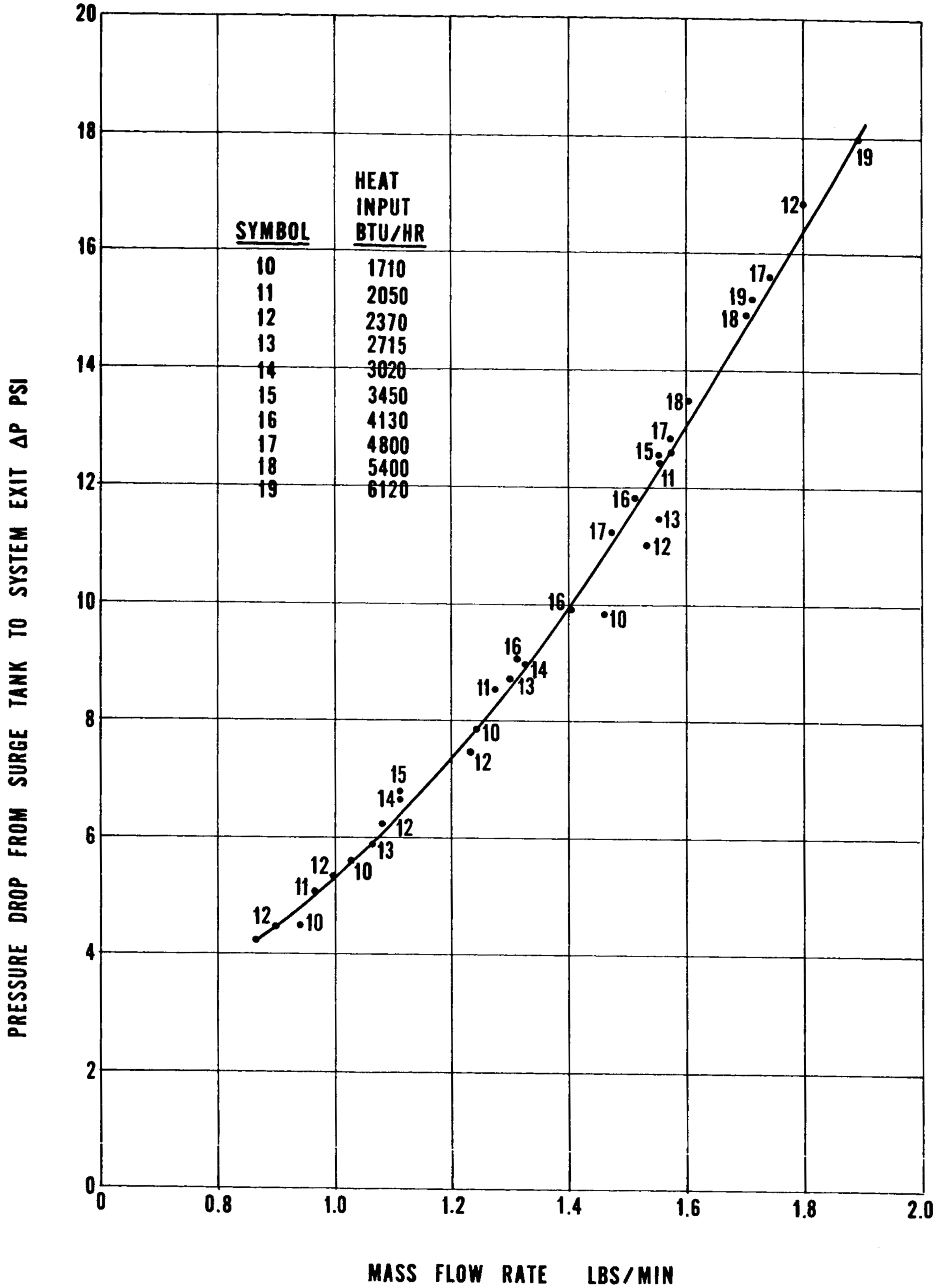

FIG. 25.– TEST SECTION PRESSURE DROP WITH LIQUID WATER

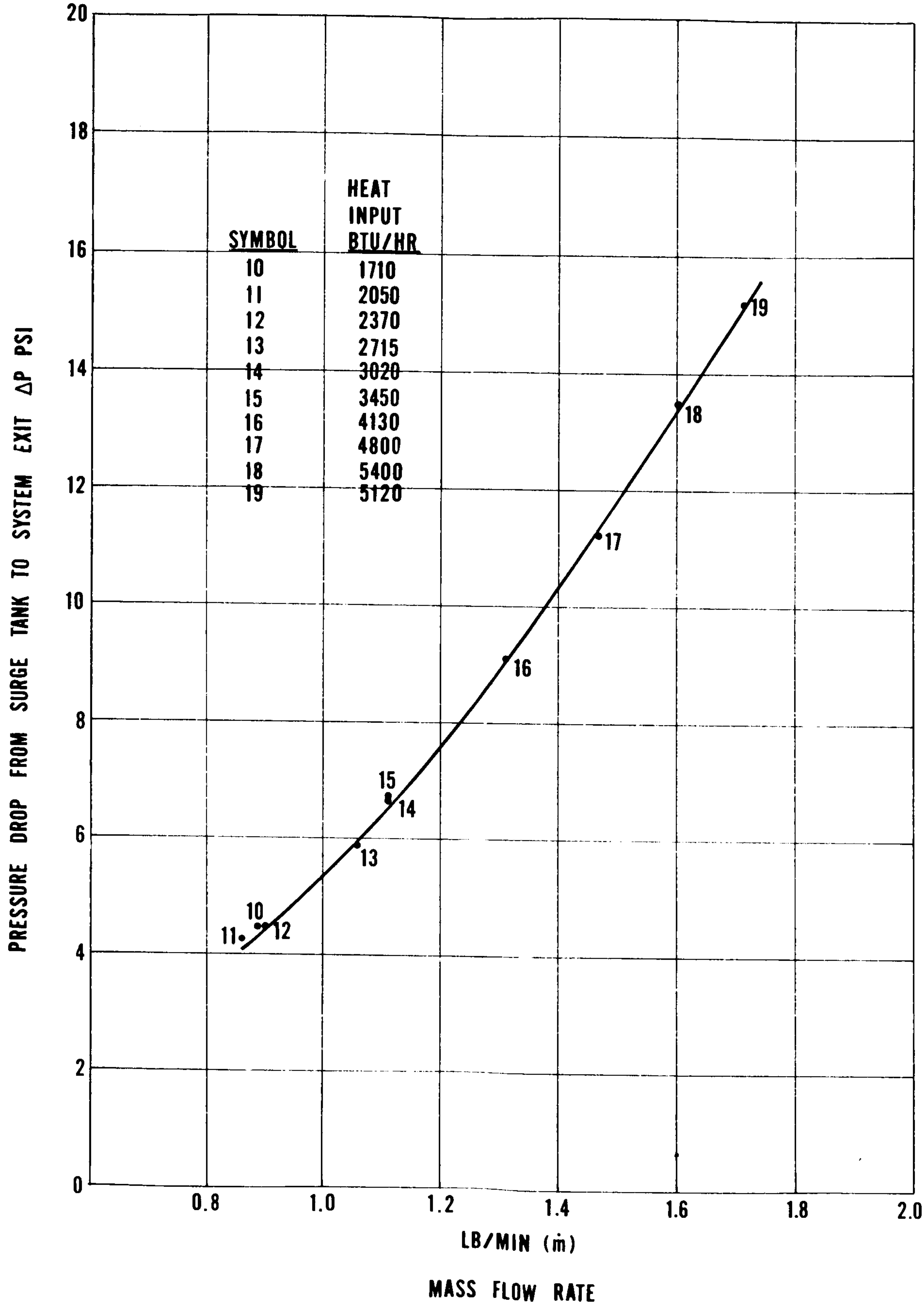

FIG. 26.- ONSET POINTS FOR TYPE I INSTABILITY WITH WATER

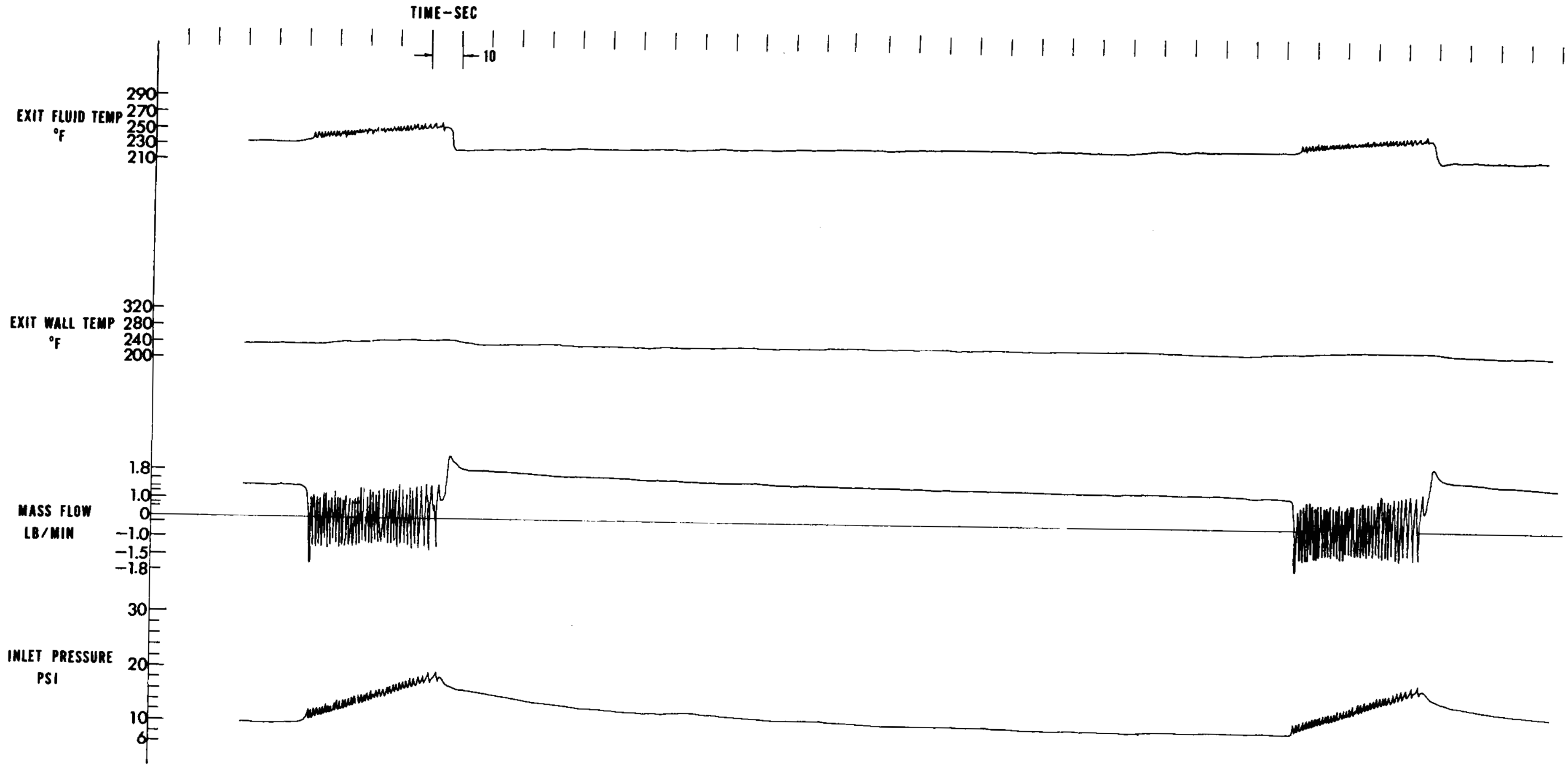

FIG.27.- RECORDINGS OF TYPE I AND TYPE II OSCILLATIONS IN WATER NEAR ONSET. POWER LEVEL 4130 BTU/HR

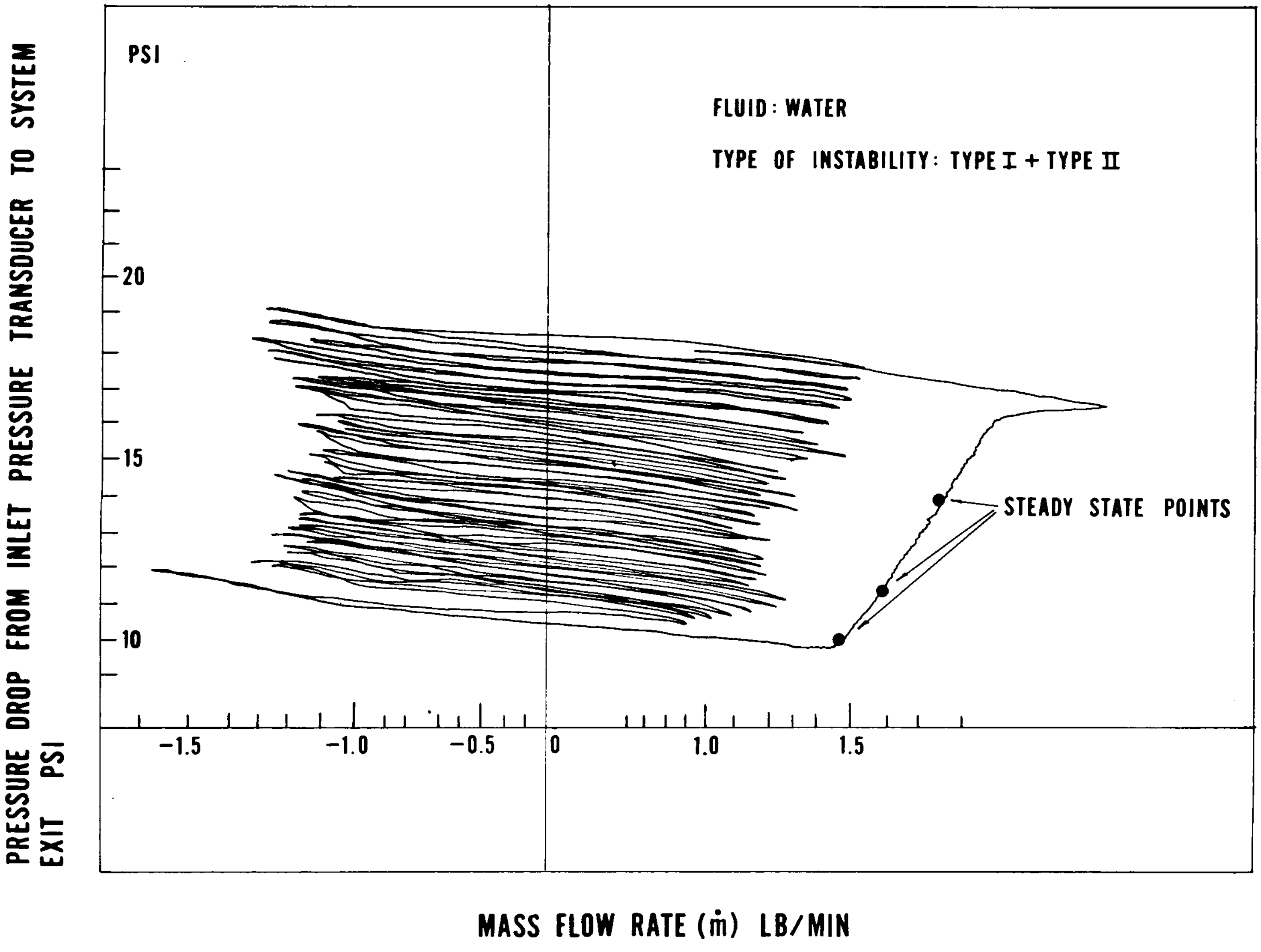

FIG. 28.— LIMIT CYCLE AT 4130 BTU/HR NEAR ONSET

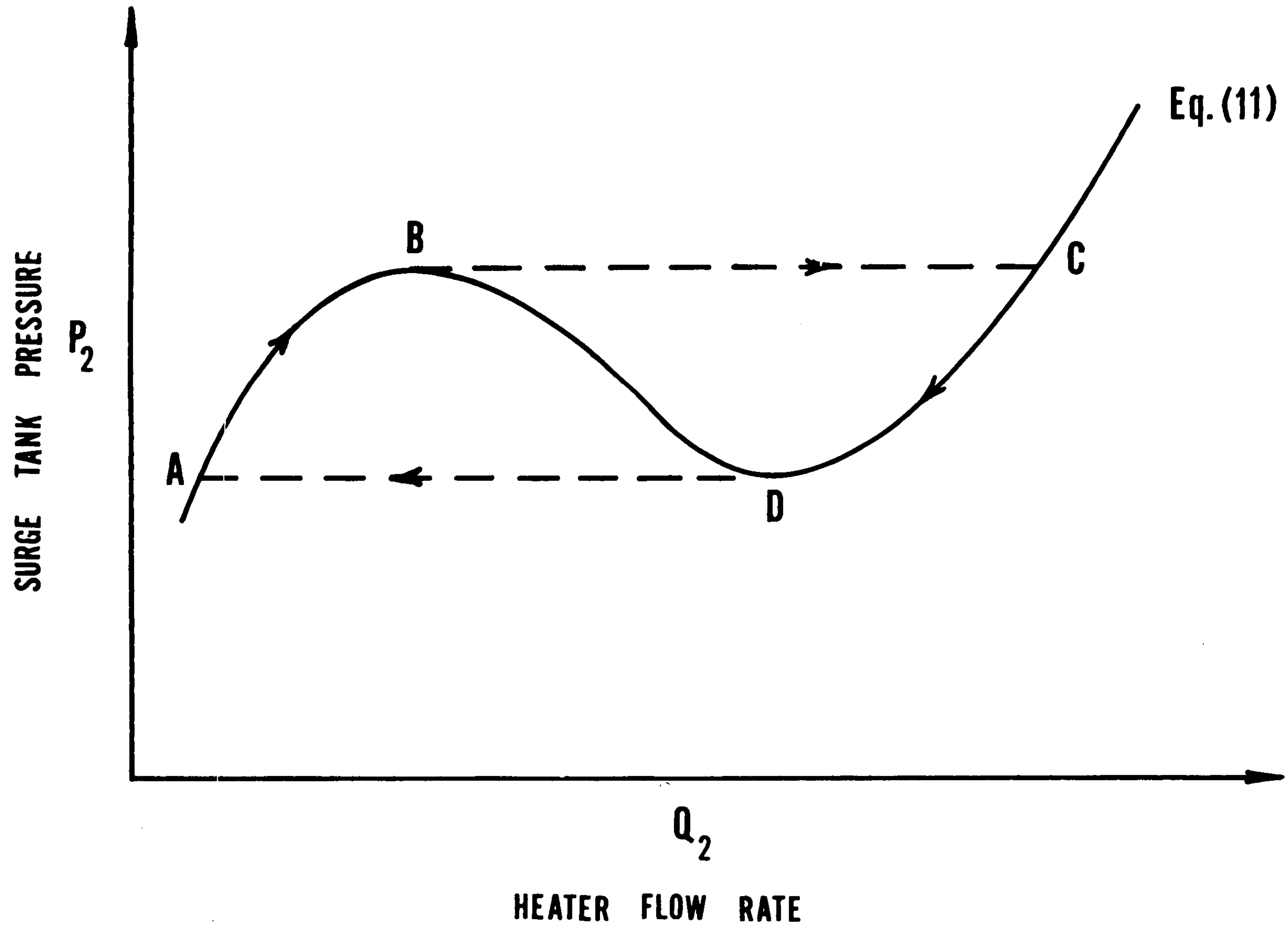

FIG. 29.– LIMIT CYCLE FOR TYPE I OSCILLATIONS WITH CONSTANT HEAT INPUT

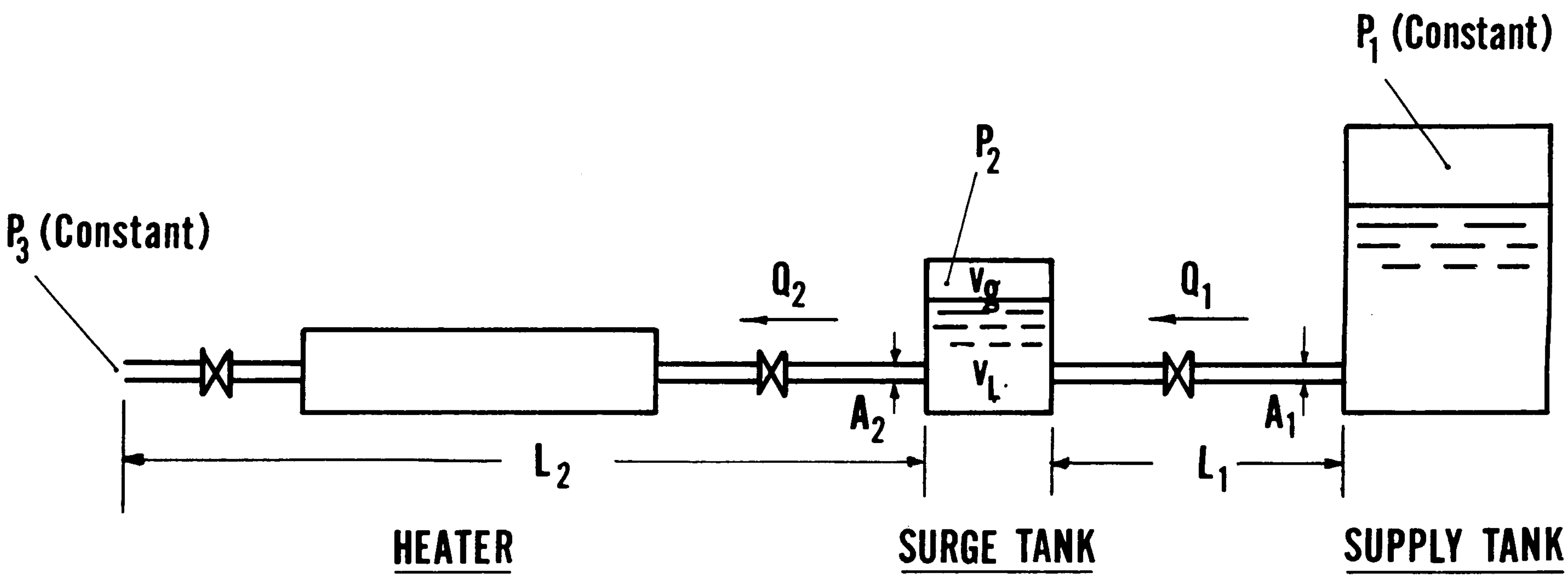

FIG. 30.-SCHEMATIC OF FLOW SYSTEM

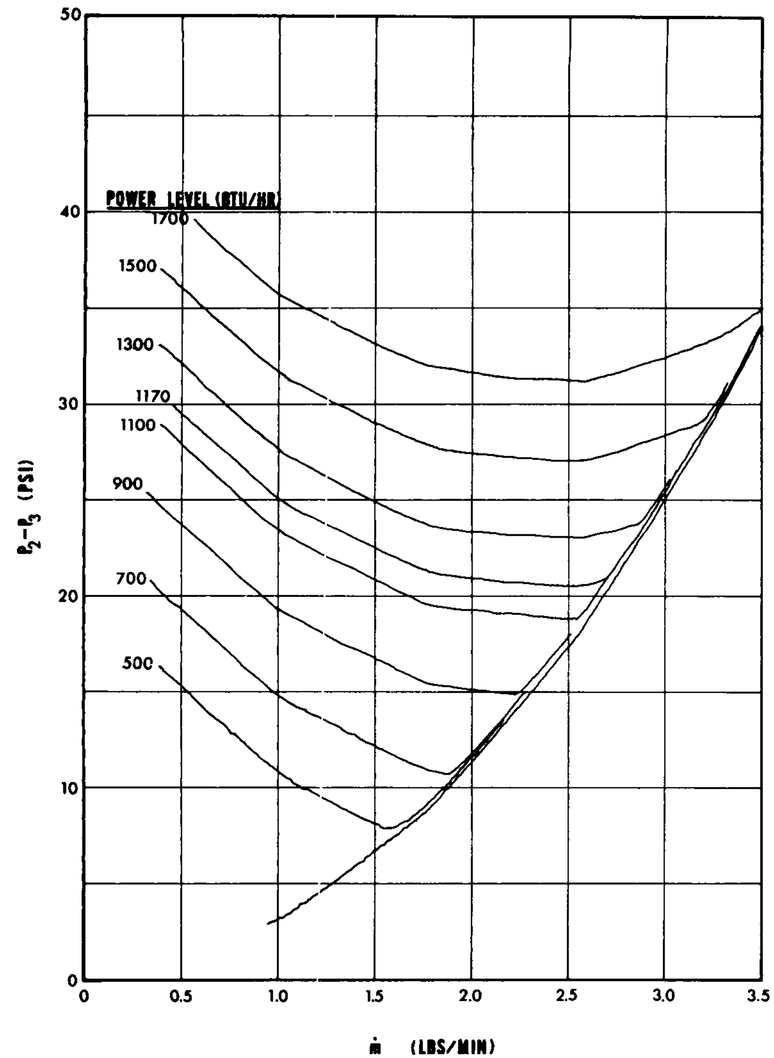

FIG. 31(a). - SYSTEM PRESSURE DROP VS MASS FLOW RATE (ANALOG SIMULATION)

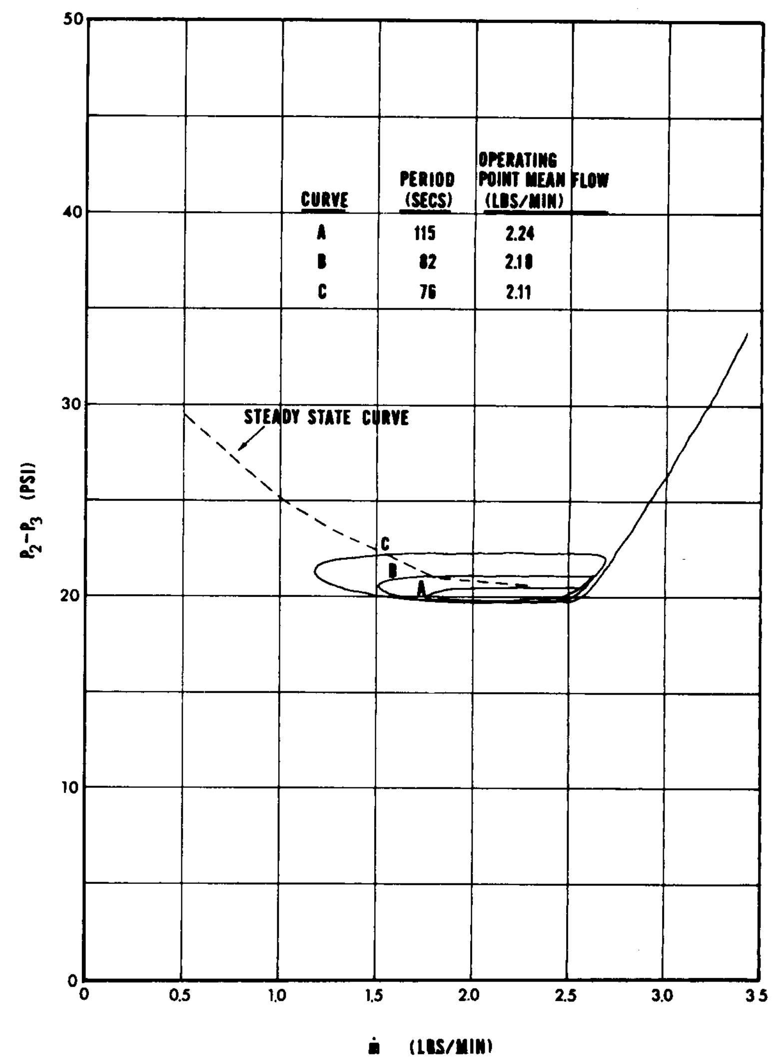

FIG. 31(b). - LIMIT-CYCLE OSCILLATIONS FOR A HEATER POWER INPUT OF 1170 BTU/HR (ANALOG SIMULATION)

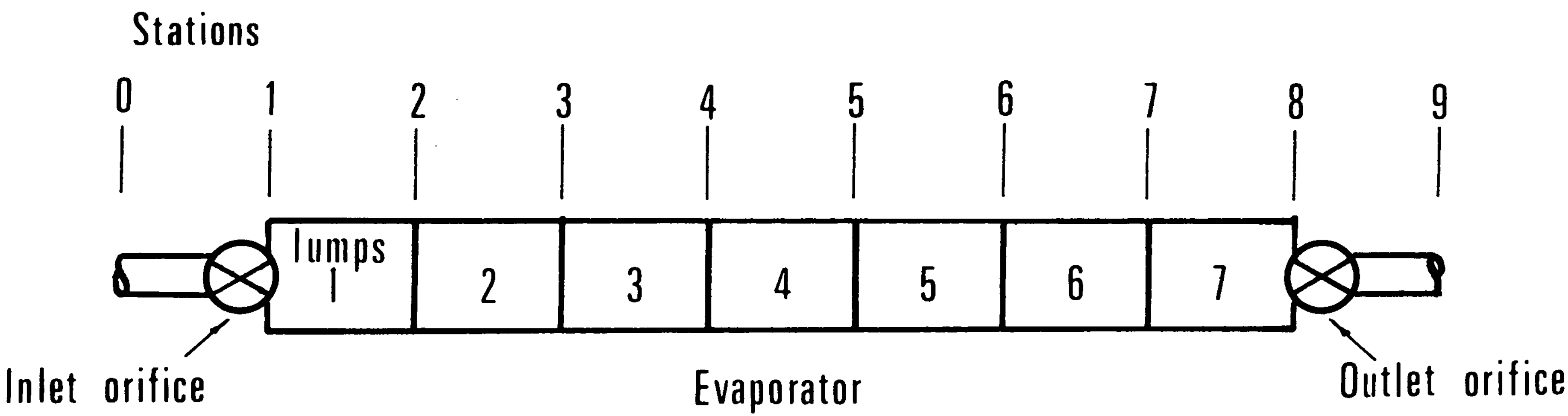

FIG. 32.– SYSTEM UNDER CONSIDERATION

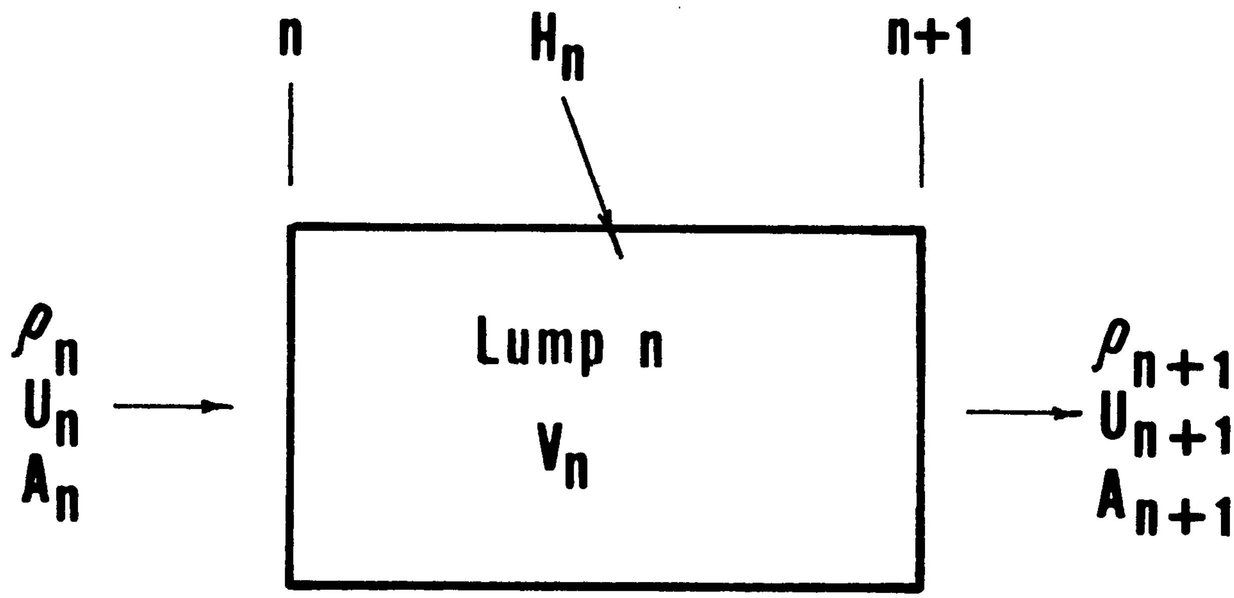

FIG. 33.— PORTION OF SYSTEM

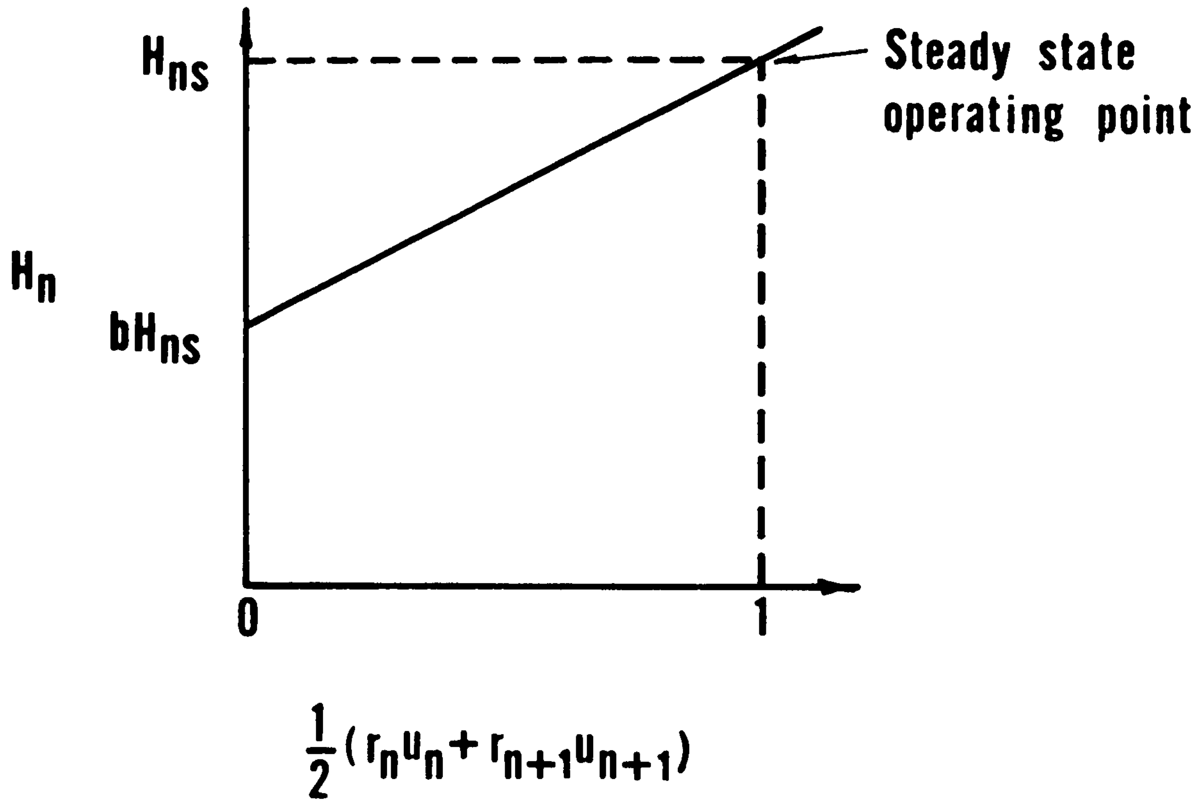

FIG. 34.– EFFECT OF MASS FLOW RATE ON HEAT TRANSFER

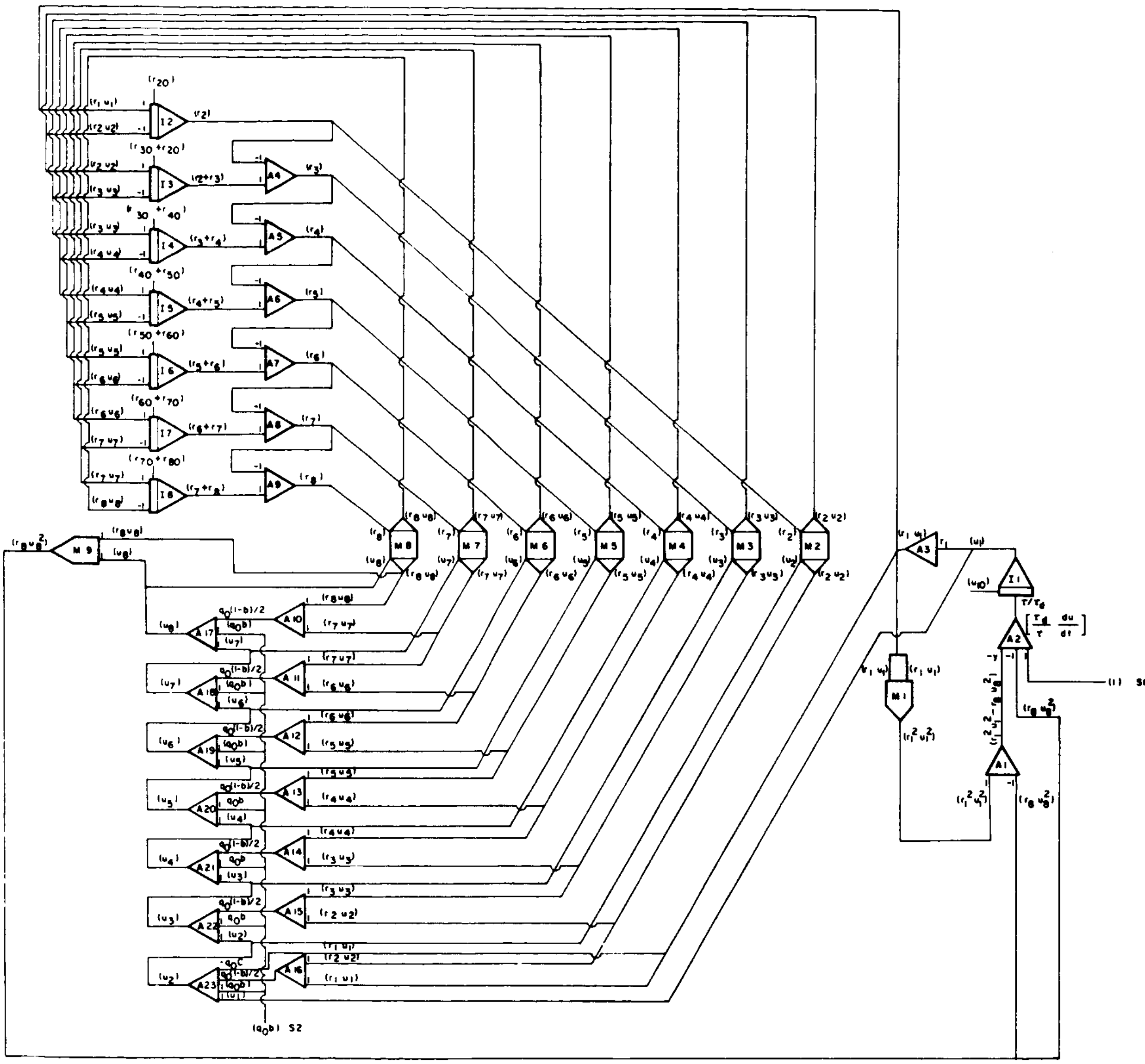

FIG. 35.– ANALOG–COMPUTER BLOCK DIAGRAM FOR TYPE II BOILING FLOW INSTABILITY

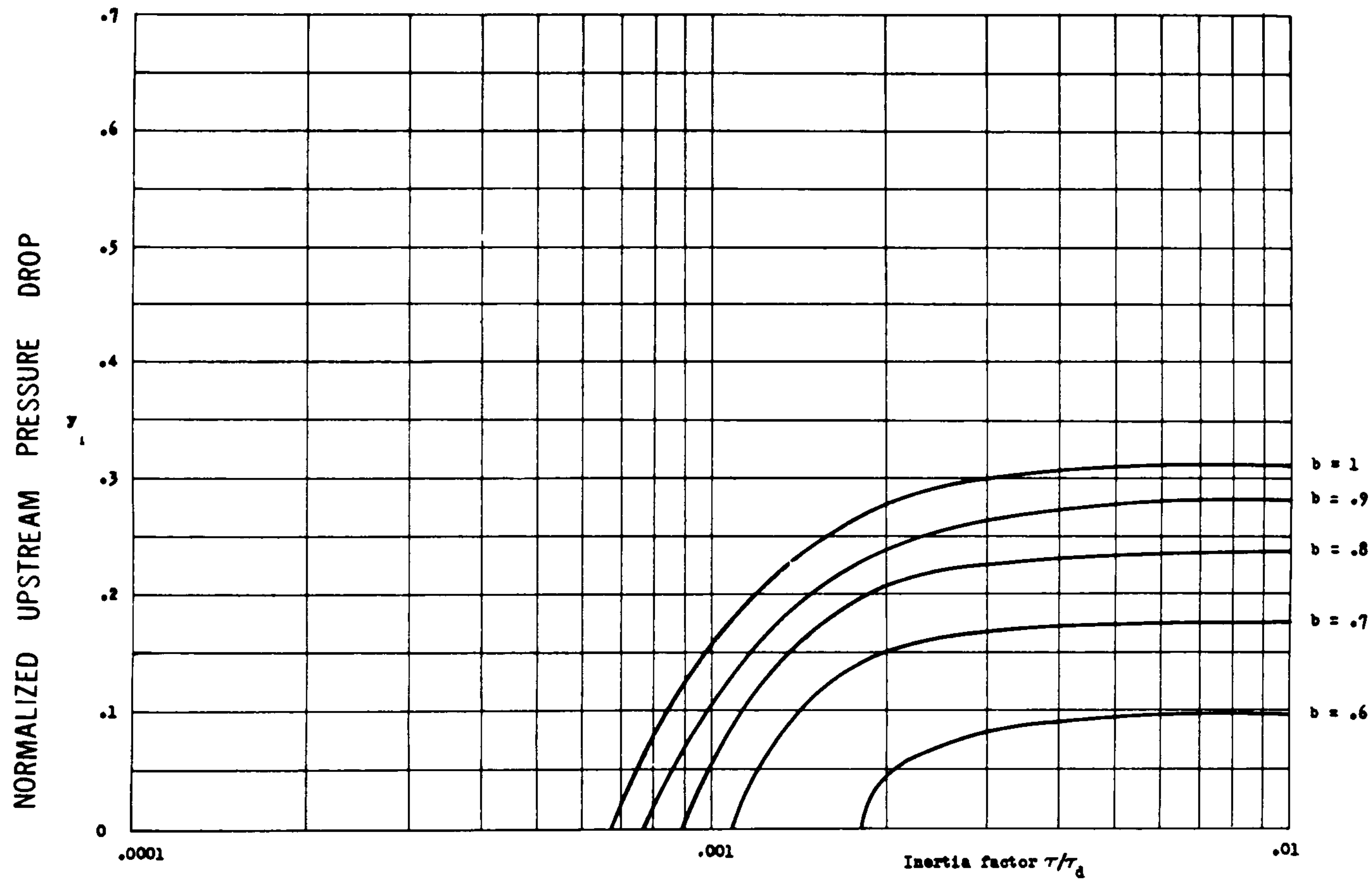

FIG. 36.– TYPE II BOILING FLOW STABILITY BOUNDARIES FOR $r_1 = 80$, $c = 0$

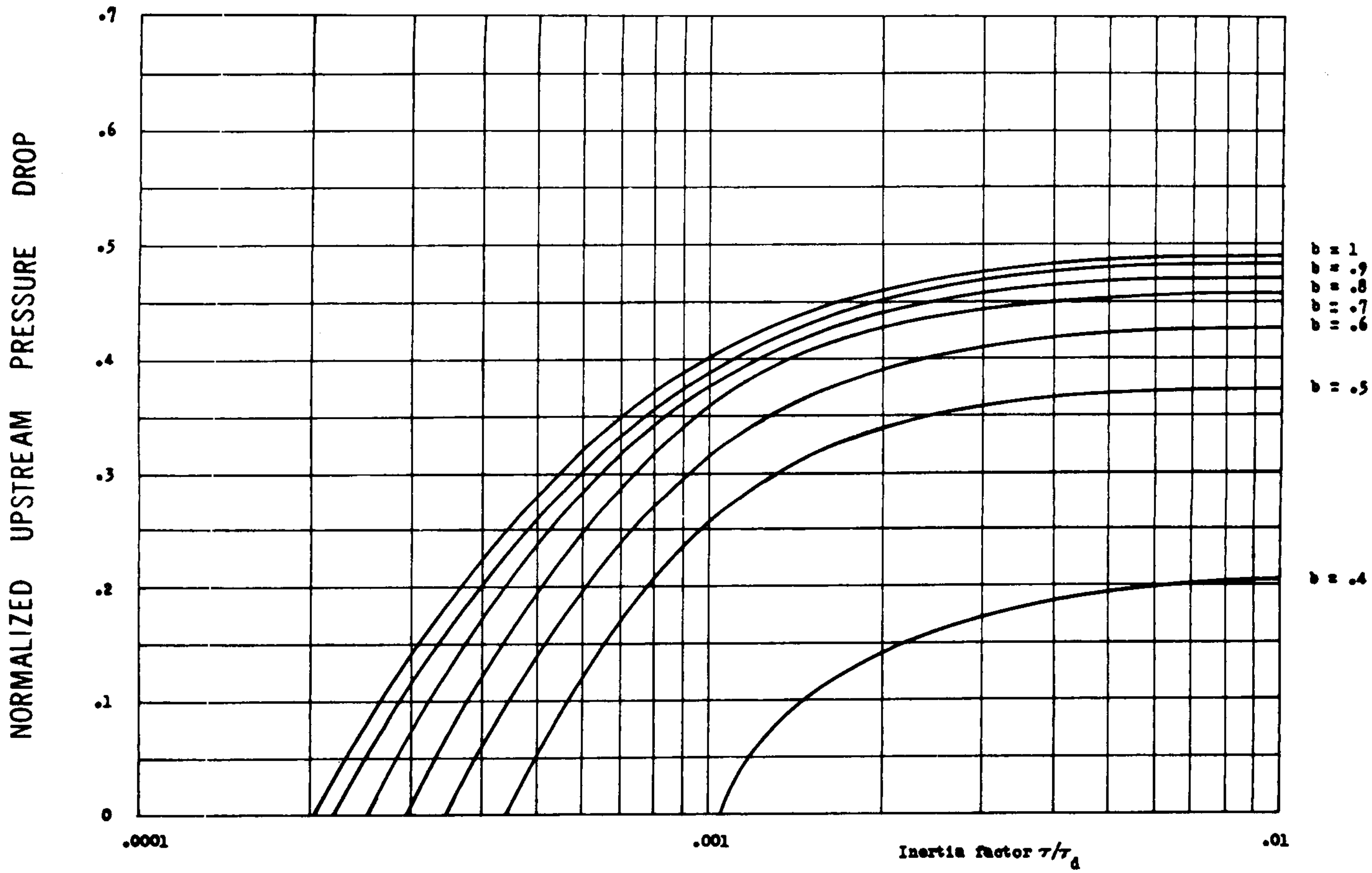

FIG. 37.– TYPE II BOILING FLOW STABILITY BOUNDARIES FOR $r_1 = 80$, $c = 0.5$

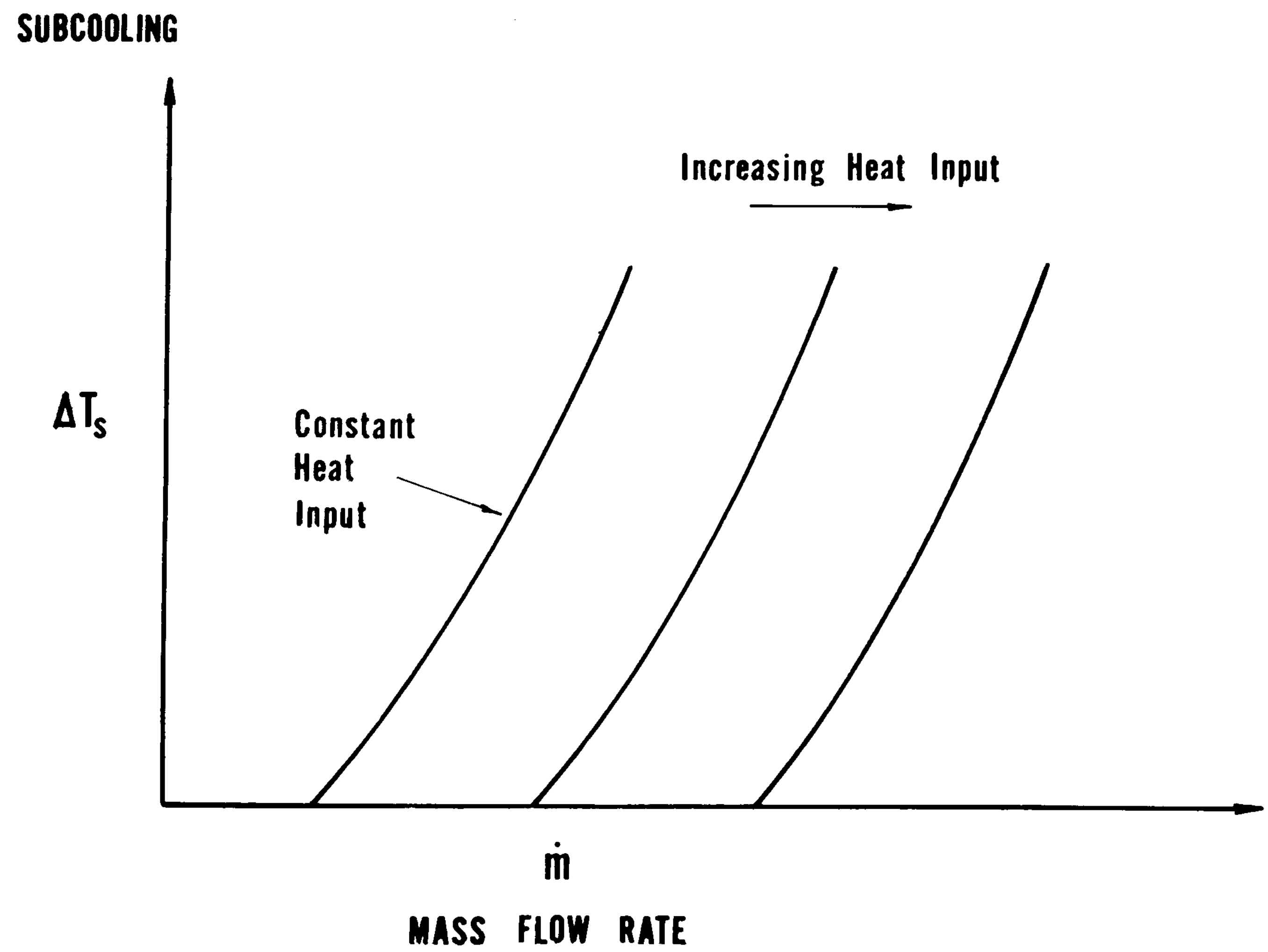

FIG. 38.- EFFECT OF SUBCOOLING ON STABILITY BOUNDARY AS PREDICTED BY ANALOG SIMULATION FOR FIXED Y

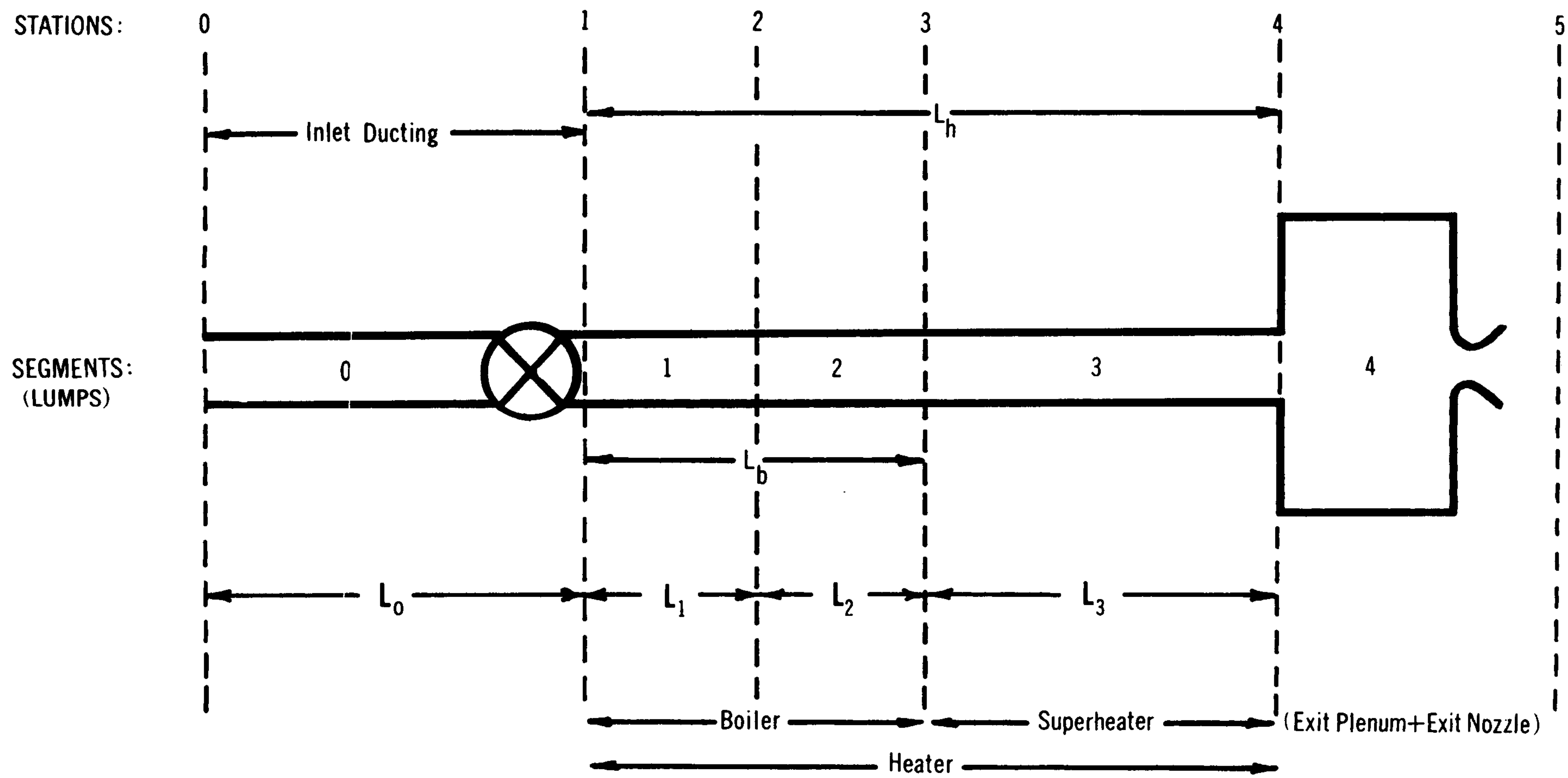

FIG. 39.- SYSTEM UNDER CONSIDERATION FOR SUPERHEAT ANALYSIS

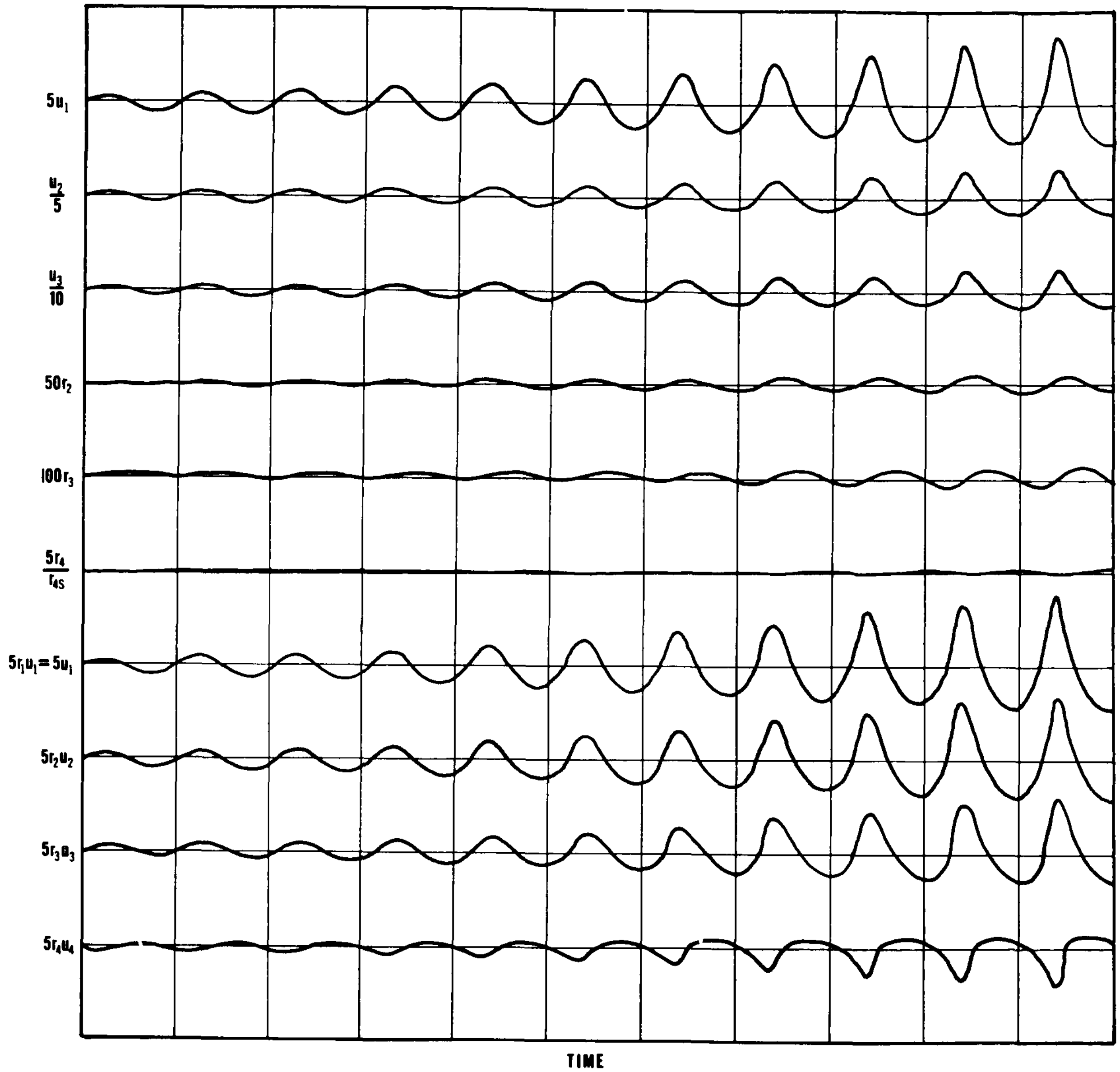

FIG. 40.- VELOCITY, DENSITY AND MASS FLOW RATE OSCILLATIONS FOR TYPE II OSCILLATIONS WITH SUPERHEAT, ANALOG SIMULATION

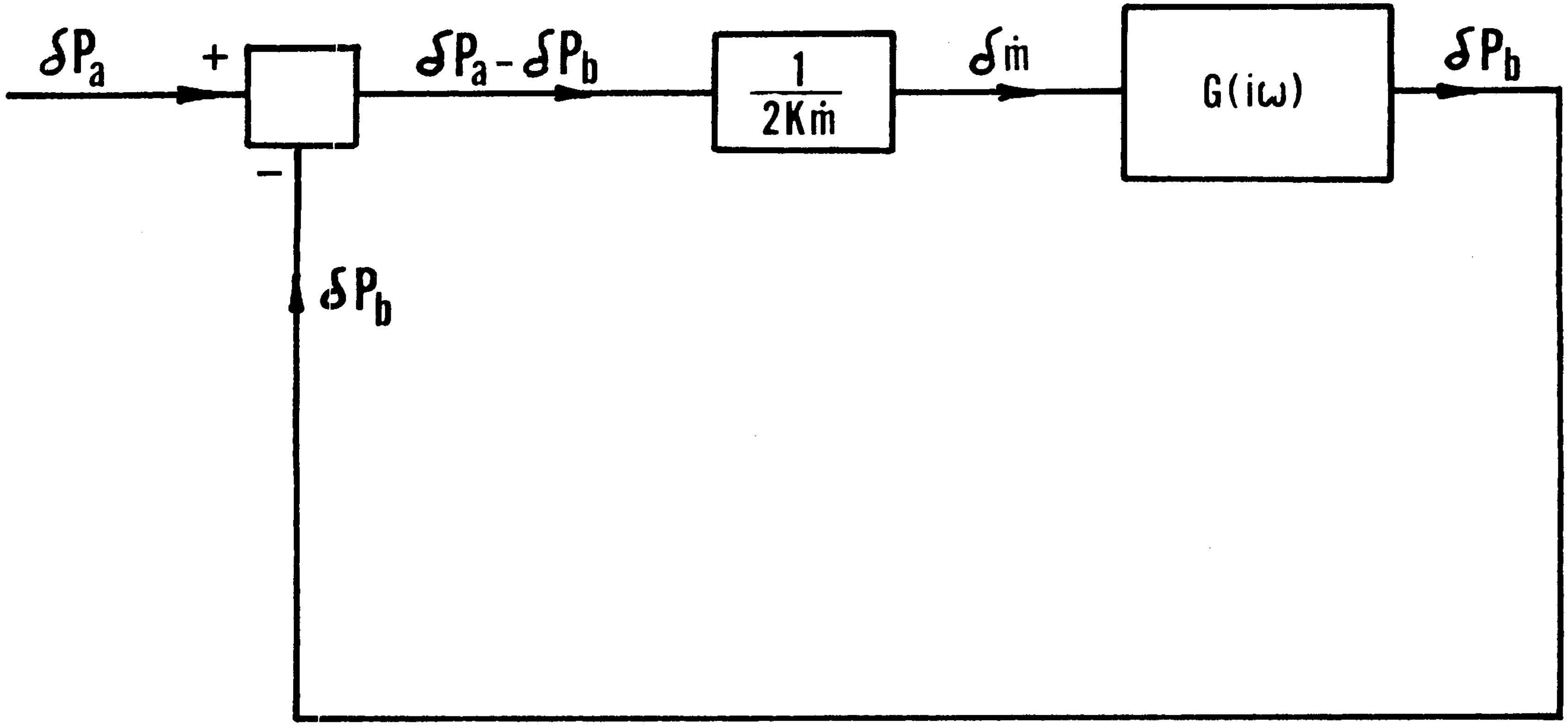

FIG. 41.– BLOCK DIAGRAM FOR FREQUENCY RESPONSE ANALYSIS OF TYPE II OSCILLATIONS

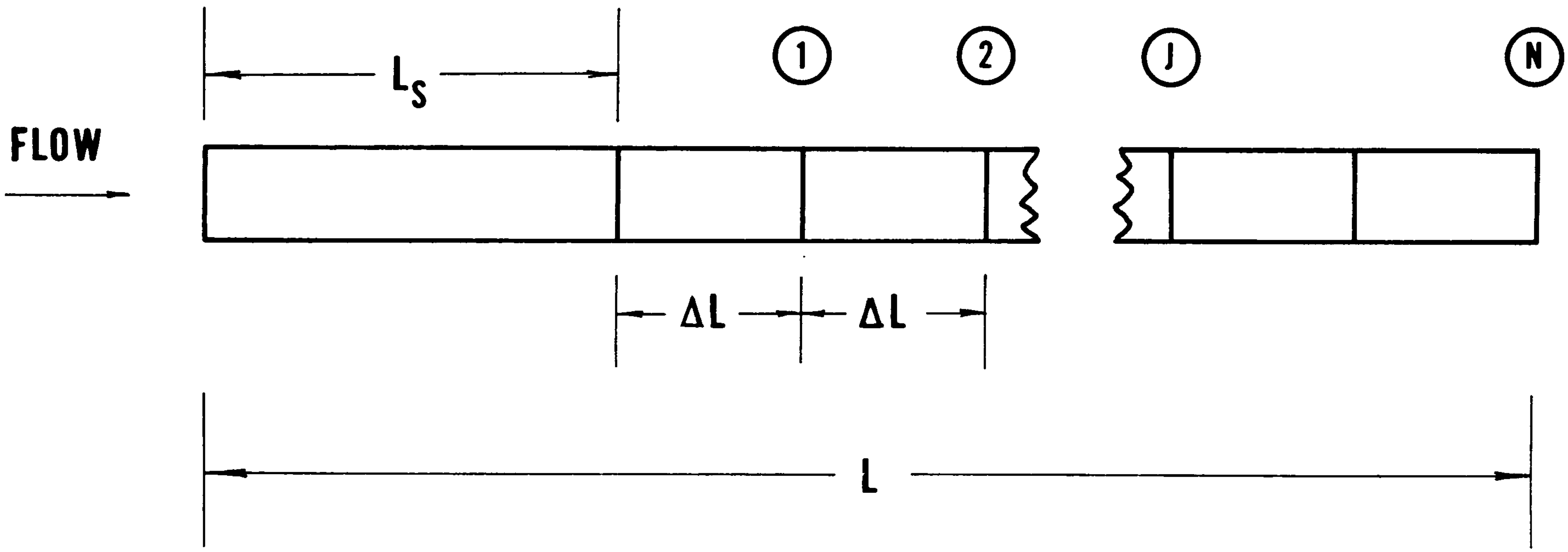

FIG. 42.–HEATER REPRESENTATION FOR FREQUENCY RESPONSE ANALYSIS

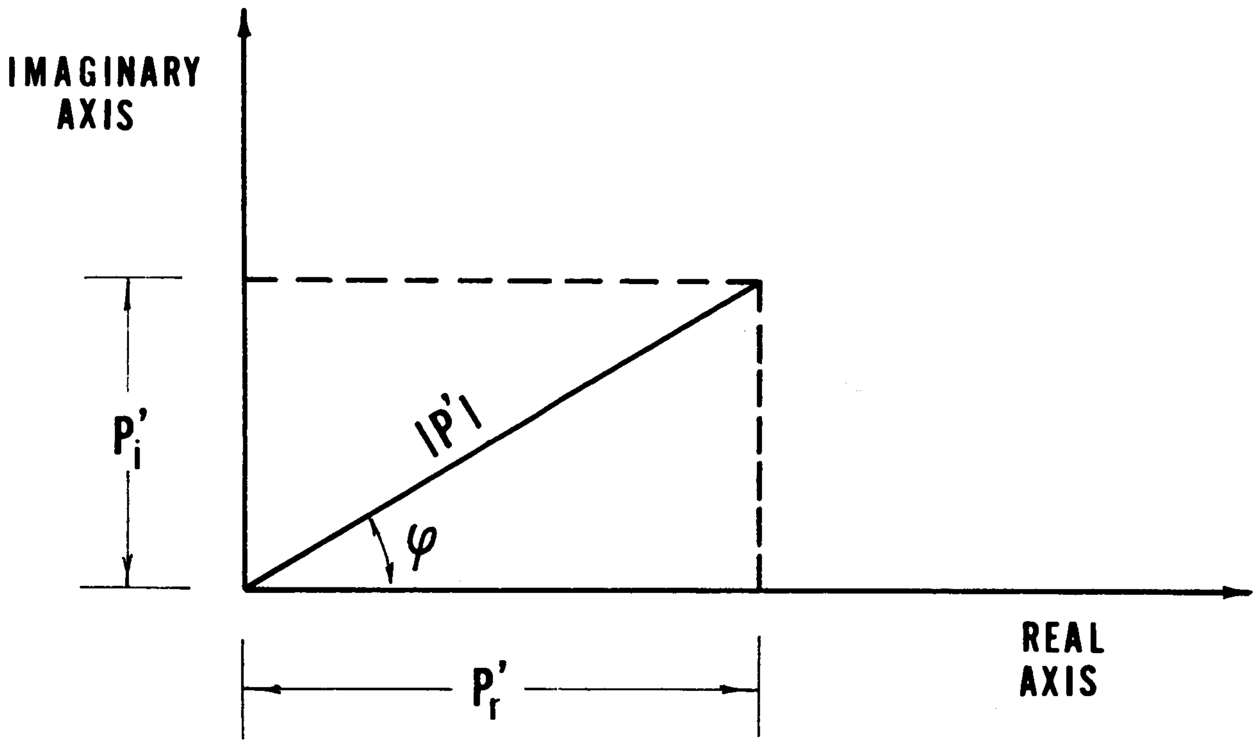

FIG. 43.- PRESSURE PERTURBATION REPRESENTED AS COMPLEX QUANTITY

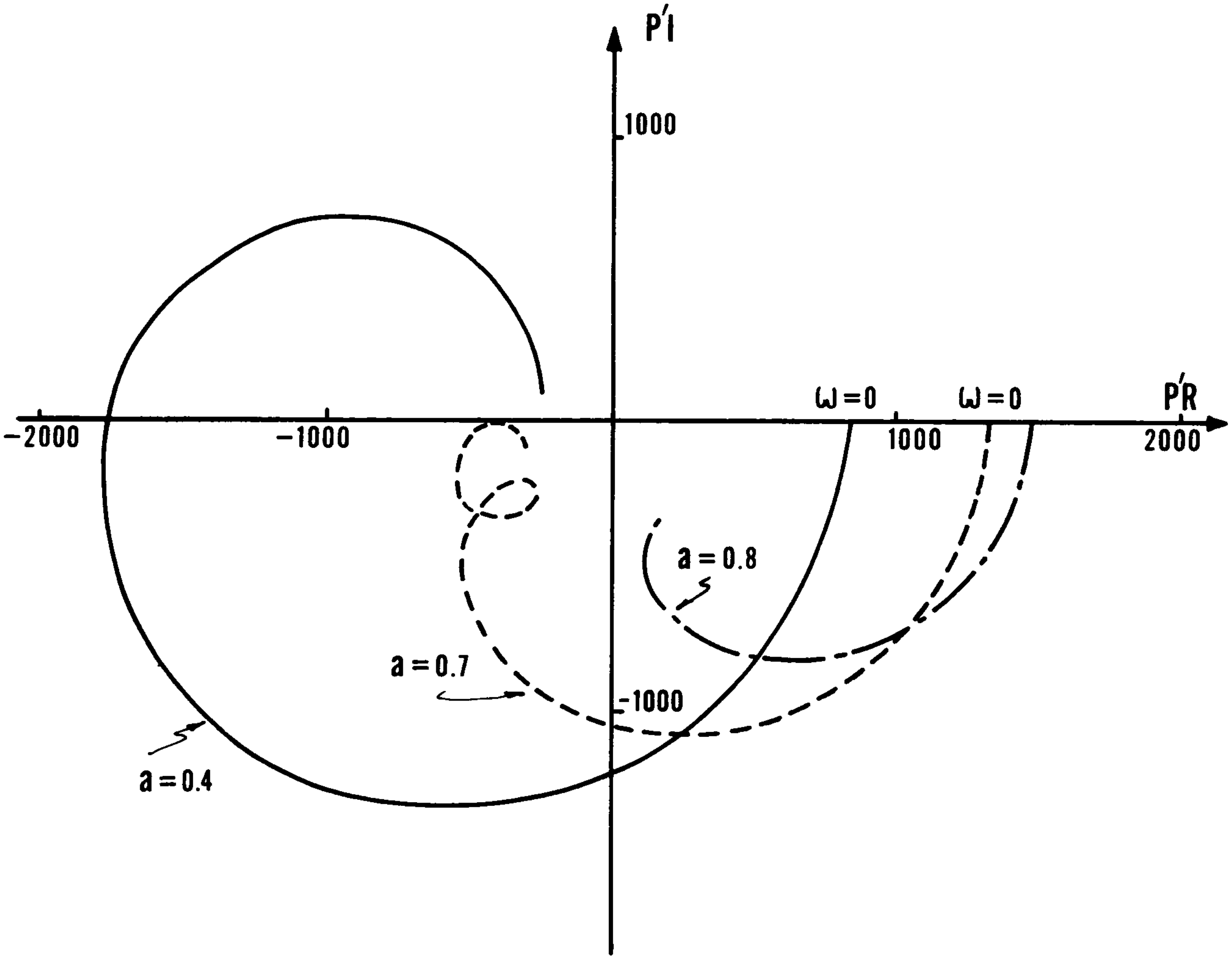

FIG. 44.- LOCUS OF PRESSURE PERTURBATION WITH VARYING FREQUENCY

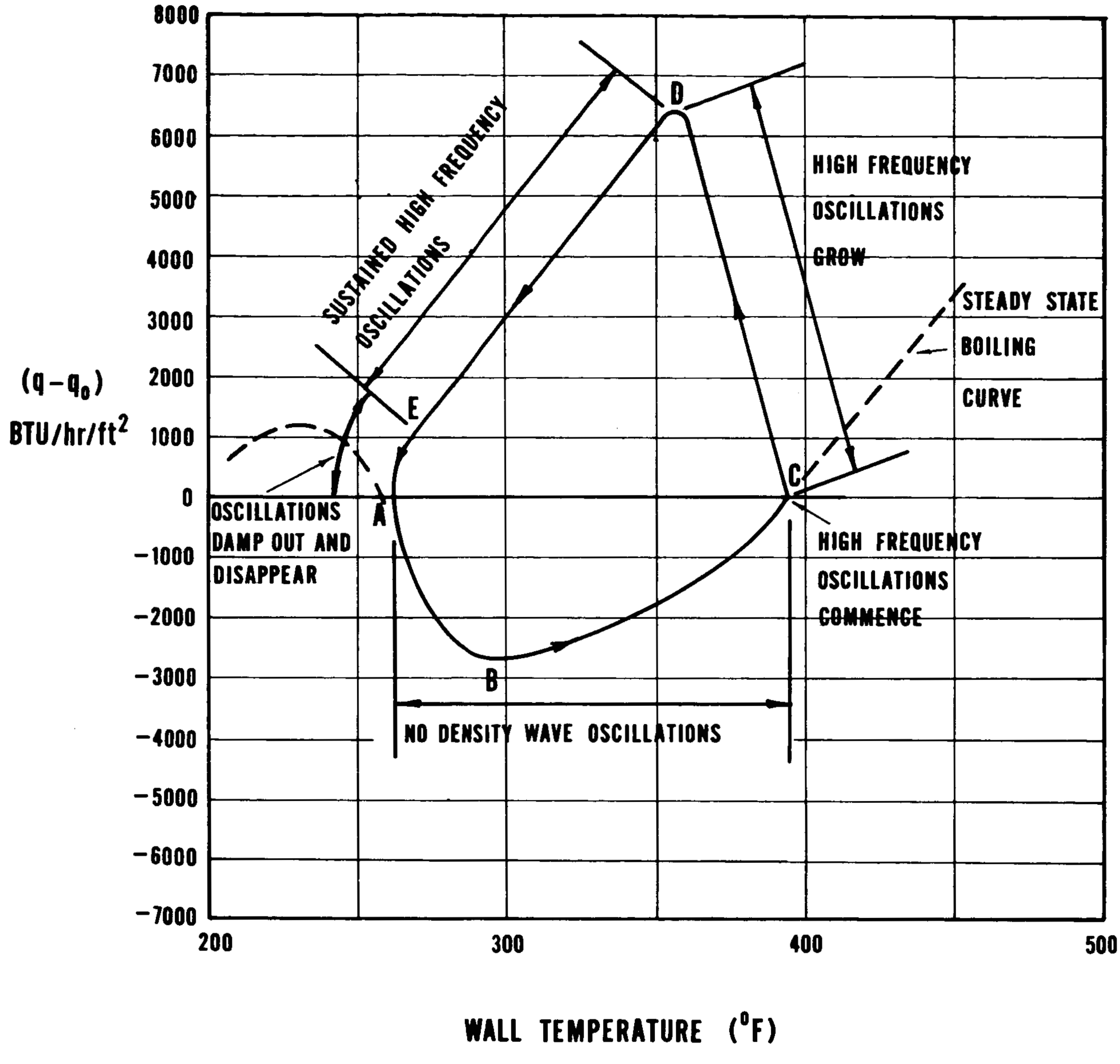

FIG.45.—HEAT FLUX VERSUS WALL TEMPERATURE FOR ONE CYCLE OF TYPE III OSCILLATIONS